Wireless Transmission with Energy Harvesting and Storage

by

Fatemeh Amirnavaei

A Thesis Submitted in Partial Fulfillment
of the Requirements for the Degree of
Doctor of Philosophy

in

The Faculty of Engineering and Applied Science
Department of Electrical and Computer Engineering
University of Ontario Institute of Technology

June, 2017

Abstract

In this dissertation, online power control strategies are proposed for wireless communication systems equipped with energy harvesting devices and finite-capacity batteries. The methods are proposed for the unbounded fading environment. Due to the time-dependent and random behavior of the energy arrival and fading, this dissertation focuses on the stochastic optimization problem to maximize the long-term average transmission rate. Leveraging the Lyapunov technique, online algorithms are designed based on the current battery energy level and fading condition. The performance gaps to the optimal scenarios are mathematically derived. The proposed algorithms do not require any statistical information (of the energy arrival and fading) and have a novel behavior of conservative energy harvesting and opportunistic transmission. The algorithms are designed for point-to-point, and relay networks.

For a point-to-point channel, a three-stage closed-form online power control policy is proposed. The proposed algorithm has an opportunistic behavior based on the energy arrival and channel fading. The proposed methodology is shown to be applicable for multi-antenna beamforming scenarios including MISO, SIMO, and MIMO. The analytical performance gap to the optimal solution is presented. The simulations are compared with other online algorithms in the literature and provides a superior performance.

A joint online power control strategy is designed for a two-hop amplify and forward (AF) network. Both transmitter and relay are equipped with finite capacity batteries and energy harvesters. The proposed algorithm is a joint closed-form scheme that has an unique behavior in terms of the channel fading and energy arrival of both hops. Analysis is provided to illustrate the performance gap of the proposed algorithm to the optimal solution. The simulation results show that the performance significantly higher than that of existing online algorithms.

To my dear mother

for her endless love and support

To my love, Javad

for his never-ending encouragement

Contents

List of Figures

List of Algorithms

Chapter 1

Introduction

1.1 Energy Harvesting in Wireless Communication

The excess carbon emission due to the growing energy demand has caused significant environmental concern. To address the increasing energy cost and reduce carbon footprint, the renewable energy has increasingly been considered as an alternative energy source. In particular, wireless communication systems equipped with energy harvesting (EH) devices have recently attracted a growing attention. Energy harvesting is a process that captures the energy from the environment, converts and stores for future transmission. Unlike the conventional fixed power supplies (either from the grid or battery), EH devices scavenge energy from the environment and provide a continuous power supply.

There are many different ambient energy sources for the energy harvesting including natural and other ambient energy sources. Natural sources such as solar, wind and water flow provide an unlimited amount of energy from the environment. Along with the natural sources, there are other methods to scavenge the ambient energy sources such as vibrational, electromagnetic, thermal, biological systems [1–8]. One of the promising source of energy harvesting is solar energy (light) which provides abundant amount of energy with-

out generating any carbon footprint. Using photovoltaic cell, light energy is converted to the electrical energy. This technique provides a higher energy level compared with that of other alternative sources of energy harvesting. This energy depends on the day time and also the geographical location. For example, this method works properly in Asian and African countries where the sun light is available throughout the day. Another natural source of energy harvesting is wind suitable for countries that their weather is mostly cloudy and windy [9].

Although the convectional renewable energies such as solar and wind energy provide a high amount of energy, the nature of these sources could be time-dependent e.g. the solar energy is not available at night. To address this concern, radio frequency (RF) has gained a great importance in various EH wireless systems. Radio frequency energy harvesting (RF EH) exploits the energy from the environmental electromagnetic signals that continuously exists in the surrounding environment [10]. Using RF EH, energy cooperation among various wireless receiver devices was recently introduced. The RF EH technique, however, has not been investigated at the transmitter side although the RF environment presents constantly.

There is a growing demand for a low-cost reliable source of energy that is applicable for a wide range of applications. The EH devices have initially gained a lot of attention in remote applications where the conventional energy supply is not accessible [11, 12]. For instance, energy harvesting devices provide an unlimited power supply for wireless sensors to maintain the lifetime network operation without the need to replenish batteries. These systems later used in biological applications where the sensors are used in the human body and not accessible for charging [13, 14].

In wireless communication, EH technique is a promising solution to provide a sustainable energy source to base stations, relay stations, routers and the mobile devices [15]. The recent technologies in wireless systems require a higher energy consumption. For example,

EH would benefit the high speed multimedia transmission in cellar networks specifically in 5G systems [10].

In practice, the ambient energy sources have a stochastic nature. In other words, the ambient energy is available at random times and in random amounts. The stochastic nature of the ambient energy is one of the challenges in energy harvesting technology specifically wireless communication. Furthermore, signal fluctuation is another challenge to design an effective wireless transmission model. Fading and path-loss are responsible for signal attenuation in wireless communication systems [16]. The channel fading has a random behavior and would greatly influence the performance of the network. Additionally, energy storage and management should be considered along with EH methods in designing a reliable EH system to address the stochastic energy arrival. EH sources should be managed effectively before utilizing and exploiting.

To address these challenges (*i.e.*, random energy arrivals and fading environment), an effective EH methodology is needed that maximizes the performance of wireless system using ambient energy sources. Based on the energy arrival process and storage structure, various methods in wireless communications were proposed [9]. Fig. 1.1 illustrates the common classification of system design with energy harvesting technology in wireless communication network. Modeling the energy arrival process can be categorized into offline and online strategies. In offline methods, the energy arrival (in terms of arrival time and arrival amount) and channel quality (in the case of considering the fading environment) are assumed to be known in advance (*i.e.*, prior to beginning of transmission) [9, 15]. In online methods, however, the energy arrival and channel fading gain are assumed to be causal where only past and current information of random events are available. offline methods are unrealistic since the nature of environment is unpredictable and has a stochastic behavior. However, these methods present an upper-bound for the performance of the online methods [17]. The online methods are challenging to be designed due the complex nature

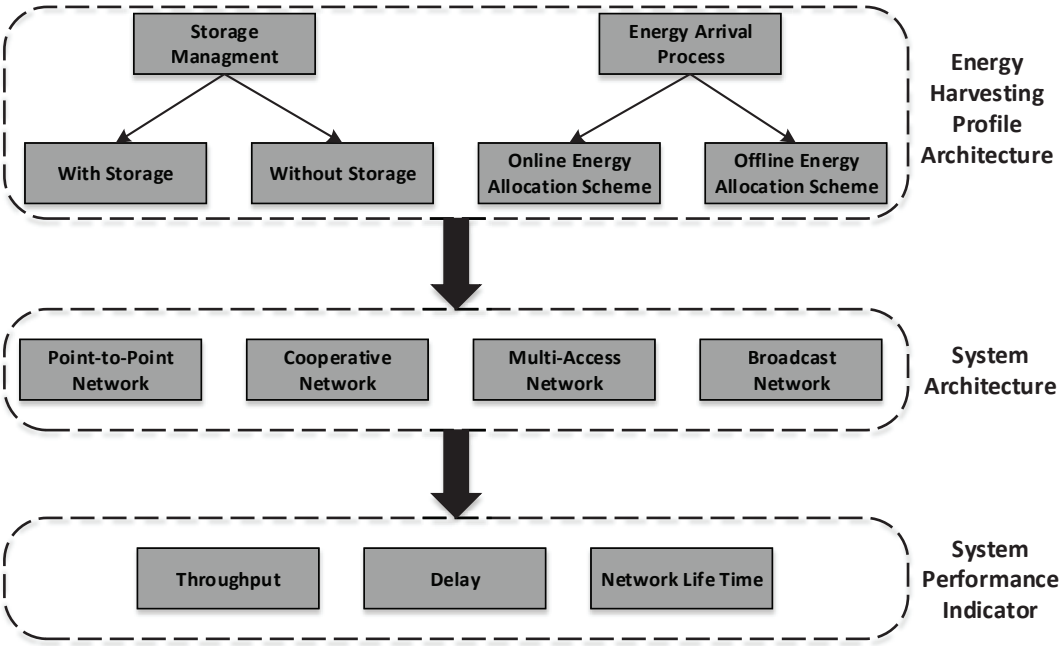

Figure 1.1: Energy harvesting systems classification

of random ambient energy sources [15].

Scavenging the ambient energy can be considered regardless of the battery storage, however, the battery storage, in practice, benefits the performance of the wireless communication system. In terms of the storage management, the EH communication systems can be divided into *with storage* and *without storage*. In *without storage* method, the harvested energy is used immediately to supply the power of the network. For a system to perform constantly, the harvested energy should be more than the minimum required energy for the network operation. EH *with storage* method uses an energy storage or rechargeable battery to save the excess amount of harvested energy. The EH *with storage* can be categorized into ideal and non-ideal in terms of battery capacity and implementation [15, 17]. EH methods (online /offline along *with storage* management) can be applied in various wireless system models including point-to-point, broadcast, multiple access, and cooperative relay

networks.

This dissertation proposes novel practical online power control strategies using EH in the fading environment to maximize the long-term average rate of wireless networks. A realistic battery storage with a finite capacity is considered in the proposed methods. The algorithms are proposed for the point-to-point and relay networks. Furthermore, an online joint power control and operation management (scheduling) is developed using RF EH at the transmitter side to maximize the long-term average rate in the multiple access network.

1.2 Literature Review and Background

In the followings sections, the existing EH works in the wireless communication are reviewed and compared.

1.2.1 EH in Wireless Communication without Storage

There are some works that focus on the capacity of a communication channel where there is no battery to store and save energy for future use. In this case, the channel input is limited to the instantaneous stochastic amplitude constraint [15]. Reference [18] considers Amplitude White Gaussian Noise (AWGN) channel with time-varying amplitude constraints and derives the capacity of this channel by using Shannon's coding scheme [11] with no battery to store energy. The transmitter has the causal information of the energy arrival, and the receiver does not have any knowledge of it. The numerical results of this work illustrate that the capacity can significantly increase with considering an unlimited battery storage. Reference [19] extends this work to a two-user multiple access channel with no batteries and assuming the static amplitude constraints. Having input distributions, they presented the boundary of the capacity region.

Besides renewable sources such as solar and wind, harvesting energy from radio-frequency energy signals has been recently considered for wireless transfer of information and power simultaneously [20–25]. First proposed in [20], simultaneous wireless information and power transfer (SWIPT) has been studied extensively under different system model assumptions. Point-to-point single antenna transmission is considered in [20, 21]. A multiple input-multiple output (MIMO) SWIPT system is first presented in [22], and then is extended to a multiple input-single output (MISO) with more than two users in [23–25]. Note that no energy storage unit is considered in these works. The SWIPT method enables the receiver to share the same antennas for receiving information and harvesting RF energy.

1.2.2 EH in Wireless Communication with Storage

For wireless transmission powered by renewable energy, typically, an energy harvesting device is implemented with a battery to store the harvested energy and provide power for the transmission. Due to the randomness of the energy source and the wireless fading channels, existing works on the transmission power control design can be grouped into two categories: offline and online power control strategies.

1.2.2.1 Offline Methods

For an offline power control design, energy arrivals and channel fades within a time period are known non-causally. In this case, typically a deterministic power optimization problem can be formulated with various criteria. Several literature works have considered offline strategies for AWGN channels [26–33]. From information theoretic point of view, the capacity of the AWGN channel with an energy harvesting transmitter has been derived in [26]. Optimal power allocation solution to minimize the transmission time for point-to-point transmission has been obtained in [27]. For the multi-user setting, optimal

power allocation are studied in [34], [35, 36], and [30] for broadcast, multiple access and interference channels, respectively. Power allocation for throughput maximization in a Gaussian relay channel under the energy harvesting has been considered in [28]. In all these works, infinite capacity of the battery is assumed for the energy storage. With finite battery capacity, power allocation policy for rate maximization has been investigated for both single user and two-user Gaussian interference channel [29, 30]. For fading channels, power allocation solutions for throughput maximization have been obtained for infinite battery capacity [31, 32, 37] and finite battery capacity cases [33, 38]. For [31], different from the commonly used harvest-store-use models for energy harvesting, the authors have considered a harvest-use-store model to improve the efficiency of energy usage.

1.2.2.2 Online Methods

online power control design based on the current and past system information, such as energy arrivals, is a more practical but much challenging problem. A few existing works have formulated the power control problems by the Markov Decision Process (MDP) and obtain the power solutions by Dynamic Programming (DP) for rate maximization or transmission error minimization [32, 33, 39–44]. For example, in [32], the online power control for the rate maximization over a fading channel in finite time slots has been considered, where the harvested energy and fading are modeled as first-order Markov processes. To compute the power solution by DP, these works generally require the statistics of harvested energy and fading channel to be certain types and known at the transmitter. In addition, the numerical solutions by DP are typically obtained with high computational complexity which is impractical for real implementation.

Some low-complexity heuristic online approaches are proposed in [33, 45–49]. However, they also assume certain known statistical information and there is no performance guarantee. Other heuristic online algorithms including competitive ratio analysis and stor-

age dam model are applied in [50] and [51], respectively. For the sensing application in a sensor network with energy harvesting, without the knowledge of energy arrival statistics, an online power control for the AWGN channel in [52] is considered. Using Lyapunov technique, an online power solution is provided to maximize the long-term average sensing rate. The maximization of utility performance for a network with energy harvesting nodes is studied in [53], where an online algorithm based on Lyapunov technique is presented to jointly manage the energy and power allocation of packet transmissions.

Heuristic online approaches are proposed in [33, 45, 46]. However, all these heuristic schemes need the statistical information of random events. Reference [33] proposes a water-filling method based on the channel fading distribution. Reference [45] considers the AWGN channel and presents a three-level power algorithm that needs the knowledge of the harvesting process distribution. Without considering fading channels, reference [46] presents a heuristic power algorithm based on the average transmit power for offline method. Note that this method requires the distribution of the harvested energy. Without knowing the energy statistics, the online power control is considered for the AWGN channel in [52] for both infinite and finite battery capacities, where Lyapunov technique [54] is used in providing an online power solution.

To the best of our knowledge, an online power control strategy for energy harvesting without considering any statistical information of harvested energy and channel fading has not been considered yet. Different from most existing online methods that suffer from high computational complexity, this dissertation aims to design a novel method based on the realistic battery charging and power output characteristics that is practical and easy to implement.

1.2.3 EH in Relay Networks

Energy harvesting has also been studied recently for relay networks [28, 55–60]. offline strategies are proposed in all these works. Gaussian relay channels are considered in [28, 55–57], where infinite battery capacity is assumed for energy harvesting. Considering EH at the relay only, throughput maximization is considered in [55, 57]. Considering only EH at the transmitter, the short-term throughput maximization and transmission time minimization is studied in [56]. In [28], power control for decode-and-forward (DF) relaying with energy harvesting nodes is considered for the throughput maximization over a finite horizon. Considering DF two-hop network with offline EH at the transmitter and relay, the maximization of transmit data by a given deadline in studied in [60]. A joint relay selection and power allocation method to maximize throughput of AF multi-relay network in high SNR values is proposed in [58].

In [58], a sub-optimal online algorithm is also proposed for joint relay selection and power allocation that depends on the statistical information of energy arrival and fading channels. In [59], for DF relaying, link selection and power control at the relay with energy harvesting is considered for the outage probability minimization by both offline and online DP approaches. Using discrete MDP, [61] studies throughput maximization of AF two-hop network by considering the non-causal (offline) and causal (online) harvested energy. However, the online solution is proposed for a special case of on-off power transmission to reduce the complexity of MDP method. Reference [62] considers a cooperative network in which multiple source-destination pairs are equipped with one energy harvesting relay. The outage probability for this network is examined by taking the spatial randomness of user locations into consideration. Moreover, [63] considers the cooperative network with transmitter nodes that are capable of transmitting and receiving from other nodes. They study offline maximization of the sum-throughput of the two-way, two-hop, and multiple

access channels by focusing jointly on the optimal transmit power and energy transfer policies. They solve the joint optimization problem by decomposing into energy transfer and consumed energy allocation problems.

Few works have studied online algorithms for a two-hop network in a fading environment. The statistical distribution of the harvested energy is assumed to be known in those studies. Most of the proposed methods suffer from high computational complexity. To the best of our knowledge, there is no comprehensive online algorithm that considers EH at both transmitter and relay with finite batteries without knowledge of statistical distribution of the energy arrival and fading condition. A joint online power strategy along with the battery storage management is developed at both transmitter and relay. The main objective is to propose a practical and easy-to-implement online algorithm that does not require any statistical information of random inputs including the energy arrival and fading channels.

1.2.4 RF-Enabled EH

The ambient radio signals provide a sustainable and reliable energy source for wireless energy harvesting (WEH). RF energy harvesting enables the wireless devices to leverage the RF environment to process their information and transmit. There are different methods to implement WEH including inductive coupling, magnetic resonant coupling and electromagnetic (EM) radiation ([64, 65]). Due to the prevalence of wireless systems, EM radiation-based RF environment is constantly available, and thus this new energy scavenging approach has attracted a significant attention [66–68].

RF-enabled devices have a wide range of applications for wireless sensor networks [69–71], wireless body networks (medical applications) [72, 73] and radio-frequency identification (RFID) tags [74, 75]. RF energy harvester enables the low-power micro size medical devices to operate without having battery. Applications of medical devices can be

found in [76, 77].

RF energy harvesting technology has gained a lot of attention in wireless communication networks [78, 79]. Since RF signals carry both information and energy, simultaneous wireless information and power transfer (SWIPT) to the receiver has been introduced [20, 21, 66], where the receiver is able to harvest the energy and decode the information simultaneously from a transmitted signal. In practice, the signal power degrades due to signal propagation and path loss. To overcome this issue in RF EH, beamforming with multi-antenna technique can be considered to increase an energy transfer efficiency of SWIPT system [65, 80, 81]. Reference [25] considers SWIPT for a multi-user wireless system with energy beamforming. Considering the *time switching* method at the receiver side and collaborative energy beamforming, [25] presents the rate-energy trade-off over fading channels.

In practice, harvesting energy and decoding information simultaneously from one signal is not possible due to the complexity involved in designing circuits. It is worth mentioning that information decoding (ID) and energy harvesting (EH) receivers work in different power levels (e.g. -10dbm for EH receivers and -60 dbm for ID receivers) [64]. To overcome this limitation of SWIPT technique, there are some works that propose the practical methods to reduce the complexity of designing receiver. Reference [82] introduces a *power splitting* method where the receiver has two co-located receivers of ID and EH. The received signal is divided into two streams with the power ratio within the range of zero to one. This work focuses on the optimal transmission strategy by studying rate-energy trade-off considering the power ratio. Recently, [83] studies SWIPT for multiple user MIMO interference channels. Using a *power splitting* technique, this work proposes a suboptimal solution to minimize the total transmission power of all transmitters subject to signal-to-interference-plus–noise ratio (SINR) and energy arrival constraints. Using *power splitting* along with SWIPT method, references [84] and [85] focus on minimizing the total

transmission power of MISO and k-user MIMO interference channels, respectively. Moreover, [86] presents an *integrated receiver* method to verify the rate-energy region where the receiver first converts the signal into DC current, then splits the signal into two streams for EH and ID. Reference [86] proposes the *energy modulation* method that encodes the data in the power of signal. Reference [87] studies the optimization of resource allocation for a two-user multiple access channels for SWIPT. It is considered that the energy harvester and information decoder are spatially separated at the receiver. A *time switching* method is proposed in [66]. The receiver consists of EH and ID parts that can either decode information or harvest energy at any time. Reference [66] studies the optimal switching mode at the receiver and presents different rate-energy region of ID and EH. Reference [88] considers the *time switching* at the receiver for multiple input-single output (MISO) multicast SWIPT network. Applying the single random beamforming, the work achieves the asymptotic optimal trade-off between the average information rate and average harvested rate when the transmit power approaches the infinity. However, for the finite transmit power, along with a large amount of energy harvesting, the simulation result demonstrates the best information and outage probability trade-off with the single random beamforming. Reference [89] considers the optimal design for SWIPT in downlink multiuser orthogonal frequency division multiplexing (OFDM) system. At the receiver side, *time switching* and *power splitting* methods are investigated to maximize the weighted sum rate. This work proposes a joint time division multiple access (TDMA)-based and frequency division multiple access (FDMA)-based transmission policies based on the *time switching* and *power splitting* methods, respectively. The authors show that for the single-receiver case, the *time switching* method outperforms *power splitting* method with either finite peak power or without any peak power constraint on each sub-carrier. Overall, *time switching* method benefits more among the other alternative methods. The main advantage of this method is a low complexity implementation. For implementing the *time switching* scheme, any

conventional decoder and energy harvester can be used and there is no need to design any sophisticated receiver. Furthermore, ID and EH components work within a different range of power consumption. Therefore, the *time switching* mode provides an effective power management scheme in terms of different applications. Last but not the least, the wireless channels suffer from fluctuation (fading) and spectrum sharing (interference). Thus, the *time switching* scheme operates dynamically to exploit the energy of signals to optimize both performance and switching operation [66].

1.2.5 EH Cognitive Radio Networks

Cognitive radio is a promising method for wireless communication to share the spectrum efficiently between the primary and secondary networks without substantial impact on the network performance. Employing energy harvesting technique in cognitive radio networks (CRN) enhances the wireless transmission in terms of energy efficiency and spectrum efficiency [90–95]. For EH CRN, an access scheme for the secondary users with EH is proposed in [96]. The secondary users are equipped with EH and a battery. The secondary users consider random spectrum sensing and random access using the primary automatic repeat request (ARQ) feedback. This work focuses on maximizing the secondary users' throughput under the constraints that both the primary and secondary queues are stable. While the primary users are only equipped with data queues, the secondary users have data and energy queues. This method has been expanded in [97] to achieve the optimal service rate of the secondary users with randomly accessing to the primary channel. Considering the channel condition and time-varying energy source, [98] investigates the maximization of the secondary users' throughput over a finite time horizon. Using the sliding window approach, [98] proposes a suboptimal algorithm for the energy allocation. Considering the probability of the available energy, a channel selection method for EH CRN is introduced

in [98]. The optimal policies for the secondary users are designed to select the channel for spectrum sensing and maximize the average spectral efficiency. In [99], the achievable throughput of the secondary users with EH is studied considering the opportunistic accessing to the spectrum licensed to the primary user. Using discrete Markov process, this work proposes the upper-bound on the achievable throughput that depends on the energy arrival rate, the primary traffic correlation and the detection threshold for a spectrum sensor. In [100], the spectrum sensing optimization is proposed for EH CRN to develop a sensing configuration under the energy causality constraint.

A self-sustainable method with RF EH in CRN is investigated in [92, 95, 101–103]. In [95], secondary transmitters can either harvest energy from the nearby primary transmitters or transmit information. The throughput maximization of the secondary network is investigated considering a stochastic-geometry model. The primary and secondary transmitters are modeled as independent homogeneous Poisson point processes. Under the given outage-probability constraints, the optimal transmission power of the secondary transmitters are derived. Applying the temporal correlation of the primary traffic, [92] aims to enable the efficient usage of the harvested energy. It proposes a technique that a secondary transmitter can opportunistically access the spectrum while harvesting energy from the ambient or wireless energy transfer. Cognitive radio sensor equipped with RF EH is studied in [92]. It aims to determine the operation mode and the decision variables for sensor nodes. In [102], a joint information and energy cooperation between the primary and secondary transmitters is investigated. Reference [103] presents the employing microwave power transfer (MPT) for the cellular networks that are recharged by microwave radiation through power stations. To utilize MPT for mobile recharging, [103] adopts the stochastic geometry and proposes a hybrid network architecture.

1.2.6 Other Types of EH Networks

Hybrid energy source combines the conventional energy source, *i.e.*, power grid, diesel generator, etc. with an EH source. A point-to-point communication system equipped with a hybrid energy source is considered in [104]. A power allocation scheme is proposed for both offline and online methods. The objective is to minimize the constant energy source while efficiently utilizing EH for the data packet transmission over a finite time slot. In [105], the throughput maximization of an EH transmitter equipped with a hybrid storage is proposed for an off-line transmission. For a base station equipped with both an EH and a power grid, [106] uses the statistical information to allocate resources for a single cell. This reference proposes a trade-off between the average grid power and outage probability for the users.

Data packet scheduling is another problem that has been gained considerable attention in EH. The proportional fairness scheme is introduced in [107]. Reference [108] uses the proportional fairness scheme to maximize the throughput of the network while considering the channel quality differences among users. The heuristic scheme is proposed for a biconvex optimization problem. Focusing on minimizing the transmission time, [27] and [109] propose optimal scheduling policies to transmit all data arrival within a certain time period. Reference [27] considers a single user network while [109] applies the method to a two-user broadcast channel. The references consider both data and energy queues and propose optimal algorithm for the off-line scheme. For a two-user multiple access channel, [110] proposes an optimal packet scheduling.

1.3 Lyapunov Optimization

Lyapunov optimization is a powerful method for optimizing time average problems in stochastic queueing networks [111–115]. Although Lyapunov techniques have a long history in the area of control theory, Lyapunov drift was first presented in [116] to build stable routing and scheduling policies for queueing networks. Reference [113] provides a drift-plus-penalty theorem that presents a technique to design control algorithms to maximize a time average network utility subject to a queue stability. The theorem also presents performance trade-offs between the utility maximization and average queue backlog. The algorithms are interesting because they only need knowledge of the current network states, and they do not need any knowledge of the probabilities associated with future random events.

Consider a stochastic network that operates in a discrete time with unit time slots $t \in \{0, 1, 2, ...\}$, [54]. The network is described by a group of queue backlog, $\mathbf{Q}(t) = (Q_1(t), Q_2(t), ..., Q_K(t))$, where K is a non-negative integer. Every slot t, a control action is taken and this action affects arrivals and departures of the queues and generates a group of real valued attribute vectors $\mathbf{x}(t)$, $\mathbf{y}(t)$ and $\mathbf{e}(t)$:

$$\mathbf{x}(t) = (x_1(t), x_2(t), ..., x_M(t)) \tag{1.1}$$

$$\mathbf{y}(t) = (y_0(t), y_2(t), ..., y_L(t)) \tag{1.2}$$

$$\mathbf{e}(t) = (e_1(t), e_2(t), ..., e_J(t)) \tag{1.3}$$

for non-negative integers M, L, J. These attributes are given by general functions:

$$x_m(t) = \hat{x}(\alpha(t), \omega(t)) \quad \forall m \in \{1, ..., M\} \tag{1.4}$$

$$y_l(t) = \hat{y}(\alpha(t), \omega(t)) \quad \forall l \in \{0, ..., L\} \tag{1.5}$$

$$e_j(t) = \hat{e}(\alpha(t), \omega(t)) \quad \forall j \in \{1, ..., J\} \tag{1.6}$$

where $\omega(t)$ is a random event observed on slot t and $\alpha(t)$ is the control action taken on slot t. The action $\alpha(t)$ is selected within a set $\mathcal{A}_{\omega(t)}$ that possibly depends on $\omega(t)$. Let $\bar{x}_m(t)$ define the time average of $x_m(t)$, under particular control algorithm, *i.e.*,

$$\bar{x}_m(t) \triangleq \frac{1}{t} \sum_{t=0}^{t-1} \mathbb{E}[x_m(\tau)]. \tag{1.7}$$

where $\mathbb{E}[\cdot]$ is the expectation over the random event $\omega(t)$. Let $\bar{y}_l(t)$ and $\bar{e}_j(t)$ represent the time average of $y_l(t)$ and $e_j(t)$, under a particular control algorithms, similarly. Let define $\bar{x}_m$ as follows

$$\bar{x}_m \triangleq \lim_{t \to \infty} \bar{x}_m(t). \tag{1.8}$$

Objective is to design an algorithm that solves the following problem:

$$\mathbf{P1}: \quad \min \overline{y_0} \tag{1.9a}$$

$$\text{s.t.} \quad \overline{y_l} \leq 0 \quad \text{for all } l \in \{1, \ldots, L\} \tag{1.9b}$$

$$\overline{e_j} = 0 \quad \text{for all } l \in \{1, \ldots, J\} \tag{1.9c}$$

$$\alpha(t) \in \mathcal{A}_{w(t)} \quad \forall t \tag{1.9d}$$

$$\text{Stability of all Network Queues} \tag{1.9e}$$

The above problem can be considered as stochastic program and is similar to the classic linear program and convex program of static optimization theory. Its solution is an algorithm to choose the control decisions over time based on the current network state, such that

satisfies all of the constraints. These types of stochastic optimization have a wide range of applications and the queueing theory plays a crucial role in them. Regardless of underlying queues in the original problems, the virtual queues is introduced as a strong method to ensure the the required time average constraints are satisfied [54]. Designing inefficient control decisions result in larger backlog in certain queues.

The general stochastic problem **P1** can be solved using the theory of Lyapunov drift and Lyapunov optimization. The virtual queues are defined to meet the desired constraints. For problem **P1**, let define virtual queues $Z_l(t)$ and $H_j(t)$ for each $l \in \{1, ..., L\}$ and $j \in \{1, ..., L\}$ with the dynamic equations:

$$Z_l(t+1) = \max\{Z_l(t) + y_l(t), 0\} \tag{1.10}$$

$$H_j(t+1) = H_j(t) + e_j(t). \tag{1.11}$$

It is worth mentioning that the virtual queue $Z_l(t)$ is designed to satisfy the constraint $\overline{y_l} \leq 0$. The virtual queue $H_j(t)$ is defined to transform the time-average constraint $\overline{e_j} = 0$ into a pure queue stability problem. Let $\mathbf{\Theta}(t) \triangleq [\mathbf{Q}(t), \mathbf{Z}(t), \mathbf{H}(t)]$ represent a vector of all actual and virtual queues. Then define Lyapunov function $L(\mathbf{\Theta}(t))$ as a sum squared of backlog in all virtual and actual queues on slot t as follows

$$L(\mathbf{\Theta}(t)) \triangleq \frac{1}{2}\sum_{k=1}^{K} Q_k(t)^2 + \frac{1}{2}\sum_{l=1}^{L} Z_l(t)^2 + \frac{1}{2}\sum_{j=1}^{J} H_j(t)^2. \tag{1.12}$$

In fact, Lyapunov function is a scalar measure of network congestion. Intuitively, if $L(\mathbf{\Theta}(t))$ is small, then all queues are small, and if $L(\mathbf{\Theta}(t))$ is large, then at least one queue is large. Define the conditional Lyapunov drift $\Delta(\mathbf{\Theta}(t))$ as follows

$$\Delta(\mathbf{\Theta}(t)) \triangleq \mathbb{E}[L(\mathbf{\Theta}(t+1)) - L(\mathbf{\Theta}(t))|\mathbf{\Theta}(t)] \tag{1.13}$$

which is the expected difference in the Lyapunov function from one slot to the next, given $\mathbf{\Theta}(t)$ as the current state at slot t.

Theorem 1.1 *([54]) Consider quadratic Lyapunov function (1.12), and assume $\mathbb{E}[L(\mathbf{\Theta}(0))] < \infty$. Suppose there are constants $B > 0$, $\epsilon \geq 0$ such that the following drift condition holds for all slots $\tau \in \{0, 1, 2, ...\}$ and all possible $\mathbf{\Theta}(\tau)$:*

$$\Delta(\mathbf{\Theta}(\tau)) \leq B - \epsilon \sum_{n=1}^{N} |\Theta_n(t)| \tag{1.14}$$

where $\Theta_n(t)$ represents the queue component in the queue vector $\mathbf{\Theta}(t)$. Then:

- *If $\epsilon \geq 0$, then all queues $\Theta_n(t)$ are mean rate stable.*
- *If $\epsilon > 0$, then all queues are strongly stable and :*

$$\limsup_{t\to\infty} \frac{1}{t} \sum_{\tau=0}^{t-1} \sum_{n=1}^{N} \mathbb{E}[|\Theta_n(t)|] \leq \frac{B}{\epsilon} \tag{1.15}$$

Proof: See [54].

Besides queues $\mathbf{\Theta}(t)$ to be stabilized, there is an associated "penalty" process $y(t)$ whose time average should be less than (or close to) some target value y^*. The process $y(t)$ represents the penalty related to the control decisions on time slot t. Suppose that the expected penalty is lower bounded by a finite value $y_{\min}$, therefore for all t and all possible control decisions, we have:

$$\mathbb{E}[y(t)] \geq y_{\min}. \tag{1.16}$$

Theorem 1.2 *([54], [113]) Suppose$L(\mathbf{\Theta}(t))$ and $y_{\min}$ are defined by (1.12) and (1.16) and assume that $\mathbb{E}[L(\mathbf{\Theta}(0))] < \infty$. Consider that there are constants $B \geq 0$, $V \geq 0$, $\epsilon \geq 0$*

and y^* such that for all slots $\tau \in \{0, 1, 2, ...\}$ and all possible values of $\mathbf{\Theta}(\tau)$, we have:

$$\Delta(\mathbf{\Theta}(t)) + V\mathbb{E}[y(t)|\mathbf{\Theta}(t)] \leq B + Vy^* - \epsilon \sum_{n=1}^{n=N} |\Theta_n(\tau)| \tag{1.17}$$

Then, all queues are mean rate stable. Further, if $V > 0$ and $\epsilon > 0$ then time average expected penalty and queue backlog satisfy:

$$\limsup_{t\to\infty} \frac{1}{t} \sum_{\tau=0}^{t-1} \mathbb{E}[y(\tau)] \leq y^* + \frac{B}{V} \tag{1.18}$$

$$\limsup_{t\to\infty} \frac{1}{t} \sum_{\tau=0}^{t-1} \sum_{n=1}^{N} \mathbb{E}[|\Theta_n(t)|] \leq \frac{B + V(y^* - y_{\min})}{\epsilon} \tag{1.19}$$

Finally,

- *If $V = 0$, then (1.19) still holds.*
- *If $\epsilon = 0$, then (1.18) still holds.*

Proof: See [54].

We can conclude the following strategy from theorems. The objective function (1.9a) is mapped to a penalty function. Therefore, instead of minimizing the existing problem, by using drift-plus-penalty theorem [113], the following expression is minimized greedily, subject to the known $\mathbf{\Theta}(t)$, in every time slot

$$\Delta(\mathbf{\Theta}(t)) + V\mathbb{E}[y_0(t)|\mathbf{\Theta}(t)] \tag{1.20}$$

where V is a non-negative weighted control parameter. It is easy to see that setting $V = 0$ leads the drift-plus-penalty to the drift alone problem, while $V > 0$ offers a trade-off between backlog reduction and penalty minimization. Reference [54] shows that this time average objective function deviates by at most $O(1/V)$ from optimality.

The drift-plus-penalty method can be viewed as a dual-based approach to the stochastic problem and it can be simplified to the well known dual subgradient algorithm for linear and convex problems when applied to non-stochastic problems [54, 117]. One of the advantage of the drift-plus-penalty approach is the explicit performance bound which results in $[O(1/V), O(V)]$ performance-delay trade-off.

The following theorem shows the convergence analysis and performance bound of drift-plus-penalty method, in terms of performance-delay trade-off. Let define $w(t)$ as a stationary process with distribution $\pi(w)$.

Theorem 1.3 *Suppose that $w(t)$ is i.i.d over slots with probabilities $\pi(t)$, the problem* **P1** *is feasible, and that $\mathbb{E}[L(\mathbf{\Theta}(0))] < \infty$. Fix a value $C \geq 0$. If we use the C-additive approximation* [1] *of the drift-plus-penalty algorithm every slot t, then:*

- *Time average expected cost satisfies*

$$\limsup_{t\to\infty} \frac{1}{t}\sum_{\tau=0}^{t-1} \mathbb{E}[y_0(\tau)] \leq y_0^{opt} + \frac{B+C}{V} \tag{1.21}$$

  where y_0^{opt} is the infimum time average cost achievable by any policy that meets the required constraints and B is defined as

$$\begin{aligned} B \geq \frac{1}{2}\sum_{k=0}^{K} \mathbb{E}[a_k^2(t) + b_k^2(t)|\mathbf{\Theta}(t)] + \frac{1}{2}\sum_{l=0}^{L} \mathbb{E}[y_l^2(t)|\mathbf{\Theta}(t)] \\ + \frac{1}{2}\sum_{j=0}^{J} \mathbb{E}[e_j^2(t)|\mathbf{\Theta}(t)] - \frac{1}{2}\sum_{k=0}^{K} \mathbb{E}[\tilde{b}_k(t)a_k(t)|\mathbf{\Theta}(t)] \end{aligned} \tag{1.22}$$

- *All queues are $Q_k(t)$, $Z_l(t)$ and $Hj(t)$ are mean rate stable, and all required constraints are satisfied.*

  Proof: See [54].

[1] C is a constant parameter proposed in [54] and later is considered to be zero without loss of generality.

1.4 Thesis Motivation

In reality, the statistics of the energy arrival for harvesting are difficult to obtain or predict accurately. More specifically, for practical system designs, both harvested energy and channel quality can only be acquired causally. Thus, it is both desirable and practical to design an online power control policy that only relies on the harvested energy and fading condition up to the current time without requiring their statistical knowledge. In addition, exploiting EH adds the new challenge of energy management in terms of battery operational constraints. These constraints limit the amount of energy that can be stored or drawn, and affect the performance of the wireless transmission. More precisely, the excessive energy usage may lead to future interruption in transmission due to energy outage. On the other hand, the conservative energy usage may cause to miss the recharging opportunity due to battery storage limitations. Thus, a more realistic battery operation model for energy harvesting and power supply should be considered in the power control design.

Due to the stochastic nature of EH sources, a time-dependent optimization (stochastic optimization) considering the energy storage management is required. to propose reliable power control policies for wireless networks. To the best of our knowledge, until now few works have proposed effective online power control methodologies for the wireless transmission over fading channels, specifically when the statistics of energy source are unknown. Online solutions obtained by DP [32, 33, 39–42] suffer from high computational complexity. Also, considering the fading environment is highly nontrivial in both design and performance analysis, where Lyapunov optimization technique cannot be directly applied. Therefore, a practical and easy-to-implement online power solution is required to address the unbounded fading environment. The cooperative relay network is a promising solution to overcome the fading and path-loss and to improve the performance of the wireless transmission. Online EH method along with the cooperative relay network can be

considered as a reliable solution to maximize the long-term transmission rate in wireless networks.

Furthermore, most existing works assume an infinite storage battery capacity which is not a realistic operational constraint in terms of storage and power supply. The energy storage not only provides a buffer for the harvested energy, but also is important for alleviating the impact on the system from a renewable energy source which is often stochastic and unpredictable. As a result, the power management at the transmitter is crucial for a reliable performance, and therefore an effective transmit power control design is needed to maximize the potential benefit of the energy harvesting technology.

1.5 Thesis Contributions

This dissertation focuses on designing online power control strategies for wireless systems equipped with energy harvesting and storage devices. In particular, the main objective of this work is to design power control policies to maximize the long-term average transmission rate over fading channels. The proposed algorithms do not require any statistical information of energy arrivals or fading profiles. The following presents the contributions of this dissertation:

- **Online Wireless Transmission in a Point-to-Point Channel with EH**

  First, an online power control policy is developed for a point-to-point fading channel equipped with EH and storage devices. A practical finite battery storage is considered to model the battery operational constraints on charging and power output. The statistics of energy arrivals and fading are unknown at the transmitter. The goal is to maximize the long-term time-averaged transmission rate under the battery operational constraints. The optimization problem is stochastic and technically chal-

lenging to solve. In particular, the finite battery storage capacity and operational constraints cause the power control decision coupled over time which complicates the control decision making. Leveraging Lyapunov optimization framework [54], an online power control strategy is proposed. However, applying Lyapunov technique to the problem is nontrivial. Specifically, a couple of issues cannot be directly handled by Lyapunov framework, including battery operational constraints and unbounded channel fading. A novel technique is developed to handle these challenges in the online power control problem. In the proposed methodology, transmission behavior is opportunistic in terms of the fading condition and the battery energy level, resembling a "water-filling" scheme. Although the policy focuses on a single-antenna transmission system, it is shown that the proposed online power control algorithm is applicable to general multi-antenna beamforming scenarios. An analysis is presented to show the bounded performance gap to the optimal solution.

- **Online Power Control for Two-Hop Network with EH**

  Next, an online joint power control policy is developed for a two-hop amplify-and-forward (AF) relaying network where both transmitter and relay are equipped with EH and finite storage devices. The proposed strategy aims to maximize the long-term time-averaged transmission rate of the relay network in a fading environment. The methodology does not require any the statistical information of random events including energy arrivals or fading channels over the two-hop network. The random behavior of energy arrival imposes a time-coupling among batteries and transmit powers. Specifically, the power control policy should tackle the time-dependent behavior of both transmit powers and batteries. A combined closed-form and numerical online power control solution is proposed employing Lyapunov optimization technique. The developed algorithm jointly controls the transmit power of both trans-

mitter and relay based on the current energy state of their battery levels and the fading environment. This method provides a deep insight into the energy management and transmission control actions. It is shown that the proposed strategy has a bounded performance gap to the optimal scenario. Simulation results demonstrate a significant improvement over the alternative approaches.

1.6 List of Publications

The following is the list of the publications corresponding to this thesis:

1. F. Amirnavaei and M. Dong, ”Online Power Control Optimization for Wireless Transmission with Energy Harvesting and Storage,” *IEEE Transactions on Wireless Communication*, vol. 15, pp. 4888-4901, July 2016.

2. F. Amirnavaei and M. Dong, ”Online Power Control Strategy for Wireless Transmission with Energy Harvesting,” *in Proc. IEEE Workshop on Signal Processing advances in Wireless Commun.(SPAWC)*, June 2015.

3. F. Amirnavaei and M. Dong, ”Online Power Control for Cooperative Relaying with Energy Harvesting,” *in Proc. of Asilomar Conf. on Signals, Systems and computers*, November 2015.

1.7 Thesis Outline

Chapter 2 considers a point-to-point fading channel that the transmitter is equipped with energy harvesting and storage devices. An online power control algorithm is proposed to maximize the long-term average rate under realistic battery operational dynamics and constraints for data transmission.

Chapter 3 considers a two-hop amplify and forward relay network equipped with energy harvesting and storage devices that supply power to both transmitter and relay. An online joint power control algorithm is developed for the transmitter and relay to maximize the long-term rate over two-hop fading channels.

Chapter 4 presents the conclusions and future work.

Chapter 2

Online Power Control for Point-to-Point Wireless Transmission with EH

2.1 Introduction

In this chapter, we consider a transmitter with energy harvesting and storage devices for transmission over fading channel. Assuming finite battery storage capacity, we design an online power control strategy aiming at maximizing the long-term time-averaged expected data rate. The design challenge is the coupling of control decision over times due to finite battery storage, besides unknown system statistics. Through problem transformation and Lyapunov optimization technique, we develop an online power control algorithm based on the current energy state of battery and fading condition. Our power solution does not require any statistical knowledge of energy arrivals and fading channel. The closed-form solution provides the insight of energy management and transmission control actions, and has minimum complexity for implementation. We also show that the proposed strategy has a bounded performance gap to the optimal performance. Simulation results demonstrate the significant gain under the proposed strategy over the greedy approach.

2.2 System Model

We consider a point-to-point wireless transmission system where the transmitter is equipped with energy harvesting and storage devices as illustrated in Fig. 2.1. The system operates in the discrete slotted time $t \in \{0, 1, 2, \ldots\}$ with duration Δt, and all operations are performed per time slot. The transmitter is powered by energy harvested from the environment (*e.g.*, solar, radio wave) using the harvesting device. Let $E_a(t)$ denote the amount of energy arrived at the harvesting device at time slot t, and $E_s(t)$ denote the amount of energy actually harvested into the battery at the end of time slot t. We have $E_s(t) \leq E_a(t)$. A battery storage device is used at the transmitter to store the harvested energy and to supply power for data transmission. Let $E_b(t)$ denote the energy state of battery (SOB) at the beginning of time slot t. This amount is bounded by

$$E_{\min} \leq E_b(t) \leq E_{\max}, \forall t, \tag{2.1}$$

where $E_{\min}$ and $E_{\max}$ represent the minimum and maximum energy levels allowed in the battery, respectively; their values depend on the type and size of the battery.

The battery has its maximum charging and discharging rates. Let $E_{c,\max}$ denote the maximum charging amount per slot. Let $P_{\max}$ denote the maximum transmit power that can be drawn from the battery, which should to satisfy $\Delta t P_{\max} \leq E_{\max} - E_{\min}$. In addition, we assume $E_{c,\max} \leq \Delta t P_{\max}$, *i.e.*, the maximum charging rate is less than or equal to the maximum discharging rate[1]. Let $P(t)$ denote the transmit power drawn from the battery at time slot t for data transmission, which is determined at each time slot t and remains

[1]Based on the battery technology, for current rechargeable batteries, it is typical that the maximum charging rate is less than the maximum discharging rate [118, 119].

unchanged during the time slot. It is bounded by

$$0 \leq P(t) \leq P_{\max}, \forall t. \tag{2.2}$$

In each time slot t, energy is harvested into the battery and power is drawn from the battery for transmission. The dynamics of SOB $E_b(t)$ over time slots is given by

$$E_b(t+1) = E_b(t) - \Delta t P(t) + E_s(t). \tag{2.3}$$

where by battery capacity constraint and dynamics of $E_b(t)$ in SOB, $P(t)$ should satisfy

$$\Delta t P(t) \leq E_b(t) - E_{\min}, \ \forall t. \tag{2.4}$$

The harvested energy $E_s(t)$ is determined by the amount of energy arrived, available room in the battery, and the maximum charging rate as follows

$$E_s(t) = \min\{E_{\max} - (E_b(t) - \Delta t P(t)), E_a(t), E_{c,\max}\}. \tag{2.5}$$

Remark: Note that, we assume perfect charging and discharging for the battery modeling. In practice, due to battery charging inefficiency, there is an energy loss during charging and discharging. The actual stored energy is less than the charging amount and the contributed power through discharging is larger than the actual power output. Let $\rho_c \in (0, 1]$ and $\rho_d \in [1, \infty)$ denote the charging efficiency and discharging efficiency coefficients, respectively. Considering the charging/discharging loss, the actual stored energy $E_s(t)$ is given by $E_s(t+1) = \min\{E_{\max} - (E_b(t) - \Delta t P(t)), \rho_c E_a(t+1), \rho_c E_{c,\max}\}$, and the actual contributed energy through discharging is $\rho_d \Delta t P(t)$. We assume $\rho_c = \rho_d = 1$. Our developed online power control algorithm and its analysis can be straightforwardly applied

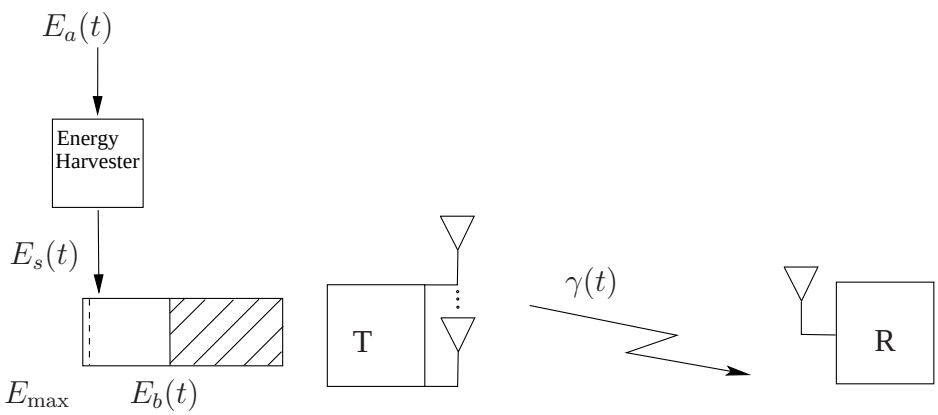

Figure 2.1: The system model with energy harvesting and storage devices.

to the battery model with general values of ρ_c and ρ_d.

For the transmission over fading, we focus on the case where both transmitter and receiver have a single antenna. In Section 2.3.5, we extend our proposed algorithm to the case of multi-antenna transmit beamforming. We assume a slow block fading scenario, where the channel, denoted by $h(t)$, is assumed to be constant during time slot t and changes over time slots. Assuming the receiver noise is additive white Gaussian noise with zero mean and variance σ_N^2, we define $\gamma(t)$ as the normalized channel gain (against receiver noise) by $\gamma(t) \triangleq |h(t)|^2/\sigma_N^2$. We assume $\gamma(t)$ is perfectly known at the transmitter at each time slot t. With transmit power $P(t)$, the instantaneous rate over the channel is given by $R(t) \triangleq \log[1 + P(t)\gamma(t)]$.

2.3 Power Control Design for Rate Maximization

Define the system state $\mathbf{s}(t) = [E_a(t), \gamma(t)]$. At the beginning of each time slot t, the transmitter observes $\mathbf{s}(t)$ and $E_b(t)$ to determine the transmit power $P(t)$ for time slot t. Our objective is to design a power control algorithm for $\{P(t)\}$ to maximize the long-term time-averaged expected rate, while satisfying the battery operational constraints. It can be formulated as the following optimization problem

$$\textbf{P1}: \quad \max_{\{P(t)\}} \lim_{T\to\infty} \frac{1}{T}\sum_{t=0}^{T-1} \mathbb{E}[R(t)]$$

$$\text{subject to} \quad 0 \le P(t) \le P_{\max},\ \forall t, \tag{2.6}$$

$$E_b(t+1) = E_b(t) - \Delta t P(t) + E_s(t), \tag{2.7}$$

$$\Delta t P(t) \le E_b(t) - E_{\min},\ \forall t, \tag{2.8}$$

where the expectation is taken with respect to the system state $\mathbf{s}(t)$.

Due to the randomness of energy arrival and fading, **P1** is a stochastic optimization problem that is challenging to solve. Furthermore, constraint (2.8) depends on the SOB $E_b(t)$, which has time-coupling dynamics over time as shown in (2.7). This results in the power control decisions $\{P(t)\}$ being correlated over time. If the random processes $\{\gamma(t)\}$ and $\{E_a(t)\}$ are Markovian and their statistics are all known, it is possible to solve **P1** through Dynamic Programming [120]. However, this approach typically faces the curse of dimensionality in computational complexity to provide a practical solution. Furthermore, in practice, the statistical information of $\{\gamma(t)\}$ and $\{E_a(t)\}$, especially the energy arrival process $\{E_a(t)\}$, is difficult to obtain ahead of time, making such an assumption less realistic.

We aim to develop an online power control algorithm without relying on the statistical knowledge of $\{\gamma(t)\}$ and $\{E_a(t)\}$. In particular, we apply the Lyapunov optimization framework [54] to design an online (sub-optimal) power control solution to **P1**. Under Lyapunov optimization, certain time-averaged constraints can be transformed into queue stability constraints and further be utilized to provide an online optimization solution. However, the transmit power constraint (2.8) on $P(t)$ is per time slot, resulting in time-coupled decision. Thus, to employ Lyapunov optimization, we first relax the per time slot constraint to

a long-term time-averaged relation between $E_b(t)$, $E_s(t)$ and $P(t)$.

2.3.1 Problem Relaxation

Define the following long-term time-averaged quantities:

$$\bar{E}_s \triangleq \lim_{T\to\infty} \frac{1}{T} \sum_{t=0}^{T-1} \mathbb{E}[E_s(t)] \tag{2.9}$$

$$\bar{P} \triangleq \lim_{T\to\infty} \frac{1}{T} \sum_{t=0}^{T-1} \mathbb{E}[P(t)] \tag{2.10}$$

We have the following long-term time-averaged relation

$$\bar{E}_s - \Delta t \bar{P} = 0. \tag{2.11}$$

To see this, note that from (2.7), the battery energy level over time T has the following relation

$$\mathbb{E}[E_b(T)] - \mathbb{E}[E_b(0)] = \sum_{t=0}^{T-1} \mathbb{E}[E_s(t) - \Delta t P(t)]. \tag{2.12}$$

By constraint (2.1), the left hand side (LHS) is bounded. Dividing both sides of (2.12) by T and taking the limit $T \to \infty$, we have (2.11). The relation in (2.11) is intuitive. It indicates that over the long run, the average energy harvested should be equal to the average energy used from the battery for transmission.

Now, replacing per-slot constraint (2.7) by the long-term time-averaged constraint (2.11), and removing battery capacity constraint (2.1), we relax the optimization problem

P1 to the following problem

$$\begin{aligned} \textbf{P2}: \quad & \max_{\{P(t)\}} \lim_{T\to\infty} \frac{1}{T}\sum_{t=0}^{T-1} \mathbb{E}[R(t)] \\ \text{subject to} \quad & 0 \le P(t) \le P_{\max},\ \forall t, \\ & \bar{E}_s - \Delta t \bar{P} = 0, \end{aligned}$$

where the dependency of power control decision $P(t)$ on $E_b(t)$ in constraint (2.8) is removed. It can be easily verified that any feasible solution to **P1** is also feasible to **P2**, but not vise versa. Thus, **P2** is indeed a relaxed problem of **P1**.

With the knowledge of only current system state $\mathbf{s}(t)$, **P2** is still challenging to solve. However, the relaxation enables us to employ the Lyapunov optimization framework to develop an online power control algorithm to solve **P2**. In the following, we develop our online algorithm. Furthermore, we will show that by our design, our proposed solution is feasible to the original problem **P1**.

2.3.2 Online Power Control via Lyapunov Optimization

We now develop an online power control algorithm to solve **P2.** Based on Lyapunov optimization [54], we introduce a virtual queue $X(t)$ for the SOB $E_b(t)$ as

$$X(t) = E_b(t) - A \tag{2.13}$$

where A is a time-independent constant. It can be shown [54] that keeping the stability of the queue $X(t)$ is equivalent to satisfying constraint (2.11). We will later determine the value of A to ensure the proposed solution is feasible to **P1**.

Since $X(t)$ is a shifted version of $E_b(t)$, by (2.7), the queuing dynamics of $X(t)$ is

given by

$$X(t+1) = X(t) - \Delta t P(t) + E_s(t). \tag{2.14}$$

Note that, although $E_b(t) \geq 0$, the value of $X(t)$ can be negative.

Define the quadratic Lyapunov function as $L(X(t)) \triangleq X^2(t)/2$. Define the per-slot Lyapunov drift, conditioned on $X(t)$ at time slot t by

$$\Delta(X(t)) \triangleq \mathbb{E}\left[L(X(t+1)) - L(X(t))|X(t)\right] \tag{2.15}$$

where the expectation is taken with respect to the random system state $\mathbf{s}(t)$. By Lyapunov optimization framework, instead of directly using the objective in **P2**, we consider the minimization of a *drift-plus-cost* metric, a technique to stabilize a queue while optimizing the time-averaged objective function. The drift-plus-cost metric is defined by

$$\Delta(X(t)) + V\mathbb{E}[-R(t)|X(t)]$$

which is a weighted sum of the per-slot Lyapunov drift $\Delta(X(t))$ and the cost function (*i.e.*, negative of the rate) conditioned on $X(t)$ with $V > 0$ being the weight.

We first provide an upper bound on the drift-plus-cost metric in the following lemma.

Lemma 2.1 *Under any control algorithm and for any values of $X(t)$ and $V \geq 0$, the drift-plus-cost expression has the following upper bound*

$$\begin{aligned} &\Delta(X(t)) - V\mathbb{E}[R(t)|X(t)] \leq \\ &B + X(t)\mathbb{E}[E_s(t) - \Delta t P(t)|X(t)] - V\mathbb{E}[R(t)|X(t)]. \end{aligned} \tag{2.16}$$

where $B \triangleq \max\{E_{c,\max},\ \Delta t P_{\max}\}^2/2$.

Proof: See Appendix 2.7.1.

Due to the dynamics involved in $\Delta X(t)$, minimizing the drift-plus-cost metric directly is still difficult. Instead, we consider minimizing its upper bound in (2.16). Specifically, we develop an online algorithm to determine $P(t)$, by minimizing the upper bound of the drift-plus-penalty in (2.16) in a *per-slot* fashion. That is, given $E_a(t), \gamma(t)$ and $X(t)$, taking the per-slot version of the upper bound in (2.16) by removing the expectation $\mathbb{E}[\cdot]$ and removing the constant B, we have the following equivalent per-slot optimization problem

$$\begin{aligned} \textbf{P3}: \min_{P(t)} \quad & X(t)[E_s(t) - \Delta t P(t)] - V \log\left(1 + P(t)\gamma(t)\right) \\ \text{subject to} \quad & 0 \leq P(t) \leq P_{\max}. \end{aligned}$$

Objective in **P3** is a summation of linear and logarithmic functions of $P(t)$, thus it is convex. Since the objective in **P3** is convex and the constraint is linear in $P(t)$, therefore **P3** is a convex optimization problem and can be solved analytically. We obtain the optimal power $P^*(t)$ in closed-form as follows.

Proposition 2.1 *The optimal transmit power $P^*(t)$ for* **P3** *is given by*

$$P^*(t) = \begin{cases} P_{\max} & \textit{for } X(t) > \frac{-V}{\Delta t(P_{\max} + \frac{1}{\gamma(t)})} \\ \frac{-V}{\Delta t X(t)} - \frac{1}{\gamma(t)} & \textit{for } \frac{-V\gamma(t)}{\Delta t} \leq X(t) \leq \frac{-V}{\Delta t(P_{\max} + \frac{1}{\gamma(t)})} \\ 0 & \textit{for } X(t) < \frac{-V\gamma(t)}{\Delta t}. \end{cases} \tag{2.17}$$

Proof: See Appendix 2.7.2.

Thus, at each time slot t, the transmitter observes the system state $\mathbf{s}(t)$ and determines the transmit power $P^*(t)$ using (2.17). It then updates $X(t)$ according to (2.14). Note that determining $P^*(t)$ does not require any statistical information of the energy arrival $E_a(t)$ or channel gain $\gamma(t)$.

As mentioned earlier, since **P2** is the relaxed problem, its solution may not be feasible to **P1**. To ensure the solution $P^*(t)$ of **P3** is feasible to **P1**, we need to guarantee the SOB $E_b(t)$ satisfies the battery capacity constraint (2.1). Recall that two parameters A and V are introduced in developing the online power solution $P^*(t)$ for **P3**. We will design the values of A and V to ensure the feasibility. However, the challenge to do so is that the normalized channel gain $\gamma(t)$ is unbounded in general for a fading channel. This prevents us to properly design A and V. To provide our online algorithm feasible to **P1**, in the following, we first consider the case where the fading channel gain is upper-bounded and derive our feasible solution. Then, we extend the solution to the case where the fading channel gain distribution has unbounded support.

2.3.3 Algorithm for Fading with Bounded Channel Gain

We first assume the channel gain $|h(t)|^2$ is upper-bounded. Consequently, the normalized channel gain $\gamma(t)$ is upper-bounded as $\gamma(t) \leq \gamma_{\max}$, where $\gamma_{\max}$ denotes the maximum gain.

As mentioned at the beginning of Section 2.3.2, maintaining the stability of $X(t)$ is equivalent to satisfying constraint (2.11). The following lemma provides the upper and lower bounds of the virtual queue $X(t)$. Define $\zeta_{\max} \triangleq \gamma_{\max}/\Delta t$.

Lemma 2.2 *With the proposed power control solution $P^*(t)$ in (2.17), the virtual queue $X(t)$ is bounded for all t as follows*

$$X_{low} \leq X(t) \leq X_{up} \tag{2.18}$$

where $X_{low} = -V\zeta_{\max} - \Delta t P_{\max}$ and $X_{up} = E_{c,\max}$.

Proof: See Appendix 2.7.3.

$$P^*(t) = \begin{cases} 0 & \text{for } E_b(t) < E_{b,\text{th1}}(t). \\ \frac{V}{\Delta t(V\zeta_{\max}+\Delta t P_{\max}+E_{\min}-E_b(t))} - \frac{1}{\gamma(t)} & \text{for } E_{b,\text{th1}}(t) \leq E_b(t) \leq E_{b,\text{th2}}(t) \\ P_{\max} & \text{for } E_b(t) > E_{b,\text{th2}}(t) \end{cases} \quad (2.21)$$

With Lemma 2.2, the following proposition provides the conditions of the shift constant A in (2.13) and the weight V for which the solution $P^*(t)$ is feasible to **P1**.

Proposition 2.2 *Assume $\gamma(t) \leq \gamma_{\max}$, $\forall t$. With the proposed online power control solution $P^*(t)$ in (2.17), if A in (2.13) is set as*

$$A = \Delta t P_{\max} + E_{\min} + V\zeta_{\max}, \quad (2.19)$$

and $V \in (0, V_{\max}]$ with

$$V_{\max} = \frac{E_{\max} - E_{\min} - E_{c,\max} - \Delta t P_{\max}}{\zeta_{\max}}, \quad (2.20)$$

then $E_b(t)$ satisfies battery capacity constraint (2.1), and the power solutions $\{P^*(t)\}$ provided by (2.17) are feasible to **P1**.

Proof: See Appendix 2.7.4.

From Proposition 2.2, substituting the expression of A in (2.19) into (2.13), we obtain the power solution $P^*(t)$ as a function of the SOB $E_b(t)$ shown in (2.21) at the top of next page, where $E_{b,\text{th1}}(t)$ and $E_{b,\text{th2}}(t)$ are two time-dependent thresholds on the battery energy level, defined by

$$E_{b,\text{th1}}(t) \triangleq \Delta t P_{\max} + E_{\min} + V\left(\zeta_{\max} - \frac{\gamma(t)}{\Delta t}\right) \quad (2.22)$$

$$E_{b,\text{th2}}(t) \triangleq \Delta t P_{\max} + E_{\min} + V\left(\zeta_{\max} - \frac{\gamma(t)}{\Delta t(P_{\max}\gamma(t)+1)}\right). \quad (2.23)$$

We summarize our proposed online power control algorithm in Algorithm 1. In addition, we provide the following remarks.

Remark 1: We see from (2.21) that the solution $P^*(t)$ in (2.21) is a three-stage solution depending on $E_b(t)$ of the battery: 1) When $E_b(t)$ is lower than certain level, the transmitter stops transmission to conserve energy for future transmission; 2) When $E_b(t)$ is sufficiently high, the maximum transmit power is used for transmission; 3) When $E_b(t)$ is between the above two energy levels, *i.e.*, the battery energy level is moderate, the transmit power is set between 0 and $P_{\max}$, depending on the current $E_b(t)$ and fading condition $\gamma(t)$.

Remark 2: In determining $P^*(t)$, the two thresholds for $E_b(t)$ depend on the normalized channel gain $\gamma(t)$ at the current time slot t. In particular, a higher value of $\gamma(t)$ (*i.e.*, good channel condition) results in lower values of the thresholds for the energy level and higher $P^*(t)$ for data transmission. On the other hand, when the channel condition is bad, the transmitter tends to conserve energy and use less power for transmission. Thus, we see that under the proposed power control algorithm, the transmission is carried out in an *opportunistic* fashion based on the channel condition. In particular, for a given $E_b(t)$ that is between the two thresholds, $P^*(t)$ in (2.21) resembles the water-filling power control strategy, where more power is allocated for a better channel condition.

To clearly demonstrate the above, consider the case when $V = V_{\max}$. The two thresholds $E_{b,\text{th1}(t)}$ and $E_{b,\text{th2}}(t)$ in (2.22) and (2.23) are respectively given by

$$E_{b,\text{th1}}(t) = E_{\max} - E_{c,\max} - \frac{\gamma(t)}{\gamma_{\max}}(E_{\max} - E_{\min} - E_{c,\max} - \Delta t P_{\max}) \tag{2.24}$$

$$E_{b,\text{th2}}(t) = E_{\max} - E_{c,\max} - \frac{\gamma(t)}{\Delta t(P_{\max}\gamma(t) + 1)}\left(E_{\max} - E_{\min} - E_{c,\max} - \Delta t P_{\max}\right). \tag{2.25}$$

We see that $E_{b,\text{th1}}(t)$ is a decreasing function of $\gamma(t)$. For $E_{b,\text{th2}}(t)$, if $\gamma(t) \gg 1/P_{\max}$, then $E_{b,\text{th2}}(t)$ is roughly constant with respect to $\gamma(t)$. The power allocation $P^*(t)$ for

Algorithm 1 Online Transmit Power Control Algorithm under Energy Harvesting ($\gamma(t) \leq \gamma_{\max}$)

Set $V \in (0, V_{\max}]$ with $V_{\max}$ given in (2.20).
At time slot t:

1: Observe the system state $\mathbf{s}(t)$.
2: Solve **P3** to obtain $P^*(t)$ as in (2.21).
3: Output transmit power solution: $P^*(t)$.

$E_{b,\text{th1}}(t) \leq E_b(t) \leq E_{b,\text{th2}}(t)$ is given by

$$P^*(t) = \frac{V_{\max}}{\Delta t(E_{\max} - E_{c,\max} - E_b(t))} - \frac{1}{\gamma(t)}. \tag{2.26}$$

It is clear that $P^*(t)$ depends on the channel condition $\gamma(t)$, and the "water line" depends on the current battery energy level $E_b(t)$. Note that the consideration of $V = V_{\max}$ is not a random choice. In Section 2.4, we will show that for the best performance, we should set $V = V_{\max}$.

Remark 4: Since $V > 0$, $V_{\max}$ in (2.20) should be positive. This means the battery energy storage capacity $E_{\max} - E_{\min}$ should be larger than the sum of maximum charging and discharging amount per slot $E_{c,\max} + \Delta t P_{\max}$. This assumption generally holds for the typical battery size and usage.

2.3.4 Algorithm for Fading with Unbounded Channel Gain

Now, we consider a more general fading scenario where the channel gain distribution has unbounded support (*e.g.*, Rayleigh fading). The normalized channel gain is unbounded, *i.e.*, $\gamma(t) < \infty$. To deal with this case, we now develop a modified algorithm from Algorithm 1 to provide a feasible power solution for the case when $\gamma(t) > \gamma_{\max}$.

Define $\mathcal{A} \triangleq [0, \gamma_{\max}]$ and $\mathcal{A}^c = (\gamma_{\max}, \infty)$. We define the case $\gamma(t) \in \mathcal{A}^c$ as an outage event. Let η denote the outage probability, *i.e.*, $\text{Prob}(\gamma(t) \in \mathcal{A}^c) = \eta$. When $\gamma(t) \in \mathcal{A}$,

Algorithm 1 still provides the feasible solution $P(t)$ to **P1**. When $\gamma(t) \in \mathcal{A}^c$, however, constraint (2.8) may be violated, and $P(t)$ in (2.21) may not be feasible. In this case, we propose the following scheme to determine $P(t)$.

Define $E_b^e(t) = E_b(t) - \Delta t P(t)$ as the SOB at the end of time slot t. Define $\bar{E}_b^e(t) \triangleq \frac{1}{t}\sum_{\tau=1}^{t} E_b^e(\tau)$ as the time-averaged $E_b^e(t)$ up to time slot t. For $\gamma(t) \in \mathcal{A}^c$ and $P^*(t)$ in (2.21) not satisfying constraint (2.8), we set the transmit power as

$$P^s(t) = \left[\frac{E_b(t) - \bar{E}_b^e(t-1)}{\Delta t}\right]^+ \tag{2.27}$$

where $[x]^+ \triangleq \max(x, 0)$.

Remark: The main idea of our scheme is that we use the time-averaged battery energy level $E_b(t)$ from the past to determine $P(t)$, so that at the end of the time slot, the battery energy level remains at its historical time-averaged level. This idea comes from the observation that in the case of $\gamma(t) \in \mathcal{A}$, our proposed algorithm under Lyapunov optimization tries to maintain the SOB $E_b(t)$ at a certain level. Thus, when the outage event occurs temporarily, we control the transmission power such that $E_b(t)$ is still roughly being maintained at its historical level as in the non-outage case. As a result, the battery energy dynamics over time will not be disturbed due to the outage event.

We summarize our online transmit power control algorithm for the general unbounded fading case in Algorithm 2. As discussed earlier, there are two main benefits provided by our proposed algorithm to improve the long-term time-averaged expected rate: 1) strategic energy conservation through energy control in the battery; 2) opportunistic transmission through power control over fading. As we will see, these benefits are evident in the simulation results in Section 2.5.

Algorithm 2 Online Transmit Power Control Algorithm under Energy Harvesting ($\gamma(t) < \infty$)

Choose η. Determine $\gamma_{\max}$ from η.
At time slot t:

1: Observe the system state $\mathbf{s}(t)$.
2: Apply Algorithm 1 to produce $P^*(t)$. Set $P^s(t) = P^*(t)$.
3: **if** $\gamma(t) \in \mathcal{A}^c$ and $P^s(t) > (E_b(t) - E_{\min})/\Delta t$ **then** obtain $P^s(t)$ as in (2.27).
4: Update $E_b^e(t) = E_b(t) - \Delta t P^s(t)$.
5: Update $\bar{E}_b^e(t) = \frac{1}{t}\left[(t-1)\bar{E}_b^e(t-1) + E_b^e(t)\right]$.
6: Output the transmit power solution $P^s(t)$.

2.3.5 Extension to Multi-antenna Beamforming Scenarios

In the above, we have focused on the single-antenna case. Our proposed algorithm can be easily extended to the scenarios of multi-antenna beamforming.For example, consider the MISO system with N transmit antennas and a single receive antenna. Under the block fading model, the channel vector between the transmitter and the receiver at time slot t is denoted by $\mathbf{h}(t) = [h_1(t), \ldots, h_N(t)]^T$. With perfect knowledge of $\mathbf{h}(t)$ at the transmitter and the optimal transmit beamforming, the normalized channel gain at time slot t is given by $\gamma(t) \triangleq ||\mathbf{h}(t)||^2/\sigma_N^2$. The instantaneous rate over the channel during time slot t has the same expression as we consider before: $R(t) = \log(1 + P(t)\gamma(t))$. Thus, the only difference is about channel gain $\gamma(t)$ and its distribution. Our proposed online algorithm (Algorithm 2) can be directly applied for this transmit beamforming scenario.

Similarly, the algorithm can be applied for the single-input multi-output (SIMO) case with receive beamforming, or MIMO beamforming. For the latter, transmit and receive beam vectors are selected as the principle right and left singular vector of the MIMO channel, denoted by $\mathbf{H}(t)$. In this case, the effective normalized channel gain is $\gamma(t) = \sigma_1^2(t)/\sigma_N^2$, where $\sigma_1^2(t)$ is the largest singular value of $\mathbf{H}(t)$. The expression of instantaneous rate $R(t)$ is still the same as before.

2.4 Performance Analysis

In this section, we analyze the performance of our proposed online power control algorithms.

2.4.1 Bounded Fading Scenario

We first consider the case where $\gamma(t) \in \mathcal{A}, \forall t$, and analyze the performance of Algorithm 1. Let $\bar{R}^s(V, \mathcal{A})$ denote the achieved objective value of **P1** under Algorithm 1. Let $\bar{R}^{\text{opt}}(\mathcal{A})$ denote the maximum objective value of **P1** under the optimal solution. The following theorem provides a bound of the performance of Algorithm 1 to $\bar{R}^{\text{opt}}(\mathcal{A})$.

Theorem 2.1 *Assume $\gamma(t) \in \mathcal{A}, \forall t$. Assume the system state $\mathbf{s}(t)$ are i.i.d over time. Under Algorithm 1, the performance is bounded from the maximum value $\bar{R}^{opt}(\mathcal{A})$ of **P1** by*

$$\bar{R}^{opt}(\mathcal{A}) - \bar{R}^s(V, \mathcal{A}) \leq \frac{B}{V} \tag{2.28}$$

where B is defined below (2.16).

Proof: See Appendix 2.7.5 .

We have the following remarks on Theorem 2.1.

Remark 1: Theorem 2.1 provides an upper bound on the gap of the long-term time-averaged expected rate of our proposed algorithm away from $\bar{R}^{\text{opt}}(\mathcal{A})$ by the optimal solution. It is in the order of $\mathcal{O}(1/V)$. Thus, larger V is desirable. However, due to battery capacity constraint, by Proposition 2.2, V has to be chosen within $(0, V_{\max}]$. Thus, to minimize the performance gap, we should always chose $V = V_{\max}$.

Remark 2: For the upper bound in (2.28), note that B is only related to the battery maximum charging and discharging rates, not the battery capacity, while $V_{\max}$ in (2.20)

increases with battery capacity. Thus, Algorithm 1 produces an asymptotic optimal solution to **P1**, as the battery storage capacity $(E_{\max} - E_{\min})$ increases .

Remark 3: Although the upper bound in (2.28) is provided under the i.i.d. assumption, the system state $\mathbf{s}(t)$ can be relaxed to accommodate the case where $\mathbf{s}(t)$ evolving in ergodic non-i.i.d. fashion. Specifically, if both normalized channel gain $\{\gamma(t)\}$ and energy arrival $\{E_a(t)\}$ processes are modeled as the finite state Markov chains, we can show a similar bound (*i.e.*, $\mathcal{O}(1/V)$) under Algorithm 1, by applying a multi-slot Lyapunov drift technique [54]. We omit details for brevity.

2.4.2 Unbounded Fading Scenario

With probability η, $\gamma(t) \in \mathcal{A}^c$. In this case, the outage event occurs, and power solution is determined differently. Let $\bar{R}^{\text{opt}}(\mathcal{A}^c)$ denote the maximum objective value of **P1** under the optimal solution and $\bar{R}^s(\mathcal{A}^c)$ denote the achieved objective using $P(t)$ in (2.27), both in the presence of the outage. The following lemma provides an upper bound on the performance when such outage occurs.

Lemma 2.3 *Assume that system state* $\mathbf{s}(t)$ *is i.i.d over time, and the channel has a normalized channel gain distribution* $f(\gamma)$*. For* $\gamma(t) \in \mathcal{A}^c$*, under Algorithm 2, the performance is bounded by*

$$\bar{R}^{opt}(\mathcal{A}^c) - \bar{R}^s(\mathcal{A}^c) \leq G \tag{2.29}$$

where constant $0 < G < \infty$ *is a function of* $f(\gamma)$ *and* $\gamma_{\max}$.

Proof: See Appendix 2.7.6 .

As indicated in Lemma 2.3, the upper bound G can be obtained for any specific channel distribution. In particular, for SIMO or MISO beamforming with channel vector $\mathbf{h}(t)$, as-

sume Rayleigh fading, *i.e.*, element $h_n(t)$ in $\mathbf{h}(t)$ is complex Gaussian with zero mean and variance σ_h^2, for $n = 1, \ldots, N$. Let $\bar{\gamma}$ represent the average received SNR per channel *i.e.*, $\mathbb{E}[|h_n(t)|^2/\sigma_N^2]$. By Lemma 2.3, we obtain the expression of G in the following corollary.

Corollary 2.1 *Assume Rayleigh fading channels. Under the assumptions of Lemma 2.3, G is given by*

$$G = C \int_{\frac{\gamma_{\max}}{\bar{\gamma}}}^{\infty} \log\left(1 + \bar{\gamma} P_{\max} \gamma\right) \gamma^{N-1} e^{-\gamma} d\gamma \tag{2.30}$$

with $C \triangleq \left[\hat{\Gamma}\left(N, \frac{\gamma_{\max}}{\bar{\gamma}}\right)\right]^{-1}$, *where* $\hat{\Gamma}(n, y) \triangleq \int_y^{\infty} x^{n-1} e^{-x} dx$ *is the upper incomplete Gamma function. In particular, for $N = 1$, we have*

$$G = \log\left(1 + P_{\max}\gamma_{\max}\right) + e^{\gamma_o} \hat{\Gamma}(0, \gamma_o) \tag{2.31}$$

where $\gamma_o \triangleq \gamma_{\max}/\bar{\gamma} + 1/(\bar{\gamma} P_{\max})$.

Proof: See Appendix 2.7.7 .

Let $\bar{R}^{\text{opt}}$ denote the the maximum objective value of **P1**. Let $\bar{R}^s(V, \eta)$ denote the achieved objective under Algorithm 2, where we emphasize the dependency of the achieved objective value on the control parameter V and the outage probability η used in our algorithm. Combining the results in Theorem 2.1 and Lemma 2.3, we have the following performance bound.

Theorem 2.2 *Assume the system state* $\mathbf{s}(t)$ *is i.i.d over time. For the fading channel with any given fading distribution, given the outage probability η, the performance under Algorithm 2 is bounded from $\bar{R}^{opt}$ by*

$$\bar{R}^{opt} - \bar{R}^s(V, \eta) \leq (1 - \eta)\frac{B}{V} + \eta G. \tag{2.32}$$

Proof: See Appendix 2.7.8.

Theorem 2.2 provides an upper bound on the performance of Algorithm 2 to the optimal solution of **P1** for Rayleigh fading scenario. The bound depends on the outage probability η we choose. So long η is chosen to be small, the effect due to outage on the bound will be small. As we will see in our simulation, the difference on the actual performance of our proposed algorithm under the bounded channel and unbounded channel is negligible, provided η is small. In Section 2.5, we show through simulation that the performance approaches to the optimal solution quickly as battery size increases.

Note that in the unbounded fading channel scenario, Algorithm 1 is used for $\gamma(t) \in \mathcal{A}$ with probability $1 - \eta$. Thus, Remarks 1 and 3 after Theorem 2.1 are also applicable to Theorem 2.2. However, due to the gap G in the case of outage $\gamma(t) \in \mathcal{A}^c$, we cannot guarantee Algorithm 2 to be asymptotically optimal for **P1**.

2.5 Simulation Results

In this section, we examine the performance of our proposed online power control algorithm. We assume that the energy arrival amount $E_a(t)$ per slot follows a compound Poisson process with a uniform distribution. We set the default Poisson arrival rate $\lambda = 0.5$ unit/slot. The amount of energy per unit is uniformly distributed between $[0, 2\alpha]J$, with the default mean amount $\alpha = 0.2J$. The battery minimum energy level is set to $E_{\min} = 0$. For the battery maximum energy level, unless specifically specified, we set the default value to $E_{\max} = 50J$. Also, the maximum charging amount per slot is $E_{c,\max} = 0.3J$, and the maximum transmission power is $P_{\max} = 0.5W$. We set time slot duration to be $\Delta t = 1$ sec.

By default, we consider single antenna $N = 1$. We generate each channel $h(t)$ as i.i.d. complex Gaussian random variable over time t with the mean normalized channel gain

$\mathbb{E}[\gamma(t)] = 10$ dB. We set the outage probability $\eta = 1\%$. This results in $\gamma_{\max} = 16.6$ dB. For comparison purpose, we consider our proposed algorithms in two fading scenarios:

(a) *Bounded fading* $\gamma(t) \leq \gamma_{\max}$: We first generate the channel as described above. If $\gamma(t) > \gamma_{\max}$, we set $\gamma(t) = \gamma_{\max}$. We apply Algorithm 1 to obtain the transmit power $P(t)$.

(b) *Unbounded fading*: The channel is generated as complex Gaussian as described above. We apply Algorithm 2 to determine the transmit power $P(t)$. For both (a) and (b), we set default $V = V_{\max}$.

To compare with other online power control algorithms, note that, as discussed in Chapter 1, existing online power control strategies ([32, 33, 39–42, 121]) are either for AWGN channels only, or based on known statistical knowledge of energy arrivals and fading channels. Also, we have a more detailed model of battery operational constraints on energy harvesting and power supply. As a result, our proposed algorithm cannot be directly compared with algorithms in [32, 33, 39–42, 121]. Nonetheless, we include a heuristic online water-filling algorithm proposed in [33] for comparison, in which the fading statistics is assumed to be known to determine the transmission power. We modify the solution to meet the battery operational constraints (2.2) and (2.5). Furthermore, for a fair comparison, we consider two alternative online algorithms that also only rely on the current system state without requiring its statistical information. The three algorithms are described below.

(c) *Energy adaptive water-filling algorithm (EAWF) [33]: Compute a cutoff fade* γ_0 *at each time slot as the solution of the following equation*

$$\int_{\gamma_0}^{\infty} \left(\frac{1}{\gamma_0} - \frac{1}{\gamma} \right) f(\gamma) d\gamma = E_b(t). \tag{2.33}$$

Then, given $\gamma(t)$, the transmission power is determined as

$$P(t) = \min\left\{\left[\frac{1}{\gamma_0} - \frac{1}{\gamma(t)}\right]^+, P_{\max}, (E_b(t) - E_{\min})/\Delta t\right\}. \tag{2.34}$$

(d) *Greedy algorithm*: At each time slot, the transmitter uses the maximum possible power based on $E_b(t)$ to maximize the transmission rate at current time slot t, *i.e.*,

$$\begin{aligned} \max_{P(t)} \quad & R(t) \\ \text{subject to} \quad & 0 \le P(t) \le P_{\max}, \ \forall t, \\ & E_b(t+1) = E_b(t) - \Delta t P(t) + E_s(t), \\ & \Delta t P(t) \le E_b(t) - E_{\min}, \forall t \end{aligned} \tag{2.35}$$

which gives $P(t) = \min\{(E_b(t) - E_{\min})/\Delta t, P_{\max}\}$.

(e) *Power halving algorithm*: At each time slot, the transmitter uses half of the maximum possible power given by the greedy algorithm in (d). Different from greedy algorithm, this simple heuristic algorithm intends to conserve harvested energy in the battery.

Note that, when implementing algorithms (c)–(e), the complex Gaussian channel is used as in (b) unbounded fading case.

Let $R^s(t)$ denote the achieved rate at time slot t. In Fig. 2.2, we plot the time-averaged expected rate $\frac{1}{T}\sum_{t=0}^{T-1} R^s(t)$, averaged over Monte Carlo runs, vs. time slots. We set $E_b(0) = E_{\max} = 50J$. As we see, with 1% outage probability setting, the performance of Algorithms 1 and 2 under the two fading scenarios (bounded and unbounded) results in nearly identical performance. Furthermore, our proposed online power control algorithm provides a significant performance improvement over all other three algorithms (c)–(e). Compared with the greedy and power halving algorithms, the achieved average rate by our Algorithm 2 is nearly 80% and 30% higher, respectively. Noticeably, compared with the

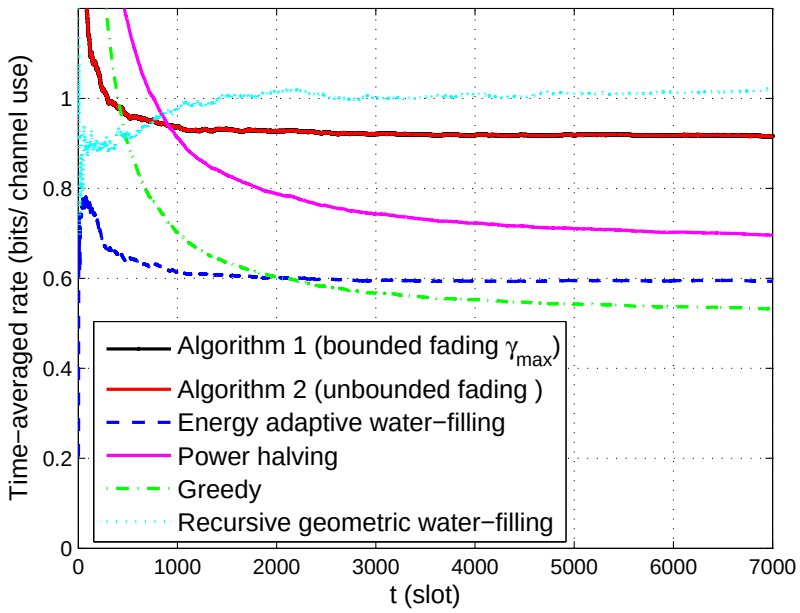

Figure 2.2: Time-averaged expected rate vs. time slot t ($E_{\max} = 50J$, $E_b(0) = E_{\max}$).

EAWF algorithm in [33] which assumes known fading statistics, Algorithm 2 still provides more than 20% improvement on the average rate without requiring any fading statistics. The performance gain of our proposed algorithm over these alternative algorithms comes from strategic energy conservation and opportunistic transmission.

The plot also shows the time-averaged expected rate for an offline optimal algorithm known as recursive geometric water-filling (RGWF) algorithm [37]. The method can be considered as an upper-bound of the time-averaged rate for $t > 1000$. As seen in Fig. 2.2, the average rate of the proposed algorithms achieves 90% of that of the RGWF. RGWF provides an optimal solution for an infinite battery capacity ($E_{\max} \gg 0$) with a known channel fading and energy arrival. This method does not consider any battery operations. The proposed algorithms, however, do not require any statical information of channel fading and energy arrival and considers a practical battery capacity ($E_{\max} = 50J$). Note that, for the $E_{\max} > 15J$, the performance of the proposed algorithms converges to that of $E_{\max} \gg 0$

(See Fig. 2.7 for further details).

Fig. 2.3 illustrates the time-averaged expected rate vs. time slot for three different channel gains with the average of $\mathbb{E}[\gamma] = \{10, 0, -10\}$ dB. In the first 3000 time slots, the average of the channel gain is $\mathbb{E}[\gamma] = 10$ dB. The average of the channel gain is $\mathbb{E}[\gamma] = 0$ dB for $t = 3000$ to $t = 6000$ and is $\mathbb{E}[\gamma] = -10$ dB for $t > 6000$. Other simulation settings are the same as the previous figures. This plot demonstrates how the performance of the algorithms evolves with the variations of the channel gain. As seen in the figure, the performance of the proposed algorithms reaches to 0.9 for $\mathbb{E}[\gamma] = 10$ dB. Once the average of the channel changes to $\mathbb{E}[\gamma] = 0$ dB, the performance of all algorithms drops significantly and then it reduces continuously. Changing the average channel gain to $\mathbb{E}[\gamma] = -10$ further reduces the average rate of all algorithms. However, the rate of change from $\mathbb{E}[\gamma] = 0$ to $\mathbb{E}[\gamma] = -10$ is not significant. As seen in the figure, the proposed algorithms outperform significantly better than all other algorithms for various fading channel statistics (average).

We repeat the experiment with a smaller battery capacity with $E_{\max} = 10J$. The initial state of battery is set to $E_b(0) = E_{\max}/2$. As shown in Figs. 2.4, similar performance comparisons after convergence can be observed. In addition, although not shown, we observe that for the same ratio of initial energy level over the battery capacity (*i.e.*, $E_b(0)/(E_{\max} - E_{\min})$), the convergence time is much shorter for a battery with smaller capacity. This behavior is intuitive since with a smaller capacity room, it takes less time slots to search for the converging energy level for $E_b(t)$ under the same system setup.

We study the dependency of power allocation by the proposed algorithm on the fading channel. For this purpose, we consider the bounded fading scenario and Algorithm 1. In Fig. 2.5, we plot the normalized channel gain $\gamma(t)$, the SOB $E_b(t)$ and thresholds $E_{b,\text{th1}}(t)$ and $E_{b,\text{th2}}(t)$, and the allocated power $P^*(t)$ by Algorithm 1 versus time slot t in the top, middle, and bottom subplots, respectively. We set $E_{\max} = 10J$. As discussed in Remarks

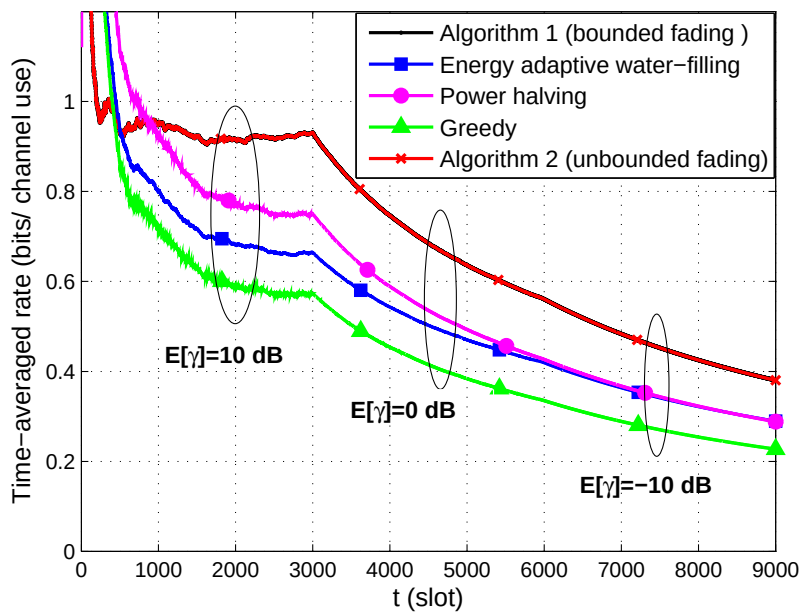

Figure 2.3: Time-averaged expected rate vs. time slot t ($E_{\max} = 50J, E_b(0) = E_{\max}$) for $\mathbb{E}[\gamma] = \{10, 0, -10\}$ dB.

3 at the end of Section 2.3.3 for $V = V_{\max}$, we see that threshold $E_{b,\text{th1}}(t)$ in (2.25) changes according to $-\gamma(t)$, while $E_{b,\text{th2}}(t)$ is roughly the constant over time. The battery energy level $E_b(t)$ roughly maintains at a level between the two thresholds. At the bottom of Fig. 2.5, we see that the power $P^*(t)$ is determined approximately according to the channel condition with a higher power for a better channel gain. This demonstrates that the transmission is opportunistic based on channel quality.

We evaluate the performance of our proposed algorithms for $V \in (0, V_{\max}]$ in Fig. 2.6. The long-term time-averaged data rate is averaged over 100 Monte Carlo runs [2]. We see that, under the proposed algorithms, the average data rate initially increases with V sharply, and then gradually converges to a stable value. This trend is consistent with results in Theorems 2.1 and 2.2, where the bounded gap to the optimal performance decreases with V. Furthermore, since the average rate quickly converges to its stable value with a relatively

[2]The mathematical expectation is calculated using Monte Carlo sampling.

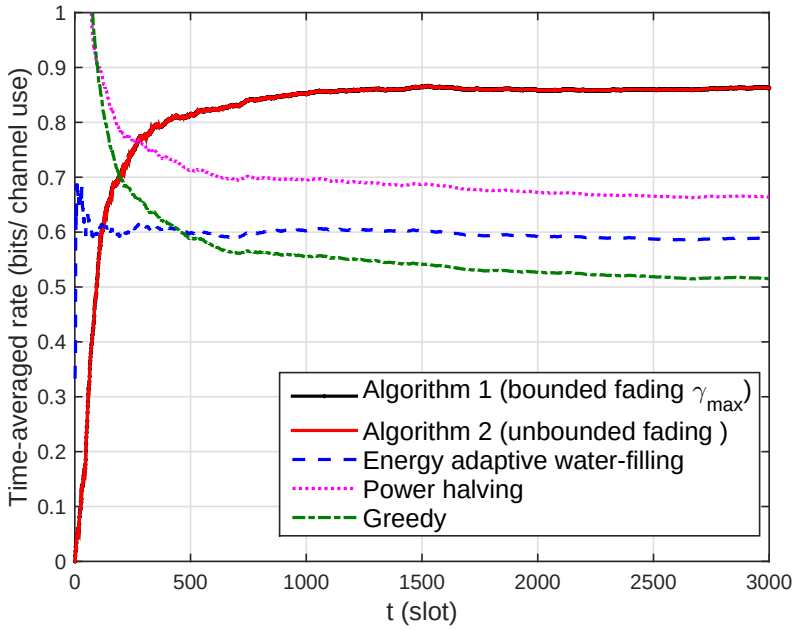

Figure 2.4: Time-averaged expected rate vs. time slot t ($E_{\max} = 10J, E_b(0) = E_{\max}/2$).

small value of V, the value of $V_{\max}$ can be relatively small. Since $V_{\max}$ is a function of battery capacity, this indicates that a smaller battery storage capacity would be sufficient to achieve a near-optimal performance. This observation is confirmed in our next study on the battery capacity. In contrast, the other three alternative algorithms does not change with V, and thus the average rate remains flat.

In Fig. 2.7, we show the long-term time-averaged expected rate under different battery capacity $E_{\max}$. We see that the performance gain over the other three alternative algorithms grows fast as the battery capacity $E_{\max}$ increases from $1J$ to $10J$ and becomes saturated afterwards. First, this demonstrates the effectiveness of our proposed online power control algorithm even for a small ratio of the battery capacity over the expected energy arrival rate $\alpha\lambda$. Second, we observe that under our proposed algorithms, the performance benefits significantly from a larger battery capacity, because the storage is crucial for better performance.

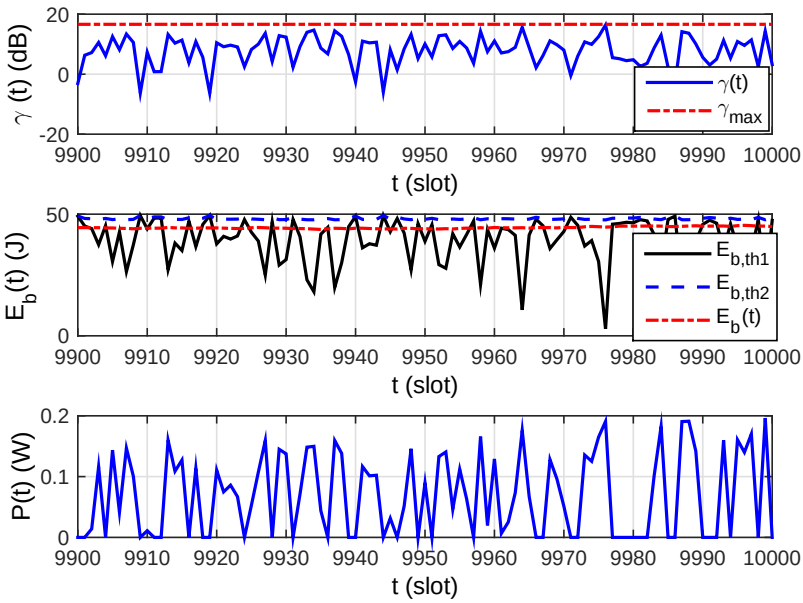

Figure 2.5: Time trajectory of system parameters: Top: $\gamma(t)$; Middle: $E_b(t)$, $E_{b,\text{th1}}(t)$, $E_{b,\text{th2}}(t)$; Bottom: $P(t)$. ($E_{\max} = 10J$)

As the battery size continues to increase, the maximum power $P_{\max}$ and charging rate $E_{c,\max}$ become the limiting factors, and as $V_{\max}$ increases with $E_{\max}$, the performance gradually converges to that of the optimal solution. This clearly shows that, under Algorithm 2, a relatively small battery storage capacity would be sufficient for a near-optimal performance. Further increasing battery size will not be effective in improving the performance. In contrast, for the greedy algorithm, due to the greedy nature, its performance is limited by $E_{c,\max}$ and $P_{\max}$, and does not change with the battery size. The same applies to the performance of the power halving and EAWF algorithms which are also unchanged with the battery size.

In Fig. 2.8, we examine the long-term average data rate under various energy arrival intensities specified by arrival rate λ and mean arrival amount α. The data rate monotonically increases with both λ and α. The rate of increment becomes smaller as α becomes larger. As more energy is stored in the battery, higher transmit power is used and the data rate is in

the non-linear region with respect to transmit power. Thus, less rate increment is observed. For the comparison purpose, the performance of the greedy algorithm is also plotted. We see the gain of our proposed algorithm over the greedy algorithm is consistent over various values of λ and α.

Next, we evaluate the performance of Algorithm 2 under different received SNR with MISO beamforming Fig. 2.9 shows the long-term time-averaged expected rate vs. the average received SNR per channel $\mathbb{E}[|h_n(t)|^2/\sigma_N^2]$, for the number of transmitter antennas $N = 1, 4$. We set $\alpha = 0.1$ and $\lambda = 0.3$. We also include the greedy and power halving algorithms for comparison. We observe that, the average rate increases with N due to the beamforming gain, as well as with SNR. As we see, Algorithm 2 outperforms both the greedy and power halving algorithms for all values of SNR and N.

In particular, as SNR becomes higher, the rate improvement by Algorithm 2 over the greedy algorithm is significantly increased. The rate improvement by Algorithm 2 over the greedy algorithm also increases with N. Comparing with the power halving algorithm, the rate improvement by Algorithm 2 is roughly consistent over SNR and N. This is because the power halving algorithm also attempt to conserve energy in the battery for the future use. This demonstrates the importance of controlling the stored energy in the battery for transmission over fading, especially as SNR and N increases.

2.6 Summary

We have designed an online transmission power control algorithm for transmission over fading with energy harvesting and storage devices at the transmitter for power supply. Aiming at maximizing the long-term time-averaged transmission rate under the battery operational constraints, we formulate the stochastic optimization problem for transmission power control. By developing a technique to transform the problem, we leverage Lyapunov

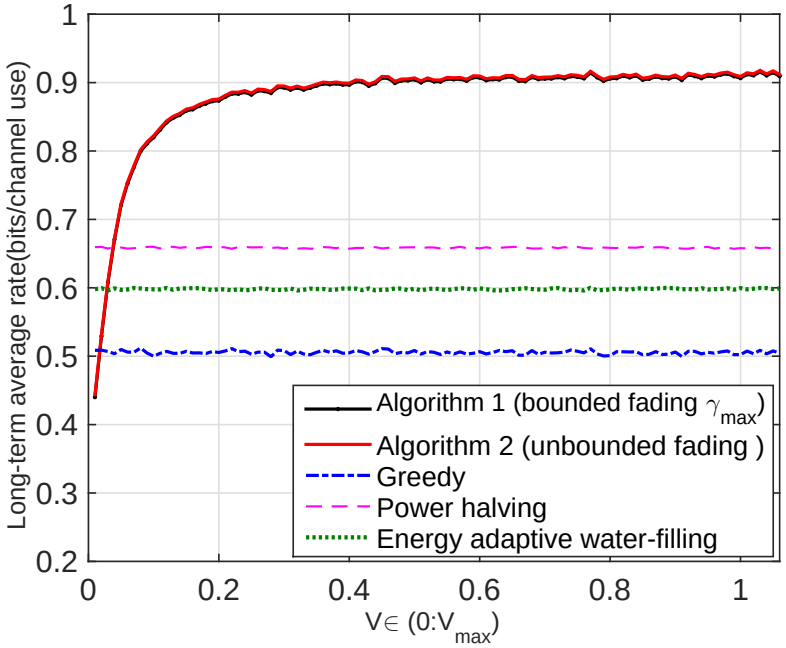

Figure 2.6: The long-term time-averaged expected rate vs. V for $V \in (0, V_{\max}]$.

optimization to propose an online power control algorithm. In particular, we develop an approach to tackle the difficulty faced in handling unbounded channel fading which otherwise cannot be dealt with directly through Lyapunov optimization. Unlike most existing online power control algorithms, our proposed algorithm only depends on the current energy arrival and channel fade condition, without requiring their statistical knowledge. In addition, our online power solution is provided in closed-form that is simple to implement. We show that our power control solution not only provides energy conservation control of the battery, but also results in an opportunistic transmission style based on fading condition, resembling a "water-filling" like solution. Through analysis, we show that our proposed algorithm provides a bounded performance gap to the optimal solution. In addition, we show that our solution applies to the general multi-antenna beamforming scenarios. Simulation studies show that our proposed online power control algorithm significantly outperforms other alternative online algorithms.

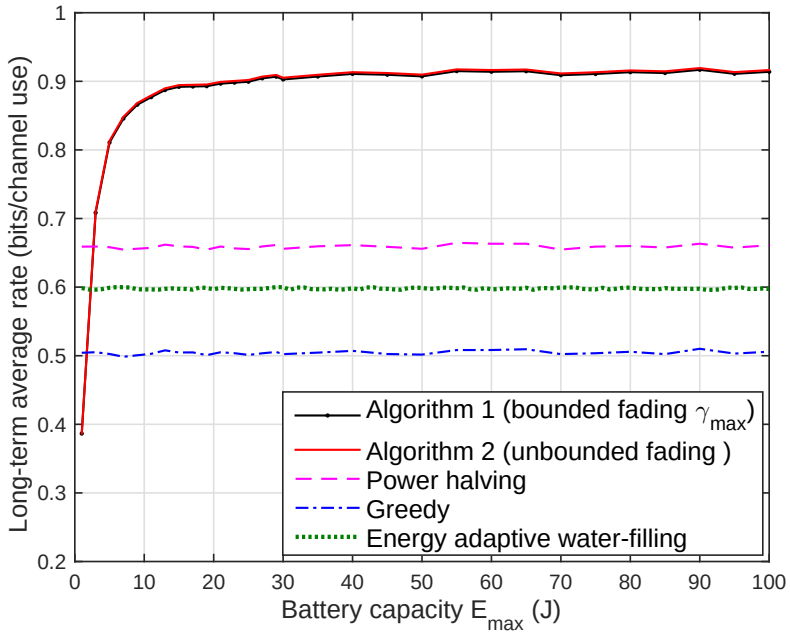

Figure 2.7: The long-term time-averaged expected rate vs. battery size $E_{\max}$.

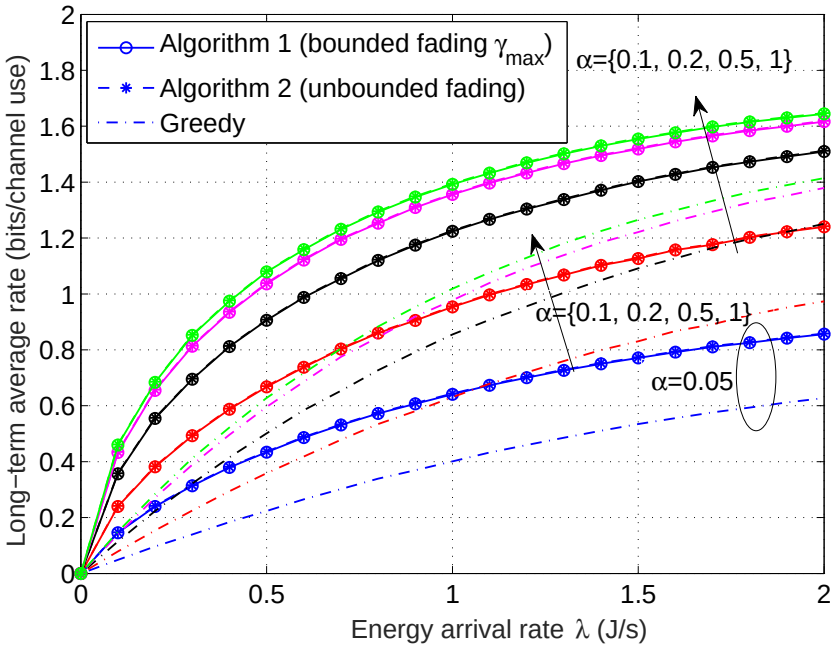

Figure 2.8: The long-term time-averaged expected rate vs. energy arrival λ.

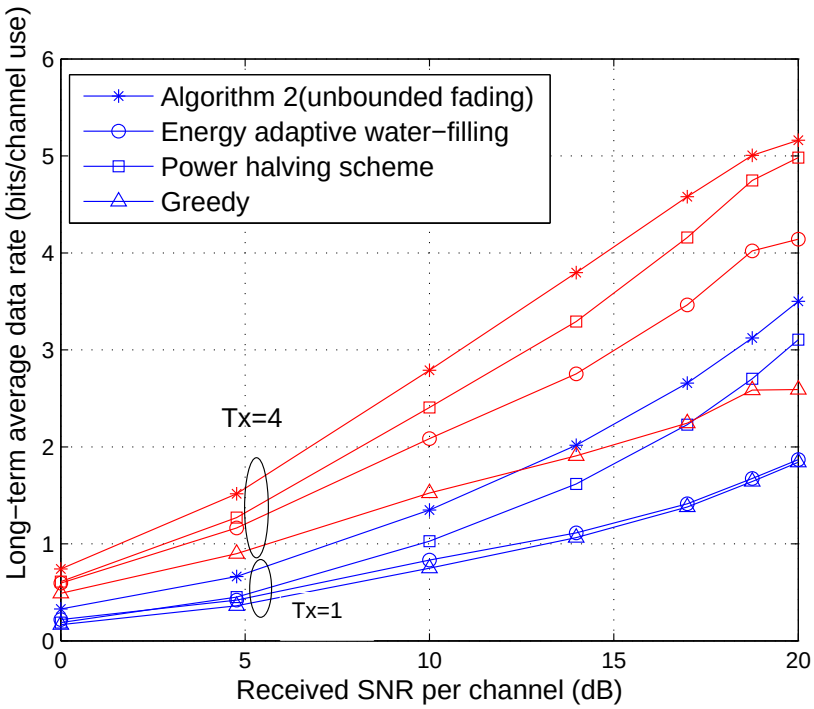

Figure 2.9: The long-term time-averaged expected rate vs. received SNR per channel.

2.7 Appendix

2.7.1 Proof of Lemma 2.1

Proof: From the dynamics of $X(t)$ in (2.14), we have

$$\begin{aligned} & L(X(t+1)) - L(X(t)) \\ &= \frac{X^2(t+1) - X^2(t)}{2} \\ &= \frac{(E_s(t) - \Delta t P(t))^2}{2} + X(t)(E_s(t) - \Delta t P(t)). \end{aligned} \tag{2.36}$$

From (2.5), we have $0 \leq E_s(t) \leq E_{c,\max}$. Along with constraint (2.6) on $P(t)$, we have

$$(E_s(t) - \Delta t P(t))^2 \leq \max\{E_{c,\max}, \Delta t P_{\max}\}^2. \tag{2.37}$$

Taking expectation at both sides of (2.36) conditioned on $X(t)$ and considering (2.37), we have the per-slot Lyapunov drift being upper bounded by

$$\begin{aligned} \Delta(X(t)) &= \mathbb{E}\left[L(t+1) - L(t)|X(t)\right] \\ &\leq B + X(t)\mathbb{E}\left[E_s(t) - \Delta t P(t)|X(t)\right] \end{aligned} \tag{2.38}$$

where $B \triangleq \max\{E_{c,\max}, \Delta t P_{\max}\}^2/2$. Adding $-V\mathbb{E}\left[R(t)|X(t)\right]$ to both sides of (2.38), we have the upper bound on the drift-plus-cost metric as in (2.16). ■

2.7.2 Proof of Proposition 2.1

Proof: Denote the objective of **P3** as $J(P(t))$

$$J(P(t)) \triangleq X(t)\left(E_s(t) - \Delta t P(t)\right) - V \log\left(1 + \gamma(t)P(t)\right).$$

Since $J(P(t))$ is convex and differentiable with respect to $P(t)$, its minimum can be found by taking derivative of $J(P(t))$ with respect to $P(t)$. Let $P'(t)$ denote the solution to $\frac{dJ(P(t))}{dP(t)} = 0$. It is given by

$$P'(t) = \frac{-V}{\Delta t X(t)} - \frac{1}{\gamma(t)}. \tag{2.39}$$

By constraint (2.6), to determine whether $P'(t)$ is an optimal solution of **P3**, we consider two cases:

2.7.2.1 If $X(t) < 0$

In this case, $J(\cdot)$ is not a monotonic function. Define $P^*(t)$ as the optimal solution of **P3**. It is determined by comparing $P'(t)$ with the two bounds 0 and $P_{\max}$ by constraint (2.6). In order for $P^*(t) = P'(t)$, it means $0 \leq P'(t) \leq P_{\max}$. By substituting $P'(t)$ in (2.39) into (2.6), the range of $X(t)$ for $P^*(t) = P'(t)$ can be found as

$$\frac{-V\gamma(t)}{\Delta t} \leq X(t) \leq \frac{-V}{\Delta t}\left(\frac{1}{P_{\max} + \frac{1}{\gamma(t)}}\right). \tag{2.40}$$

Thus, if $X(t) < \frac{-V\gamma(t)}{\Delta t}$, then $P^*(t) = 0$. If $X(t) > \frac{-V}{\Delta t}\left(\frac{1}{P_{\max}+\frac{1}{\gamma(t)}}\right)$, then $P^*(t) = P_{\max}$.

2.7.2.2 If $X(t) \geq 0$

In this case, $J(\cdot)$ is a decreasing function of $P(t)$. Since $P'(t) < 0$, it does not satisfy constraint (2.6). Therefore, the minimum value of P3 is found by $P^*(t) = P_{\max}$. ■

2.7.3 Proof of Lemma 2.2

Proof: We first present the following lemma that will be used to prove Lemma 2.2.

Lemma 2.4 *The optimal power allocation of problem* **P3** *has the following properties:*

- *If* $X(t) > 0$ *then the optimal solution always chooses* $P^*(t) = P_{\max}$.
- *If* $X(t) < -V\zeta_{\max}$ *then the optimal solution always chooses* $P^*(t) = 0$.

Proof:

Based on Proposition 2.1, we know that if $X(t) < \frac{-V\gamma(t)}{\Delta t}$, then $P^*(t) = 0$. For $\zeta_{\max} = \frac{\gamma_{\max}}{\Delta t}$, the sufficient condition for $P^*(t) = 0$ is $X(t) < -V\zeta_{\max}$. Similarly, we can derive the sufficient condition for $P^*(t) = P_{\max}$, which is $X(t) > 0$. ■

Using Lemma 2.4 and Algorithm 1, we now prove the bounds in (2.18). Note that by Lemma 2.4, when $X(t) < -V\zeta_{\max}$, in the next time slot, $X(t+1)$ in (2.14) is always increasing, *i.e.*, $X(t+1) \geq X(t)$. When $-V\zeta_{\max} \leq X(t)$, by Algorithm 1, we have $P^*(t) > 0$. From (2.14), the maximum possible decrease of $X(t)$ to $X(t+1)$ is when $P^*(t) = P_{\max}$ and $E_s(t) = 0$, *i.e.*, using maximum transmit power and no energy harvested. In this case, we have

$$X(t+1) \geq X(t) - \Delta t P_{\max} \geq -V\zeta_{\max} - \Delta t P_{\max}.$$

Since the above inequality holds for any t, we conclude that $X(t) \geq X_{\text{low}}$ where

$$X_{\text{low}} = -V\zeta_{\max} - \Delta t P_{\max}. \tag{2.41}$$

From (2.5), we have $E_s(t) \leq \min\{E_{\max} - E_b(t-1) + \Delta t P(t-1), E_{c,\max}\}$. Combining this with (2.14), we have

$$X(t+1) \leq X(t) - \Delta t P(t) + \min\{E_{\max} - X(t-1) - A + \Delta t P(t-1), E_{c,\max}\}. \tag{2.42}$$

If $X(t) > 0$, by Lemma 2.4, $P^*(t) = P_{\max}$. This means $X(t+1) \leq X(t) - \Delta t P_{\max} + E_{c,\max} \leq X(t)$. Thus, $X(t+1)$ is decreasing. If $X(t) \leq 0$, we have $P^*(t) \in [0, P_{\max})$. In this case, the maximum increase from $X(t)$ to $X(t+1)$ is when $P^*(t) = 0$ and $E_s(t) = E_{c,\max}$. In this case, we have $X(t+1) \leq X(t) + E_{c,\max} \leq E_{c,\max}, \forall t$. It follows that $X(t)$ is upper bounded as $X(t) \leq E_{c,\max} \triangleq X_{\text{up}}$. ■

2.7.4 Proof of Proposition 2.2

Proof: In order for $P^*(t)$ to be a feasible solution to **P1**, $E_b(t)$ needs to meet the battery capacity constraint (2.1). Since $X(t) \geq X_{\text{low}}$, by (2.13) and (2.41) , we have $E_b(t) - A \geq -V\zeta_{\max} - \Delta t P_{\max}$. This means $A \leq E_b(t) + V\zeta_{\max} + \Delta t P_{\max}, \forall t$. It follows that set

$$A = E_{\min} + V\zeta_{\max} + \Delta t P_{\max} \tag{2.43}$$

would satisfy the above constraint. In order for $P^*(t)$ to be feasible, it requires $X(t) = E_b(t) - A \leq E_{\max} - A$. Since $X(t) \leq X_{\text{up}} = E_{c,\max}$, the feasibility is guaranteed if $E_{c,\max} \leq E_{\max} - A$. Replacing A in this inequality by the expression in (2.43), we have

$$V \leq \frac{E_{\max} - E_{\min} - E_{c,\max} - \Delta t P_{\max}}{\zeta_{\max}}. \tag{2.44}$$

■

2.7.5 Proof of Theorem 2.1

Proof: We adopt the approach in Lyapunov optimization theory [54] to derive the bound. We first show that there exists a stationary, randomized power control policy $\{P^r(t)\}$ for **P2**, where $P^r(t)$ only depends on the current system state $\mathbf{s}(t)$, and we can

bound the expected values of the cost objective and the constraints per slot. Using these bounds and the upper bound of drift-plus-cost metric in (2.16), we derive the bound in (2.28).

The following lemma can be obtained straightforwardly from the results in [54].

Lemma 2.5 *For system state* $\mathbf{s}(t)$ *i.i.d. over time, there exists a stationary randomized power control solution* $P^r(t)$ *that only depends on the current state* $\mathbf{s}(t)$ *and guarantees*

$$\mathbb{E}_{\mathcal{A}}[R^r(t)] \triangleq \bar{R}^r(\mathcal{A}) = \bar{R}^o(\mathcal{A}), \tag{2.45}$$

$$\mathbb{E}_{\mathcal{A}}[E_s^r(t)] = \mathbb{E}_{\mathcal{A}}[\Delta t P^r(t))] \tag{2.46}$$

where $R^r(t)$ *and* $E_s^r(t)$ *are instantaneous rate and harvested energy under the stationary randomized solution,* $\mathbb{E}_{\mathcal{A}}[\cdot]$ *is taken with respect to the random system state* $\mathbf{s}(t)$ *conditioned on* $\gamma(t) \leq \gamma_{\max}$ *and the randomized power solution* $P^r(t)$*, and* $\bar{R}^r(\mathcal{A})$ *and* $\bar{R}^o(\mathcal{A})$ *are the objectives of* **P2** *achieved under* $P^r(t)$ *and under the optimal solution, respectively.*

Our proposed algorithm is to solve per slot optimization problem **P3**, which minimizes the upper bound in (2.16) over all possible power control solutions, including the optimal stationary randomized solution $P^r(t)$ in Lemma 2.5. Plugging $P^r(t)$ into the right hand side of (2.16) and by Lemma 2.5, we have

$$\begin{aligned}
&\Delta(X(t)) - V\mathbb{E}_{\mathcal{A}}[R^s(t)|X(t)] \\
&\leq B + X(t)\mathbb{E}_{\mathcal{A}}[E_s^r(t) - \Delta t P^r(t)|X(t)] - V\mathbb{E}_{\mathcal{A}}[R^r(t)|X(t)] \\
&= B + X(t)\mathbb{E}_{\mathcal{A}}[E_s^r(t) - \Delta t P^r(t)] - V\mathbb{E}_{\mathcal{A}}[R^r(t)] \\
&= B - V\bar{R}^o(\mathcal{A}) \\
&\leq B - V\bar{R}^{\text{opt}}(\mathcal{A})
\end{aligned} \tag{2.47}$$

where the first equality is due to $P^r(t)$ only depending on $\mathbf{s}(t)$, the second equality is by (2.45) and (2.46) of Lemma 2.5, and the last inequality is because **P2** is a relaxed version of **P1** and therefore we have $\bar{R}^{\text{opt}} \leq \bar{R}^o(\mathcal{A})$.

By the definition of $\Delta(X(t))$ in (2.15), taking expectations of both sides in (2.47) over $X(t)$, and summing over t from 0 to $T-1$, we have

$$\begin{aligned}
&V\sum_{t=0}^{T-1}\mathbb{E}_{\mathcal{A}}[R^s(t)] \\
&\geq TV\bar{R}^{\text{opt}}(\mathcal{A}) - TB + \mathbb{E}_{\mathcal{A}}[L(X(T))] - \mathbb{E}_{\mathcal{A}}[L(X(0))] \\
&\geq TV\bar{R}^{\text{opt}}(\mathcal{A}) - TB - \mathbb{E}_{\mathcal{A}}[L(X(0))]
\end{aligned}$$

where the last inequality is due to $L(X(T))$ being non-negative by definition. Dividing both sides by VT and taking limits over T, and noting that $L(X(0))$ is bounded, we have

$$\lim_{T\to\infty}\frac{1}{T}\sum_{t=0}^{T-1}\mathbb{E}_{\mathcal{A}}[R^s(t)] \geq \bar{R}^{\text{opt}}(\mathcal{A}) - \frac{B}{V} \tag{2.48}$$

where the left hand side of (2.48) is $\bar{R}^s(V,\mathcal{A})$. ■

2.7.6 Proof of Lemma 2.3

Proof: To find an upper bound, we know that in each time slot, an optimum rate $R^{\text{opt}}(t)$ is less or equal to the maximum achievable rate which is $R_{\max}(t)$:

$$R^{\text{opt}}(t) \leq \log\left(1 + P_{\max}\gamma(t)\right) \triangleq R_{\max}(t) \tag{2.49}$$

So (2.49) can be written as

$$R^{\text{opt}}(t) - R(t) \leq R_{\max}(t) - R(t) \tag{2.50}$$

where $R(t)$ is the instantaneous rate under random event $\gamma(t) \in \mathcal{A}^c$. RHS of (2.50) can be written as

$$R_{\max} - R(t) = \log\left(\frac{1 + P_{\max}\gamma(t)}{1 + P^s(t)\gamma(t)}\right) \tag{2.51}$$

By taking expectation of (2.50) over $\gamma(t)$ and considering (2.51), (2.50) can be written as

$$\mathbb{E}_{\mathcal{A}^c}[R^{\text{opt}}(t)] - \mathbb{E}_{\mathcal{A}^c}[R(t)] \leq \mathbb{E}_{\mathcal{A}^c}\left[\log\left(\frac{1 + P_{\max}\gamma(t)}{1 + P^s(t)\gamma(t)}\right)\right] \tag{2.52}$$

where $\mathbb{E}_{\mathcal{A}^c}[\cdot] \triangleq E[\cdot|\gamma(t) \in \mathcal{A}^c]$. Define $g(t) \triangleq \mathbb{E}_{\mathcal{A}^c}\left[\log\left(\frac{1+P_{\max}\gamma(t)}{1+P^s(t)\gamma(t)}\right)\right]$. Summing both sides of (2.52) over T, and let $T \to \infty$, we have

$$\lim_{T\to\infty} \frac{1}{T}\sum_{t=0}^{T-1} \mathbb{E}_{\mathcal{A}^c}[R(t)] \geq \bar{R}^{\text{opt}} - g(t) \tag{2.53}$$

where LHS of (2.53) is $\bar{R}^s(\mathcal{A}^c)$. From the definition of $g(t)$, we have

$$\begin{aligned} g(t) &= \int_{\gamma_{\max}}^{\infty} \log\left(\frac{1 + P_{\max}\gamma}{1 + P_{\mathcal{A}^c}(t)\gamma}\right) f(\gamma|\gamma > \gamma_{\max}) d\gamma \\ &\leq \int_{\gamma_{\max}}^{\infty} \log\left(1 + P_{\max}\gamma\right) f(\gamma|\gamma > \gamma_{\max})\, d\gamma \\ &= \frac{1}{1 - F(\gamma_{\max})} \int_{\gamma_{\max}}^{\infty} \log\left(1 + P_{\max}\gamma\right) f(\gamma) d\gamma \\ &\triangleq G \end{aligned} \tag{2.54}$$

where for simplicity, we let $\gamma(t) = \gamma$, and $f(\gamma|\gamma > \gamma_{\max})$ denotes the conditional probability density function (pdf); also, $F(\gamma_{\max}) = \text{Prob}(\gamma \leq \gamma_{\max})$, *i.e.*, the cumulative distribution function (cdf) of γ. Note that $G < \infty$ since the integration in the second equality is finite. Thus, combining (2.53) and (2.54), we have $\bar{R}^s(\mathcal{A}^c) \geq R^{\text{opt}} - G$ as in (2.29). ■

2.7.7 Proof of Corollary 2.1

Proof: Note that for $h_n(t)$ being complex Gaussian with variance σ_h^2, for $n = 1, \cdots, N$, $\gamma(t)$ has the χ-square distribution with $2N$ degree of freedom. Thus, we have

$$\begin{aligned} f(\gamma) &= \frac{1}{\bar{\gamma}^N (N-1)!} \gamma^{N-1} e^{-\frac{\gamma}{\bar{\gamma}}} \\ 1 - F(\gamma_{\max}) &= \frac{1}{(N-1)!} \hat{\Gamma}(N, \frac{\gamma_{\max}}{\bar{\gamma}}). \end{aligned} \tag{2.55}$$

where $\hat{\Gamma}(n, y) \triangleq \int_y^\infty x^{n-1} e^{-x} dx$. The upper bound G of $g(t)$ is given by

$$G = C \int_{\frac{\gamma_{\max}}{\bar{\gamma}}}^{\infty} \log\left(1 + \bar{\gamma} P_{\max} \gamma\right) \gamma^{N-1} e^{-\gamma} d\gamma$$

as shown in (2.30), where $C \triangleq \left[\hat{\Gamma}\left(N, \frac{\gamma_{\max}}{\bar{\gamma}}\right)\right]^{-1}$. A special case is when $N = 1$. The channel has a Rayleigh fading and $\gamma(t)$ has an exponential distribution. Therefore,

$$\frac{f(\gamma)}{1 - F(\gamma_{\max})} = \frac{1}{\bar{\gamma}} e^{-\frac{\gamma}{\bar{\gamma}} + \frac{\gamma_{\max}}{\bar{\gamma}}}. \tag{2.56}$$

It follows that

$$G = \frac{1}{\bar{\gamma}} e^{\frac{\gamma_{\max}}{\bar{\gamma}}} \int_{\gamma_{\max}}^{\infty} \log\left(1 + P_{\max} \gamma\right) e^{-\frac{\gamma}{\bar{\gamma}}} d\gamma. \tag{2.57}$$

By using integral by part, we have

$$\frac{1}{\bar{\gamma}}\int_{\gamma_{\max}}^{\infty}\log\left(1+P_{\max}\gamma\right)e^{-\gamma/\bar{\gamma}}d\gamma=\log(1+P_{\max}\gamma_{\max})e^{-\frac{\gamma_{\max}}{\bar{\gamma}}}+\int_{\frac{\gamma_{\max}}{\bar{\gamma}}}^{\infty}\frac{\bar{\gamma}P_{\max}}{1+\bar{\gamma}P_{\max}\gamma}e^{-\gamma}d\gamma$$

For the second term above, we use the following result

$$\int_{u}^{\infty}\frac{1}{\beta+x}e^{-x}dx=e^{\beta}\hat{\Gamma}(0,u+\beta) \tag{2.58}$$

Thus, we have G as in (2.31) ■

2.7.8 Proof of Theorem 2.2

Proof: The achieved long-term time-averaged expected rate under Algorithm 2 can be written as

$$\bar{R}^{s}(V,\eta)=(1-\eta)\bar{R}^{s}(V,\mathcal{A})+\eta\bar{R}^{s}(\mathcal{A}^{c}) \tag{2.59}$$

where $\bar{R}^{s}(V,\eta)=\lim_{T\to\infty}\frac{1}{T}\sum_{t=0}^{T-1}\mathbb{E}[R(t)]$. Also, the optimal solution of **P1** can be written as

$$\bar{R}^{\text{opt}}=(1-\eta)\bar{R}^{\text{opt}}(\mathcal{A})+\eta\bar{R}^{\text{opt}}(\mathcal{A}^{c}) \tag{2.60}$$

By subtracting (2.59) from (2.60), we can write

$$\begin{aligned}\bar{R}^{\text{opt}}-\bar{R}^{s}(V,\eta)=(1-\eta)&\left(\bar{R}^{\text{opt}}(\mathcal{A})-\bar{R}^{s}(V,\mathcal{A})\right)\\&+\eta\left(\bar{R}^{\text{opt}}(\mathcal{A}^{c})-\bar{R}^{s}(\mathcal{A}^{c})\right).\end{aligned} \tag{2.61}$$

Combining the results of Theorems 2.1 and 2.2 , the performance gap of Algorithm 2 to the optimal solution for **P1** in (2.32) follows. ■

Chapter 3

Online Joint Power Control in EH Relay Network

3.1 Introduction

In this chapter, we consider a two-hop amplify and forward (AF) relay network equipped with energy harvesters and batteries in the fading environment. We assume the statistics of energy arrivals and fading are unknown at the transmitter and relay. Our objective is to maximize the log-term time-averaged expected rate in a two-hop network with finite batteries. We design an online joint power control strategy. Using Lyapunov optimization technique, we develop an algorithm to determine joint transmit powers of the transmitter and relay based on the current energy level of the batteries and channel fade conditions. The joint power control algorithm is provided in a closed form and numerically. We propose a scheme to tackle the problem of unbounded fading channels that cannot be addressed with Lyapunov technique directly. We further bound the performance of the proposed algorithm to that of the optimal solution.

3.2 System Model

We consider a half duplex two-hop AF relaying network consisted of a pair of source and destination nodes and a relay, as illustrated in Fig. 3.1. We assume the source and destination are far apart and no direct link is assumed from the source to the destination. The system operates in a slotted time $t \in \{0, 1, 2, ...\}$ with slot duration Δt. The channel coefficients on the first and second hops are denoted by $h_s(t)$ and $h_r(t)$, respectively. We assume a slow block fading scenario, where $h_s(t)$ and $h_r(t)$ remain unchanged during time slot t and change from slot to slot. Assuming the receiver noise at the relay and the destination are additive white Gaussian with zero mean and variance $\sigma_s^2 = \sigma_r^2 = 1$, we define $\gamma_s(t)$ and $\gamma_r(t)$ as the normalized channel gain given by $\gamma_i(t) \triangleq |h_i(t)|^2/\sigma_i^2 = |h_i(t)|^2$, where $i = s, r$ is the node index denoting the source or the relay. In addition, we assume the channel gains are known at both the source and the relay in every time slot.

We assume the source and the relay are stand-alone devices powered by the energy harvesting and storage devices. Let $E_a^s(t)$ and $E_a^r(t)$ be the amount of energy arrived at the harvesting device of the source and the relay, respectively, at the end of time slot t. Let $E_h^s(t)$ and $E_h^r(t)$ be the amount of energy harvested into the battery of at the source and the relay, respectively, at the end of time slot t. We have $E_h^i(t) \in [0, E_a^i(t)]$, where $i = s, r$. A battery storage unit is used at the source and the relay to store the harvested energy and supply power for data transmission in each hop. Let $E_b^s(t)$ and $E_b^r(t)$ be battery energy level at the source and the relay at the beginning of time slot t, which are bounded by the battery storage capacity as

$$E_{\min} \leq E_b^i(t) \leq E_{\max}, \quad i = s, r \tag{3.1}$$

where $E_{\min}$ and $E_{\max}$ represent the minimum and maximum energy levels allowed in the

battery, which depend on the battery specifications.

Each battery has its own charging and discharging rate limit. In the thesis, we assume identical storage batteries at the source and the relay. [1] Let $E_{c,\max}$ be the maximum charging amount per slot and $P_{\max}$ the maximum transmit power drawn from the battery. [2] At time slot t, the transmission power at the source and the relay, denoted by $P_s(t)$ and $P_r(t)$, respectively, should satisfy

$$0 \leq P_i(t) \leq P_{\max}, \quad i = s, r. \tag{3.2}$$

By the battery capacity constraint (3.1), $P_i(t)$ should also satisfy

$$0 \leq \Delta t P_i(t) \leq E_b^i(t) - E_{\min}, \quad i = s, r. \tag{3.3}$$

The energy level in each battery $E_b^i(t)$ evolves over time as follows

$$E_b^i(t+1) = E_b^i(t) - \Delta t P_i(t) + E_h^i(t)\ , \quad i = s, r, \tag{3.4}$$

where the harvested energy $E_h^i(t)$ depends on energy arrival and $E_{c,\max}$ and available room in the battery as

$$E_h^i(t) = \min\{E_{\max} - (E_b^i(t) - \Delta t P_i(t)), E_a^i(t), E_{c,\max}\}. \tag{3.5}$$

By the AF relaying strategy, the received SNR at the destination at time slot t is given

[1] Extension to different batteries at each node is straightforward.
[2] It is clear that the maximum power satisfies $\Delta t P_{\max} \leq E_{\max} - E_{\min}$

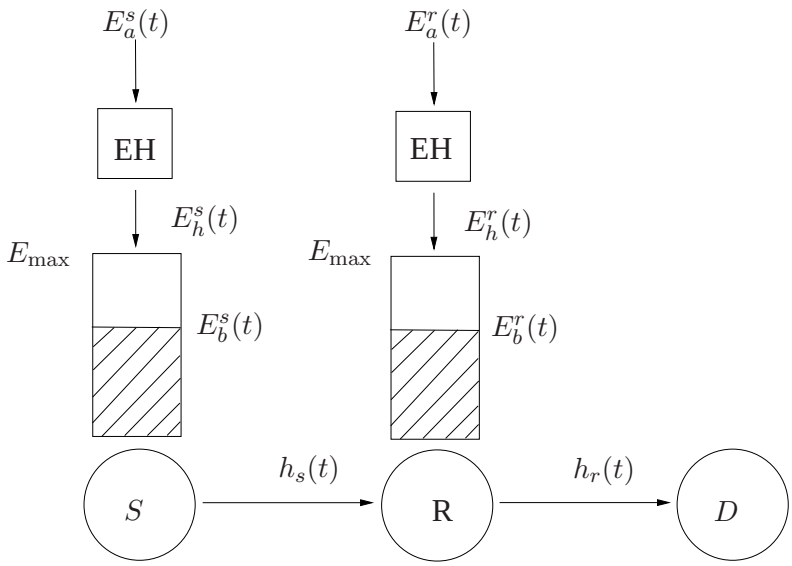

Figure 3.1: A two-hop network with energy harvesting and storage devices.

by

$$\text{SNR}_d(t) = \frac{\gamma_s(t)\gamma_r(t)P_s(t)P_r(t)}{\gamma_r(t)P_r(t) + \gamma_s(t)P_s(t) + 1}. \tag{3.6}$$

in which it is assumed that $\sigma_s^2 = \sigma_r^2 = 1$. The instantaneous rate at time slot t is given by $R(t) \triangleq \frac{1}{2}\log\left(1 + \text{SNR}_d(t)\right)$.

3.3 Long-Term Rate Maximization

At the beginning of time slot t, the relay network system state is given by

$$\mathbf{s}(t) \triangleq [\gamma_s(t), \gamma_r(t), E_a^s(t), E_a^r(t), E_b^s(t), E_b^r(t)]. \tag{3.7}$$

Our objective is to design a joint power control policy, *i.e.*, a mapping $\pi(t) : \mathbf{s}(t) \rightarrow \{P_s(t), P_r(t)\}$, to maximize the long-term time-averaged expected data rate, while satisfying all the battery operation constraints at the source and the relay. The joint optimization

problem is given by

$$\begin{aligned}
\textbf{P1}: \max_{\{P_s(t),P_r(t)\}} \lim_{T\to\infty} \frac{1}{T}\sum_{t=0}^{T} \mathbb{E}[R(t)] \\
\text{subject to } 0 \le P_i(t) \le P_{\max}, \quad i=s,r \\
0 \le \Delta t P_i(t) \le E_b^i(t) - E_{\min}, \quad i=s,r. \\
E_b^i(t+1) = E_b^i(t) - \Delta t P_i(t) + E_h^i(t)\ , \quad i=s,r,
\end{aligned}$$

where $\mathbb{E}[\cdot]$ is the expectation taken with respect to $\gamma_s(t)$, $\gamma_r(t)$, $E_a^s(t)$, and $E_a^r(t)$.

In practice, the distribution or statistics of the energy arrivals $\{E_a^s(t)\}$ and $\{E_a^r(t)\}$ are difficult to predict. This makes the existing methods relying on the distribution of system inputs difficult to apply (*e.g.*, Dynamic Programming). Instead, we develop an online power control policy which does not require the distribution or statistics of the energy arrivals $\{E_a^i(t), i=s,r\}$ and channel gains $\{\gamma_i(t), i=s,r\}$.

P1 is a joint stochastic optimization problem which is difficult to solve. The control decisions $P_s(t)$ and $P_r(t)$ are correlated over time, because $E_b^s(t)$ and $E_b^r(t)$ in (3.4) are coupled over time as a result of the finite transmit power constraint (3.1). To handle this, we first relax the per time slot battery capacity constraint (3.3) to a long-term time-averaged energy input and output relation. This enables us to employ Lyapunov optimization to design an online control policy. From (3.4), the expected battery energy level and the expected energy input and output over time duration T have the following relation

$$\mathbb{E}[E_b^i(T)] - \mathbb{E}[E_b^i(0)] = \sum_{t=0}^{T-1} \mathbb{E}[E_h^i(t) - \Delta t P_i(t)], \quad i=s,r. \tag{3.8}$$

By (3.1), the left hand side of (3.8) is bounded. Dividing both sides of (3.8) by T and taking the limit $T\to\infty$, we arrive at a long-term time-averaged battery energy input and output

relation

$$\bar{E}_h^i - \Delta t \bar{P}_i = 0, \quad i = s, r \tag{3.9}$$

where $\bar{E}_h^i \triangleq \lim_{T\to\infty} \frac{1}{T} \sum_{t=0}^{T-1} \mathbb{E}[E_h^i(t)]$ and $\bar{P}_i \triangleq \lim_{T\to\infty} \frac{1}{T} \sum_{t=0}^{T-1} \mathbb{E}[P_i(t)]$, $i = s, r$. **P1** is now relaxed to the following problem

$$\begin{aligned} \textbf{P2}: \max_{\{P_s(t), P_r(t)\}} \lim_{T\to\infty} \frac{1}{T} \sum_{t=0}^{T-1} \mathbb{E}[R(t)] \\ \text{subject to } \ 0 \le P_i(t) \le P_{\max}, \quad i = s, r, \\ \bar{E}_h^i = \Delta t \bar{P}_i. \end{aligned}$$

where per slot power constraint (3.3) is replaced by time averaged power constraint (3.9). As a result, per slot battery capacity constraint (3.1) is removed. Note that since the power control decision $P_s(t)$ and $P_r(t)$ on $E_b^s(t)$ and $E_b^r(t)$ are removed, **P2** is the relaxed problem of **P1**. Thus, any feasible solution to **P1** is also feasible to **P2**, but not vise versa. In fact, **P2** is still a challenging joint stochastic problem to solve. In following, we first develop an online power control policy to find a solution for **P2** by using Lyapunov optimization [54]. We then design the system parameters to ensure that our proposed solution is feasible to **P1**.

3.4 Online Control Policy via Lyapunov Optimization

We now apply Lyapunov optimization to develop an online power control algorithm to solve **P2**. We first define two virtual queues for the battery energy levels $E_b^s(t)$ and $E_b^r(t)$

at the source and the relay, respectively, as

$$X_i(t) \triangleq E_b^i(t) - A_i \ , \quad i = s, r, \tag{3.10}$$

where A_i, $i = s, r$, are constants. The value of A_i will be determined later to ensure the solution being feasible to **P1**. Since $X_i(t)$ is a shifted version of $E_b^i(t)$, from (3.4), the queue $X_i(t)$ evolves over time as

$$X_i(t+1) = X_i(t) - \Delta t P_i(t) + E_h^i(t) \quad i = s, r. \tag{3.11}$$

The purpose of introducing virtual queues $X_i(t)$'s is to enforce constraint (3.9) to be met through Lyapunov optimization. Let $\mathbf{X}(t) \triangleq [X_s(t), X_r(t)]$. Define the quadratic Lyapunov function as

$$L(\mathbf{X}(t)) \triangleq \frac{1}{2}(X_s^2(t) + X_r^2(t)). \tag{3.12}$$

Define a per-slot Lyapunov drift, conditioned on $\mathbf{X}(t)$ at time slot t, as

$$\Delta(\mathbf{X}(t)) \triangleq \mathbb{E}[L(\mathbf{X}(t+1)) - L(\mathbf{X}(t))|\mathbf{X}(t)], \tag{3.13}$$

where $\mathbb{E}[\cdot]$ is taken with respect to the system random inputs $\gamma_s(t)$, $\gamma_r(t)$, $E_a^s(t)$, and $E_a^r(t)$.

By the Lyapunov optimization framework, instead of using the objective in **P2**, we minimize a *drift-plus-cost* metric. The drift-plus-cost metric consists of the weighted sum of the per-slot Lyapunov drift $\Delta(\mathbf{X}(t))$ and the cost objective function (the negative of the rate), conditioned on $X_s(t)$ and $X_r(t)$ given by $\Delta(\mathbf{X}(t)) - 2V\mathbb{E}\left[R(t)|\mathbf{X}(t)\right]$, where $V > 0$ is the weight between the drift and the cost. Note that factor 2 is used to cancel out factor $1/2$ in $R(t)$ to simply our derivation later. It does not affect our solution.

3.4.1 Transformation to Online Optimization

We now provide an upper bound on the drift-plus-cost metric, which enables us to design online joint power control algorithm.

Lemma 3.1 *Under any control policy and for any queue lengths $X_s(t)$ and $X_r(t)$, the drift-plus-cost metric is upper bounded by*

$$\Delta\left(\mathbf{X}(t)\right) - V\mathbb{E}\left[R(t)|\mathbf{X}(t)\right] \leq B + \sum_{i=s,r} X_i(t)\mathbb{E}[E_h^i(t) - \Delta t P_i(t)|\mathbf{X}(t)] - V\mathbb{E}[R(t)|\mathbf{X}(t)] \tag{3.14}$$

where $B \triangleq \max\{E_{c,\max}^2, (\Delta t P_{\max})^2\}/2$.

Proof: See Appendix 3.8.1.

Considering the upper bound in (3.14) on the drift-plus-cost metric, we design an online control policy to minimize it *per slot* by removing the expectation. Let $\mathbf{P}(t) \triangleq [P_s(t), P_r(t)]$. The per-slot optimization is given by the following problem

$$\textbf{P3}: \min_{\mathbf{P}(t)} \sum_{i=s,r} X_i(t)(E_h^i(t) - \Delta t P_i(t)) - V\log\left(1 + \frac{\gamma_s(t)\gamma_r(t)P_s(t)P_r(t)}{\gamma_r(t)P_r(t) + \gamma_s(t)P_s(t) + 1}\right)$$

$$\text{subject to} \quad 0 \leq P_s(t) \leq P_{\max},\ 0 \leq P_r(t) \leq P_{\max}.$$

where we have removed the constant terms in the upper bound on the drift-plus-cost metric to arrive at the objective expression in **P3**. Note that the objective of **P3** is not jointly convex with respect to $P_s(t)$ and $P_r(t)$. By approximating the last term in the objective, the

rate, with its upper bound, we modify **P3** into a jointly convex problem as follows

$$\textbf{P3}' : \min_{\mathbf{P}(t)} \sum_{i=s,r} X_i(t)(E_h^i(t) - \Delta t P_i(t)) - V \log\left(1 + \frac{\gamma_s(t)\gamma_r(t)P_s(t)P_r(t)}{\gamma_r(t)P_r(t) + \gamma_s(t)P_s(t)}\right)$$

$$\text{subject to} \quad 0 \le P_s(t) \le P_{\max},\ 0 \le P_r(t) \le P_{\max}.$$

Comparing **P3**′ and **P3**, **P3**′ is minimizing a lower bound of the objective of **P3**. Furthermore, the bound is tight when the received SNR at either hop is high. In the following, we show that **P3**′ is a convex optimization problem. Denote the objective of **P3**′ by $f(\mathbf{P}(t))$.

For notational convenience, we remove (t) from $P_i(t)$, $X_i(t)$ and $\gamma_i(t)$ for $i = s, r$ in the following equations. To verify that the objective function $f(\mathbf{P}(t))$ is convex, first we write the Hessian matrix of f as follows

$$\nabla^2 f = \begin{bmatrix} \frac{\partial^2 f}{\partial P_s^2} & \frac{\partial^2 f}{\partial P_s \partial P_r} \\ \frac{\partial^2 f}{\partial P_r \partial P_s} & \frac{\partial^2 f}{\partial P_r^2} \end{bmatrix} \tag{3.15}$$

where

$$\frac{\partial^2 f}{\partial P_s^2} = V(\gamma_s\gamma_r P_r)^2 \frac{2(\gamma_s\gamma_r P_s P_r + \gamma_r P_r + \gamma_s P_s) + (\gamma_r P_r)^2}{(\gamma_r P_r + \gamma_s P_s)^2(\gamma_r P_r + \gamma_s P_s + \gamma_s\gamma_r P_s P_r)^2}, \tag{3.16}$$

$$\begin{aligned} \frac{\partial^2 f}{\partial P_s \partial P_r} &= -V \frac{2\gamma_s\gamma_r^2 P_r}{(\gamma_r P_r + \gamma_s P_s)(\gamma_r P_r + \gamma_s P_s + \gamma_s\gamma_r P_s P_r)} \\ &\quad + \frac{(\gamma_r P_r)^2 \gamma_s\gamma_r \left((\gamma_r P_r + \gamma_s P_s + \gamma_s\gamma_r P_s P_r) + (\gamma_r P_r + \gamma_s P_s)(\gamma_s P_s + 1)\right)}{(\gamma_r P_r + \gamma_s P_s)^2(\gamma_r P_r + \gamma_s P_s + \gamma_s\gamma_r P_s P_r)^2}. \end{aligned} \tag{3.17}$$

It can be seen that the Hessian matrix is symmetric and its determinant is as follows

$$\det(\nabla^2 f) = \frac{2(VP_rP_s)^2(\gamma_s\gamma_r)^4}{(P_s\gamma_s + P_r\gamma_r)^2(P_s\gamma_s + P_r\gamma_r + P_sP_r\gamma_s\gamma_r)^3}. \tag{3.18}$$

Since $\frac{\partial^2 f}{\partial P_s^2} \geq 0$ and $\det(\nabla^2 f) \geq 0$, the Hessian matrix is positive semi definite [122]. Therefore, we conclude that the $f(\mathbf{P}(t))$ is a convex function with respect to $P_s(t)$ and $P_r(t)$. As the constraints are linear functions, **P**3′ is a joint optimization problem [123].

Since **P3′** is convex, we obtain the optimal $P_s^*(t)$ and $P_r^*(t)$ by analyzing the partial derivative of $f(\mathbf{P}(t))$ and considering the range constraint (3.2). Denote $\hat{R} \triangleq \log\left(1 + \frac{\gamma_s(t)\gamma_r(t)P_s(t)P_r(t)}{\gamma_r(t)P_r(t)+\gamma_s(t)P_s(t)}\right)$. Depending on the sign of $X_s(t)$ and $X_r(t)$, we have the following four cases.

3.4.1.1 Case 1: $X_s(t) \geq 0$ and $X_r(t) \geq 0$

Taking partial derivative of $f(\mathbf{P}(t))$ with respect to $P_i(t)$, $i = s, r$, we have

$$\frac{\partial f(\mathbf{P}(t))}{\partial P_i(t)} = -\Delta t X_i(t) - V\frac{\partial \hat{R}}{\partial P_i(t)}, \quad i = s, r. \tag{3.19}$$

It is easy to verify that $\partial\hat{R}/\partial P_i(t) \geq 0$. Since $X_i(t) \geq 0$ and $V \geq 0$, we have $\partial f(\mathbf{P}(t))/\partial P_i(t) \leq 0$. Thus, given $P_r(t)$, $f(\mathbf{P}(t))$ is a decreasing function of $P_s(t)$, and vise versa. Therefore, $P_s^*(t) = P_r^*(t) = P_{\max}$.

3.4.1.2 Case 2: $X_s(t) \geq 0$ and $X_r(t) < 0$

From the discussion in Case 1, when $X_s(t) \geq 0$, we have $P_s^*(t) = P_{\max}$. With $P_s^*(t) = P_{\max}$ in $f(\mathbf{P}(t))$, we have

$$f([P_{\max}, P_r(t)]) = X_s(t)(E_h^s(t) - \Delta t P_{\max}) + X_r(t)(E_h^r(t) - \Delta t P_r(t)) - V\hat{R}_r(t) \tag{3.20}$$

where $\hat{R}_r(t) \triangleq \log\left(1 + \frac{\gamma_s(t)\gamma_r(t)P_{\max}P_r(t)}{\gamma_r(t)P_r(t)+\gamma_s(t)P_{\max}}\right)$. For $X_r(t) < 0$, $\partial f(\mathbf{P}(t))/\partial P_r(t)$ in (3.19) is no longer monotonic in $P_r(t)$. The root of $\partial f([P_{\max}, P_r(t)])/\partial P_r(t) = 0$, denoted by $P_r^o(t)$, is derived as

$$P_r^o(t) = \frac{\eta_s(t)P_{\max}}{2(1+\gamma_s(t)P_{\max})}\left(-(2+\gamma_s(t)P_{\max}) + C_r\right) \tag{3.21}$$

where $C_r \triangleq \sqrt{(\gamma_s(t)P_{\max})^2 - 4\frac{\gamma_r(t)V}{\Delta t X_r(t)}(1+\gamma_s(t)P_{\max})}$ and $\eta_s(t) \triangleq \gamma_s(t)/\gamma_r(t)$. With the power constraint $0 \leq P_r(t) \leq P_{\max}$, the optimal $P_r^*(t)$ is

$$P_r^*(t) = \max\{\min\{P_r^o(t), P_{\max}\}, 0\}. \tag{3.22}$$

3.4.1.3 Case 3: $X_s(t) < 0$ and $X_r(t) \geq 0$

Following the similar discussion in Case 2, we obtain the optimal solution as $P_r^*(t) = P_{\max}$, and

$$P_s^*(t) = \max\{\min\{P_s^o(t), P_{\max}\}, 0\} \tag{3.23}$$

where

$$P_s^o(t) = \frac{\eta_r(t)P_{\max}}{2(1+\gamma_r(t)P_{\max})}\left(-(2+\gamma_r(t)P_{\max}) + C_s\right) \tag{3.24}$$

with $C_s \triangleq \sqrt{(\gamma_r(t)P_{\max})^2 - 4\frac{\gamma_s(t)V}{X_s(t)\Delta t}(1+\gamma_r(t)P_{\max})}$ and $\eta_r(t) \triangleq \gamma_r(t)/\gamma_s(t)$.

3.4.1.4 Case 4: $X_s(t) < 0$ and $X_r(t) < 0$

In this case, the objective function of $f(\mathbf{P}(t))$ is not monotonic with respect to either $P_s(t)$ or $P_r(t)$. However, we show in Section 3.4.1 that $f(\mathbf{P}(t))$ is convex and problem **P3′** is

a joint convex optimization problem with respect to $P_s(t)$ and $P_r(t)$. The optimal solution $P_s^*(t)$ and $P_r^*(t)$ can be numerically obtained by the standard convex optimization solver like fmincon solver in MATLAB.

The optimal solution of **P3′** is summarized in Proposition 3.1 below

Proposition 3.1 *The optimal solution of* **P3′** *is given by*

1. *If* $X_s(t) \geq 0$ *and* $X_r(t) \geq 0$*, then* $P_s^*(t) = P_r^*(t) = P_{\max}$*;*
2. *If* $X_s(t) \geq 0$ *and* $X_r(t) < 0$*, then* $P_s^*(t) = P_{\max}$ *and* $P_r^*(t) = \max\{\min\{P_r^o(t), P_{\max}\}, 0\}$*, where* $P_r^o(t)$ *is given by* (3.21)*;*
3. *If* $X_s(t) < 0$ *and* $X_r(t) \geq 0$*, then* $P_s^*(t) = \max\{\min\{P_s^o(t), P_{\max}\}, 0\}$*, where* $P_s^o(t)$ *is given by* (3.24)*, and* $P_r^*(t) = P_{\max}$*;*
4. *If* $X_s(t) < 0$ *and* $X_r(t) < 0$*, then* $P_s^*(t)$ *and* $P_r^*(t)$ *can numerically be obtained.*

3.4.2 Online Power Control Algorithm

The optimal solution to **P3′** has some structural properties that will be useful in analyzing its performance later. These characteristics are presented in the following Lemma.

Lemma 3.2 *Define* $\zeta_{\max,i} \triangleq \frac{1}{\Delta t}\gamma_{i,\max}$ *for* $i = s, r$*. The optimal solution of problem* **P3′** *has the following properties:*

(i) *If* $X_s(t) \geq 0$ *and* $X_r(t) \geq 0$*, then the optimal solution is always given by* $P_s^*(t) = P_r^*(t) = P_{\max}$.

(ii) *If* $X_s(t) \geq 0$ *and* $X_r(t) \leq -V\zeta_{\max,r}$*, then the optimal solution is always given by* $P_s^*(t) = P_{\max}$ *and* $P_r^*(t) = 0$.

(iii) *If* $X_s(t) \leq -V\zeta_{\max,s}$ *and* $X_r(t) \geq 0$*, then the optimal solution is always given by* $P_s^*(t) = 0$ *and* $P_r^*(t) = P_{\max}$.

Proof: See Appendix 3.8.2.

Using properties of Lemma 3.2, we show below that the virtual queues $X_s(t)$ and $X_r(t)$ are bounded.

Lemma 3.3 *Under the proposed power solution, the virtual queues $X_s(t)$ and $X_r(t)$ are bounded for all t's as*

$$X_{low,i} \leq X_i(t) \leq X_{up,i} \quad i = s, r \ , \tag{3.25}$$

where $X_{low,i} \triangleq -V\zeta_{\max,i} - \Delta t P_{\max}$ and $X_{up,i} \triangleq E_{c,\max}$.

Proof: See Appendix 3.8.3.

Remark 1: The optimal solution $P_s^*(t)$ and $P_r^*(t)$ of **P3′** depends on the values of $X_s(t)$ and $X_r(t)$. To help summarize the solution, based on Proposition 3.1 and Lemmas 3.2 and 3.3, we partition the values of $(X_s(t), X_r(t))$ into six regions as follows

$$\begin{aligned}
\mathcal{R}_1 &\triangleq \{(X_s(t), X_r(t)) : \quad X_s(t) \in [0, X_{\text{up},s}], X_r(t) \in [0, X_{\text{up},r}]\} \\
\mathcal{R}_2 &\triangleq \{(X_s(t), X_r(t)) : \quad X_s(t) \in [0, X_{\text{up},s}], X_r(t) \in [-V\zeta_{\max,r}, 0]\} \\
\mathcal{R}_3 &\triangleq \{(X_s(t), X_r(t)) : \quad X_s(t) \in [-V\zeta_{\max,s}, 0], X_r(t) \in [0, X_{\text{up},r}]\} \\
\mathcal{R}_4 &\triangleq \{(X_s(t), X_r(t)) : \quad X_s(t) \in [0, X_{\text{up},s}], X_r(t) \in [-X_{\text{low},r}, -V\zeta_{\max,r}]\} \\
\mathcal{R}_5 &\triangleq \{(X_s(t), X_r(t)) : \quad X_s(t) \in [-X_{\text{low},s}, -V\zeta_{\max,s}], X_r(t) \in [0, X_{\text{up},r}]\} \\
\mathcal{R}_6 &\triangleq \{(X_s(t), X_r(t)) : \quad X_s(t) \in [X_{\text{low},s}, 0], X_r(t) \in [X_{\text{low},r}, 0]\}.
\end{aligned} \tag{3.26}$$

Fig. 3.2 shows the six regions for $(X_s(t), X_r(t))$. In each region, the optimal solution of P3′ is given with a unique form, shown as follows

(i) For $(X_s(t), X_r(t)) \in \mathcal{R}_1$: $P_s^*(t) = P_r^*(t) = P_{\max}$;

(ii) For $(X_s(t), X_r(t)) \in \mathcal{R}_2$: $P_s^*(t) = P_{\max}$, $P_r^*(t)$ in (3.22);

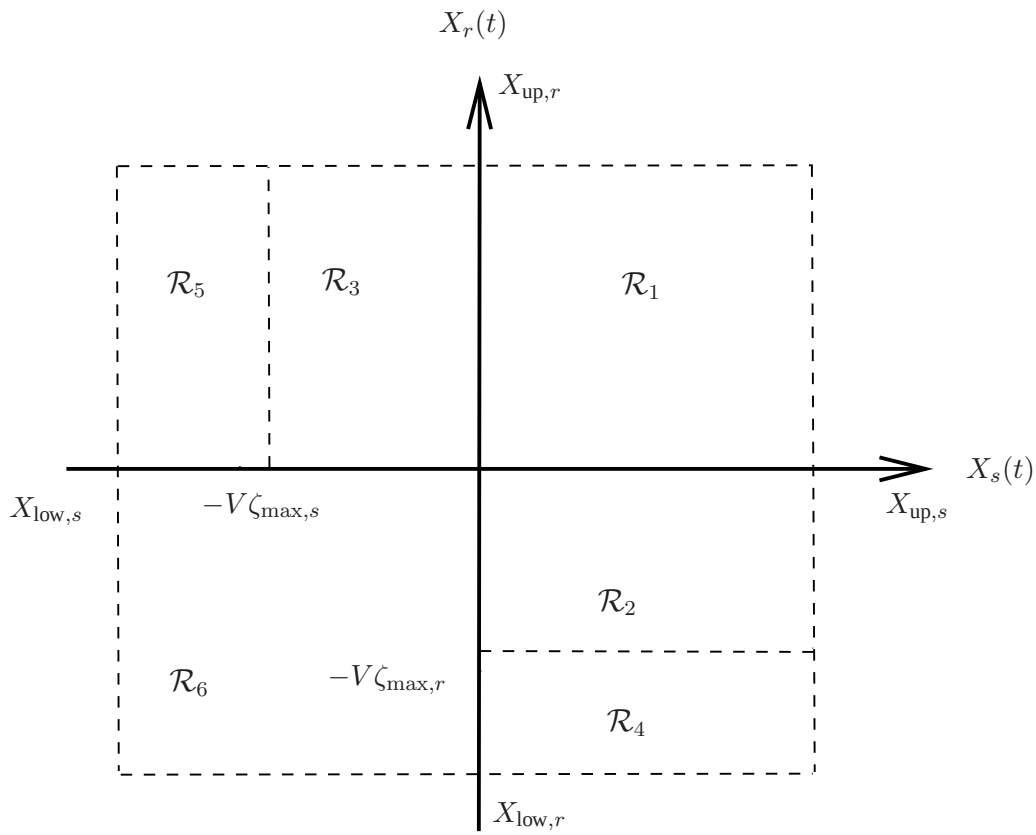

Figure 3.2: Power control policy at virtual queues

(iii) For $(X_s(t), X_r(t)) \in \mathcal{R}_3$: $P_s^*(t)$ in (3.23), $P_r^*(t) = P_{\max}$;

(iv) For $(X_s(t), X_r(t)) \in \mathcal{R}_4$: $P_s^*(t) = P_{\max}$, $P_r^*(t) = 0$;

(v) For $(X_s(t), X_r(t)) \in \mathcal{R}_5$: $P_s^*(t) = 0$, $P_r^*(t) = P_{\max}$;

(vi) For $(X_s(t), X_r(t)) \in \mathcal{R}_6$: $P_s^*(t)$ and $P_r^*(t)$ can numerically be solved.

Note that in **P3′**, we have removed the battery capacity constraint (3.1). By the bounded-ness of $X_s(t)$ and $X_r(t)$ given in Lemma 3.3, we can design parameters A_s, A_r and V to ensure that the optimal power solution of **P3′** is feasible to **P1**. The results are shown in the following proposition

Proposition 3.2 *Under the optimal solution of problem* **P3′**, *if* $A_i,\ i = s, r$ *in* (3.10) *satisfies*

$$A_i = \Delta t P_{\max} + E_{\min} + V\zeta_{\max,i}, \quad i = s, r, \tag{3.27}$$

and $V \in (0, V_{\max}]$ *with*

$$V_{\max} = \min\{V_{\max,s}, V_{\max,r}\} \tag{3.28}$$

where

$$V_{\max,i} = \frac{E_{\max} - E_{\min} - E_{c,\max} - \Delta t P_{\max}}{\zeta_{\max,i}}, \quad i = s, r, \tag{3.29}$$

then $E_b^s(t)$ *and* $E_b^r(t)$ *satisfy the battery capacity constraints* (3.1), *and the optimal power solution* $(P_s^*(t), P_r^*(t))$ *of* **P3′** *in Proposition 3.1 is feasible to* **P1** *for all* t*'s.*

Proof: See Appendix 3.8.4.

Substituting the expression of A_i in (3.27) into (3.10) and from Proposition 3.1, we express the joint power control solution $(P_s^*(t), P_r^*(t))$ as a function of battery energy levels and the channel fading condition. Define three energy state thresholds for the batteries as follows

$$E_{b,\text{th1}}^i \triangleq \Delta t P_{\max} + E_{\min} + V\zeta_{\max,i} \tag{3.30}$$

$$E_{b,\text{th2}}^i \triangleq \Delta t P_{\max} + E_{\min} + V(\zeta_{\max,i} - \alpha_i(t)) \tag{3.31}$$

$$E_{b,\text{th3}}^i \triangleq \Delta t P_{\max} + E_{\min} + V(\zeta_{\max,i} - \frac{\gamma_i(t)}{\Delta}) \tag{3.32}$$

Algorithm 3 Online Transmit Power Control Algorithm with EH
($\gamma_i(t) \leq \gamma_{i,\max}$, for $i = s, r$)

Set $V \in (0, V_{\max}]$ with $V_{\max}$ given in (3.28).
At time slot t:

1: Compute $E^i_{b,\text{th}j}(t)$ for $i = s, r$ and $j = 1, 2, 3$ by (3.30)-(3.32).
2: Obtain $P^*_s(t)$ and $P^*_r(t)$ according to the following cases:

S1) If $E^s_b(t) \geq E^s_{b,\text{th1}}$ and $E^r_b(t) \geq E^r_{b,\text{th2}}$, then $P^*_s(t) = P^*_r(t) = P_{\max}$;

S2) If $E^s_b(t) \geq E^s_{b,\text{th1}}$ and $E^r_{b,\text{th3}} < E^r_b(t) < E^r_{b,\text{th2}}$, then $P^*_s(t) = P_{\max}$ and $P^*_r(t) = P^o_r(t)$;

S3) If $E^s_b(t) \geq E^s_{b,\text{th1}}$ and $E^r_b(t) \leq E^r_{b,\text{th3}}$, then $P^*_s(t) = P_{\max}$ and $P^*_r(t) = 0$;

S4) If $E^s_{b,\text{th2}} \leq E^s_b(t) < E^s_{b,\text{th1}}$ and $E^r_b(t) \geq E^r_{b,\text{th1}}$, then $P^*_s(t) = P^*_r(t) = P_{\max}$;

S5) If $E^s_{b,\text{th3}} < E^s_b(t) < E^s_{b,\text{th2}}$ and $E^r_b(t) \geq E^r_{b,\text{th1}}$, then $P^*_s(t) = P^o_s(t)$ and $P^*_r(t) = P_{\max}$.

S6) If $E^s_b(t) \leq E^s_{b,\text{th3}}$ and $E^r_b(t) \geq E^r_{b,th1}$, then $P^*_s(t) = 0$ and $P^*_r(t) = P_{\max}$;

S7) If $E^s_b(t) < E^s_{b,\text{th1}}$ and $E^r_b(t) < E^r_{b,\text{th1}}$, then $P^*_s(t)$ and $P^*_r(t)$ can numerically be obtained.

3: Update $E^i_b(t+1)$ and $X_i(t+1)$ with $P^*_i(t)$, for $i = s, r$, using (3.4) and (3.10), respectively.
4: Output source and replay transmit power solutions: $P^*_s(t)$ and $P^*_r(t)$.

for $i = s, r$, where

$$\alpha_s(t) \triangleq \frac{\eta_r^2(t)\gamma_s(t)/\Delta t}{\eta_r(t)^2 + \eta_r(t)(2 + \gamma_r(t)P_{\max}) + (1 + \gamma_r(t)P_{\max})},$$
$$\alpha_r(t) \triangleq \frac{\eta_s^2(t)\gamma_r(t)/\Delta t}{\eta_s(t)^2 + \eta_s(t)(2 + \gamma_s(t)P_{\max}) + (1 + \gamma_s(t)P_{\max})}.$$

The joint power control solution $(P^*_s(t), P^*_r(t))$ in terms of $E^s_b(t)$ and $E^r_b(t)$ is provided in Algorithm 3, where we summarize our proposed joint power control strategy.

Remark 2: Note that for Cases S3 and S6 in Algorithm 3, the power solution is such that the transmit power of either source or relay is 0 , while that of the other node is $P_{\max}$. Both of these cases will result in $R(t) = 0$. Thus, in practical design, to save energy consumption, both powers should be set to 0 if one of them is 0, *i.e.*, $P_s(t) = 0$ or $P_r(t) = 0$

Algorithm 4 Online Modified Transmit Power Algorithm with EH
($\gamma_i(t) \leq \gamma_{i,\max}$, for $i = s, r$)

Set $V \in (0, V_{\max}]$ with $V_{\max}$ given in (3.28).
At time slot t:

1: Compute $E^i_{b,\text{th}j}(t)$ for $i = s, r$ and $j = 1, 2, 3$ by (3.30)-(3.32);
2: Obtain $P^*_s(t)$ and $P^*_r(t)$ according to S1)-S7) in Algorithm 3, except S3) and S6) which modify to S3′) and S6′) as follows

S3′) If $E^s_b(t) \geq E^s_{b,\text{th1}}$ and $E^r_b(t) \leq E^r_{b,\text{th3}}$, then $P^*_s(t) = P^*_r(t) = 0$.

S6′) If $E^s_b(t) \leq E^s_{b,\text{th3}}$ and $E^r_b(t) \geq E^r_{b,th1}$, then $P^*_s(t) = P^*_r(t) = 0$.

3: Update $E^i_b(t+1)$ and $X_i(t+1)$ with $P^*_i(t)$, for $i = s, r$, using (3.4) and (3.10), respectively.
4: Output source and replay transmit power solutions: $P^*_s(t)$ and $P^*_r(t)$.

replace with $P_s(t) = P_r(t) = 0$. Considering this condition, we modify the solutions of S3 and S6 in Algorithm 3 to be $P^*_s(t) = P^*_r(t) = 0$, as shown in the modified version Algorithm 4, where we replaced S3 and S6 of Algorithm 3 with Cases S3′ and S6′.

3.4.3 Algorithm for Fading with Unbounded Channel Gain

So far, we assume that the normalized channel gain is bounded $\gamma_i(t) \leq \gamma_{i,\max}, i = s, r$. For a more general fading scenario, the distributions of channel fading over two hops *i.e.*, $h_s(t)$ and $h_r(t)$ have unbounded support (*e.g.*, complex Gaussian distributions). Thus, the normalized channel gains $\gamma_s(t)$ and $\gamma_r(t)$ are unbounded. Our previous approach for online power control decision cannot directly accommodate the unbounded channel gain. In the following, we develop a modified algorithm from Algorithm 4 to provide source and relay transmit power solutions when $\gamma_s(t) > \gamma_{s,\max}$ and/or $\gamma_r(t) > \gamma_{r,\max}$.

Define $\mathcal{A}_i \triangleq [0, \gamma_{i,\max}]$ and $\mathcal{A}^c_i = (\gamma_{i,\max}, \infty)$, $i = s, r$. When $\gamma_i(t) \in \mathcal{A}^c_i$, $i = s, r$, we call an outage event occurs over that hop (in terms of the condition to execute Algorithm 4). The outage event for the relay network occurs when either of the two hops has an

outage. The corresponding outage probability, denoted by $\{p_o\}$, is given by

$$p_{\text{o}} = P(\{\gamma_s(t) \in \mathcal{A}_s^c\} \cup \{\gamma_r(t) \in \mathcal{A}_r^c\}) = p_{\text{o},s} + p_{\text{o},r} - p_{\text{o},s}p_{\text{o},r}, \tag{3.33}$$

where $p_{o,i} \triangleq P(\gamma_i(t) \in \mathcal{A}_i^c)$ is the outage probability for each hop. The channels over two hops are statistically independent, therefore the above equation is simplified as shown in the last part of equation. For Rayleigh fading channels as an example, assume h_i being complex Gaussian with zero mean and variance $\sigma_{h,i}^2$, $i = s, r$. The outage probability for each hop is $P(\gamma_i(t) \in \mathcal{A}_i^c) = \exp(-\gamma_{i,\max}/\sigma_{h,i}^2)$, and the outage probability for the network is $p_{\text{o}} = \exp(-\gamma_{s,\max}/\sigma_{h,s}^2) + \exp(-\gamma_{r,\max}/\sigma_{h,r}^2) - \exp(-\gamma_{s,\max}/\sigma_{h,s}^2 - \gamma_{r,\max}/\sigma_{h,r}^2)$.

Note that, when $\gamma_s(t) \in \mathcal{A}_s$ and $\gamma_r(t) \in \mathcal{A}_r$, Algorithm 4 still provides a feasible power solution to **P1**. However, when outage occurs, $P_s^*(t)$ or $P_r^*(t)$ in Algorithm 4 may not be feasible. In other words, the battery capacity constraint (3.3) may be violated. In this case, we propose the following method to determine $P_s(t)$ and $P_r(t)$.

Define $E_b^{i,e}(t) \triangleq E_b^i(t) - \Delta t P_i(t)$, $i = s, r$, as the battery energy level (at the source or relay) at the end of time slot t, before the energy is harvested into the battery. Define $\bar{E}_b^{i,e}(t) \triangleq \frac{1}{t}\sum_{\tau=1}^{t} E_b^{i,e}(t)$ as the time-averaged $E_b^{i,e}$ up to time slot t. When $\gamma_i(t) \in \mathcal{A}_i^c$, if $P_j^*(t)$, $j = s, r$, in Proposition 3.2 does not satisfy constraint (3.3), we set the transmit power as

$$P_j^o(t) = \left[\frac{E_b^i(t) - \bar{E}_b^{i,e}(t-1)}{\Delta t}\right]^+, \text{ for } j = s, r \tag{3.34}$$

where $[a]^+ \triangleq \max\{a, 0\}$.

Remark 3: Note that, first, $P_j^o(t)$ in (3.34) is clearly feasible to **P1**; second, whenever in outage Algorithm 4 produces an infeasible solution, our proposed method above is to control the power such that at the end of the time slot, the remaining energy level (excluding

Algorithm 5 Online Transmit Power Control Algorithm with EH (OTPC-EH) ($\gamma_i(t) < \infty$ for $i = s, r$)

Choose $p_{\mathrm{o},i}$, and obtain $\gamma_{i,\max}$ using $p_{\mathrm{o},i}$, for $i = s, r$.
At time slot t:

1: Observe the system state $\mathbf{s}(t)$.
2: Apply **Algorithm 4** to produce $P_s^*(t)$ and $P_r^*(t)$. Set $P_s^o(t) = P_s^*(t)$ and $P_r^o(t) = P_r^*(t)$.
3: **if** $\gamma_s(t) \in \mathcal{A}_s^c$ or $\gamma_r(t) \in \mathcal{A}_r^c$ **then**
4: **for** $i = s, r$ **do**
5: **if** $P_i^*(t) > (E_b^i(t) - E_{\min})/\Delta t$ **then** obtain $P_i^o(t)$ in (3.34).
6: Update $E_b^{i,e}(t) = E_b^i(t) - \Delta t P_i^o(t)$.
7: Update $\bar{E}_b^{i,e}(t) = \frac{1}{t}\left[(t-1)\bar{E}_b^{i,e}(t-1) + E_b^{i,e}(t)\right]$.
8: Output source and replay transmit power solutions: $P_s^o(t)$ and $P_r^o(t)$.

the harvested energy) would be roughly maintained at its historical average level. The reason to do so is that in the case of bounded channel gains, the online algorithm by Lyapunov technique converges to and maintain a steady-state battery energy level at the long-term. When in outage, which happens only occasionally, we set the transmit power such that the battery energy level is maintained at its steady-state without being disturbed.

We summarize our online transmit power control with EH algorithm for the general fading scenario in Algorithm 5 (OTPC-EH).

3.5 Performance Analysis

We first analyze the performance of our proposed algorithms for the bounded fading channels; then we study the performance for general unbounded fading channels.

3.5.1 Bounded Fading Channels

We first consider the case where $\gamma_i(t) \in \mathcal{A}_i$, $\forall t$ and $i = s, r$, and analyze the performance of Algorithm 4. Let $\bar{R}^s(V, \mathcal{A}_s, \mathcal{A}_r)$ denote the achieved objective value of the long-term time-

averaged expected rate of **P1** by Algorithm 4 under a chosen V value. Let $\bar{R}^{\text{opt}}(\mathcal{A}_s, \mathcal{A}_r)$ denote the maximum objective value of **P1** under the optimal power control policy.

We show below the performance gap of Algorithm 4 to $\bar{R}^{\text{opt}}(\mathcal{A}_s, \mathcal{A}_r)$.

Theorem 3.1 *Assume $\gamma_i(t) \in \mathcal{A}_i$, $\forall t$ and $i = s, r$. Assume the system state $\mathbf{s}(t)$ being i.i.d over time. The performance gap between Algorithm 4 and the optimal power control policy of **P1** is upper-bounded as*

$$\bar{R}^{opt}(\mathcal{A}_s, \mathcal{A}_r) - \bar{R}^{s}(V, \mathcal{A}_s, \mathcal{A}_r) \leq \frac{B}{V} \tag{3.35}$$

where B is defined below (3.14)*.*

Proof: See Appendix 3.8.5.

From (3.35) we note that the bound on the performance gap of our proposed Algorithm 4 to the optimal one decreases with V. Due to the battery capacity constraint, V has to be chosen within $(0, V_{\max}]$. Thus, to minimize the gap to the maximum performance, we should chose $V = V_{\max}$. Furthermore, from (3.28) and (3.29), $V_{\max}$ increases with the battery capacity. Thus, Algorithm 4 is asymptotically optimal for **P1** as the battery capacity goes to infinity. Finally, the i.i.d. assumption of $\{\gamma_s(t)\}$, $\{\gamma_r(t)\}$, $\{E_a^s(t)\}$ and $\{E_a^r(t)\}$ can be relaxed to accommodate the case where these processes are modeled as finite state Markov chains. By applying a multi-slot Lyapunov drift technique [54], a similar bound can be shown for our proposed power control algorithm.

3.5.2 Unbounded Fading Channels

As we mentioned earlier in Section 3.4.3, the outage event happens when at least one channel gain locates in $\gamma_i(t) \in \mathcal{A}_i^c$ region. (3.34) shows how to obtain the source and relay transmission powers when the outage happens. In this part, we present the upper-

bound on the performance of power control strategy in the presence of an outage event. Let $\bar{R}^{\text{opt}}(\mathcal{A}_s^c, \mathcal{A}_r^c)$ denote the maximum objective of problem **P1** under the optimal solution and $\bar{R}^s(\mathcal{A}_s^c, \mathcal{A}_r^c)$ denote the achieved rate of problem **P1** using (3.34), both in the presence of outage.

In the following lemma, we propose an upper-bound on the performance of Algorithm 5 in the outage event. For simplicity, without causing any confusion, we drop the time notation and let $\gamma_i(t) = \gamma_i$ in the following

Lemma 3.4 *Assume that the system state* ***s****(t) is i.i.d. over time. For* $\gamma_i \in \mathcal{A}_i^c$*, the performance gap of Algorithm 5 and the optimal policy is upper-bounded as*

$$\bar{R}^{opt}(\mathcal{A}_s^c, \mathcal{A}_r^c) - \bar{R}^s(\mathcal{A}_s^c, \mathcal{A}_r^c) \leq G. \tag{3.36}$$

where $0 < G < \infty$ *is a constant as a function of the channel gains distribution* $f(\gamma_i)$ *and* $\gamma_{i,\max}$.

Proof: See Appendix 3.8.6.

For the general fading case, where $\gamma_i(t) < \infty$, let $\bar{R}^{\text{opt}}$ denote the maximum objective value of **P1**. Let $\bar{R}^s(V, p_o)$ denote the achieved objective by Algorithm 5, where the value depends on both the control parameter V and the outage probability p_o in our algorithm. Combining the results in Theorem 3.1 and Lemma 3.4, we have the performance bound in our proposed (OTPC-EH) algorithm at Algorithm 5 as follows

Theorem 3.2 *Assume the system state* $\mathbf{s}(t)$ *is i.i.d over time. For the fading channel with any given fading distribution, given the outage probability* p_o*, the performance under Algorithm 5 (OTPEH) is bounded from* $\bar{R}^{opt}$ *by*

$$\bar{R}^{opt} - \bar{R}^s(V, p_o) \leq (1 - p_o)\frac{B}{V} + p_o G. \tag{3.37}$$

Proof: See Appendix 3.8.7.

3.6 Simulation Results

We now evaluate the performance of our proposed algorithms in a two-hop relay network. For the batteries at both source and relay, the default maximum and minimum energy levels are set to $E_{\max} = 50J$ and $E_{\min} = 0$, respectively. The maximum charging amount per slot is set to $E_{c,\max} = 0.3J$, and the maximum transmission power is $P_{\max} = 0.5$ W. We set the time slot duration $\Delta t = 1$ sec. We assume that the independent energy arrival $E_s^i(t)$ for $i = s, r$ follows a compound Poisson process with the arrival rate as $\lambda_i(t)$ unit/slot for the source and relay. For each unit arrival, the amount of $E_a^i(t)$ is i.i.d. and uniformly distributed between $[0, 2a_i]$, where a_i is the mean for $i = s, r$. The energy arrival for both channels have a same statistical setting,*i.e.*, , $a_i = 0.3$J and $\lambda_i = 0.5$, for $i = s, r$.

We generate the channels $h_s(t)$ and $h_r(t)$ as i.i.d complex Gaussian random variable with the normalized channel gain $\mathbb{E}[\gamma_i(t)] = 10$ dB; then set the outage probability over each hop to be $p_{o,i} = 0.01$ which results in $\gamma_{i,\max} \approx 16$ dB. Finally, we set $V = V_{\max}$ in verifying the algorithms performance. We study our proposed algorithms under two fading scenarios

(a) *Bounded fading* $\gamma_i(t) \leq \gamma_{i,\max}$: We assume the same channel setting as described above. If $\gamma_i(t) > \gamma_{i,\max}$, we set $\gamma_i(t) = \gamma_{i,\max}$. Under this scenario, we perform Algorithm 4 to find source and relay transmit powers.

(b) *Unbounded fading* $\gamma_i(t) < \infty$: We apply Algorithm 5 (OTPC-EH) to obtain source and relay transmit powers.

To the best of our knowledge, the online methods in the literature rely on the statistical information of energy arrival and random events. In order to verify the our methodology,

the proposed algorithms are compared with three online algorithms in the literature. These algorithms were proposed for different system models and therefore, we modify them based on our problem setting. In addition, in Chapter 2, the online power control policy for a point-to-point channel is proposed that only relies on the current energy arrival and fading condition. As a benchmark, we extend the proposed Algorithm 2 to a two-hop network. The four algorithms are described below

(c) *Energy adaptive water-filling algorithm (EAWF)*: In [33], EAWF is proposed for a SISO network. This heuristic algorithm determines the power transmission based on the channel distribution and computes a cutoff fade γ_0 at each time slot for the channel. Then, by finding cutoff fade and given channel gain of each time slot, the transmit power is computed based on water-filling method. The battery operational constraint (3.5) is first imposed to EAWF scheme. Then the scheme is applied to each hop to find the instantaneous cutoff fade $\gamma_{i,0}$ for the corresponding hop. Note that the channels are statistically independent. Therefore, the cutoff fade $\gamma_{i,0}$ is the solution of the following equation

$$\int_{\gamma_{i,0}}^{\infty} \left(\frac{1}{\gamma_{i,0}} - \frac{1}{\gamma_i} \right) f(\gamma_i) d\gamma_i = E_b^i(t), \quad i = s, r. \tag{3.38}$$

Then, given $\gamma_i(t)$, the transmission power of each hop is determined as

$$P_i(t) = \min \left\{ \left[\frac{1}{\gamma_{i,0}} - \frac{1}{\gamma_i(t)} \right]^+, P_{\max}, (E_b^i(t) - E_{\min})/\Delta t \right\} \tag{3.39}$$

(d) *Greedy algorithm*: At each time slot, the transmitter at each hop uses the maximum possible power based on $E_b^i(t)$ to maximize the transmission rate at current time slot

t, *i.e.*,

$$\max_{P_s(t),P_r(t)} R(t) \tag{3.40}$$

$$\begin{aligned} \text{subject to} \quad & 0 \le P_i(t) \le P_{\max}, \quad i = s, r \\ & 0 \le \Delta t P_i(t) \le E_b^i(t) - E_{\min}, \quad i = s, r. \\ & E_b^i(t+1) = E_b^i(t) - \Delta t P_i(t) + E_h^i(t)\ , \quad i = s, r, \end{aligned}$$

which gives $P_i(t) = \min\{(E_b^i(t) - E_{\min})/\Delta t, P_{\max}\}$.

(e) *Power halving algorithm*: At each time slot, the source and relay use half of the maximum possible powers given by the greedy algorithm in (d). Although greedy and power halving algorithms are both heuristic algorithms, unlike the greedy algorithm, power halving scheme works to conserve the harvested energy in the batteries.

(f) *Algorithm 2*: In Chapter 2, Algorithm 2 is presented for a point-to-point channel. The proposed online power control policy only relies on the current energy arrival and fading condition. We apply Algorithm 2 for the two-hop network. At each time slot, the source and relay use Algorithm 2 to determine the transmission powers.

Algorithms (d) and (f) only depend on the current system state without requiring their statistical information. Note that, when implementing algorithms (c)–(f), the complex Gaussian channel is used as in (b) fading scenario. As we mention in Section 3.4.2, we modify the power allocation solution of S3 and S6 of Algorithm 3 to S3′ and S6′ in Algorithm 4 to save energy consumption. In order to provide a consistent comparison, we apply this energy saving approach for all algorithms (c) to (f). If the transmit power of either transmitter or relay is 0 while the other node is $P_{\max}$, we set both transmit powers to 0, *i.e.*,

$P_s(t) = P_r(t) = 0$.

In Figs. 3.3 and 3.4, we plot the time-averaged expected rate vs. time slots for two different initial battery settings. Each time-averaged rate is averaged over 50 Monte Carlo runs. We set the initial state of batteries to $E_{\max}/2$ and $E_{\max}$ for Figs. 3.3 and 3.4, respectively. The performance of Algorithms 4 and 5 under fading scenarios (a) and (b) is almost identical and 1.5 times higher than that of Algorithm 2. It can be seen that the transmission rate for the proposed algorithms are nearly doubled over that of the power halving and EAWF algorithms and more than two times of greedy algorithm. The proposed algorithms outperform significantly the EAWF algorithm while the latter one uses the fading statistics to determine the transmission power. It is worth mentioning that the proposed algorithms benefit from the energy preservation and opportunistic transmission based on the energy levels of batteries and fading conditions.

Moreover, we study the effect of fading condition on the performance of the proposed algorithms. In Fig. 3.5, we plot the normalized relay-destination channel gain, the state of relay battery level and the transmission power of relay $P_r^*(t)$ vs. time slot t. We examine the performance of Algorithm 5 under the bounded fading scenario (b). The middle subplot shows the relay battery level along with the three threshold levels defined in (3.30)-(3.32). We can see that $E_{b,\text{th3}}^r$ varies by $-\gamma_r(t)$. Threshold $E_{b,\text{th1}}^r$ is a constant value based on the maximum transmission power, the minimum battery energy level and weight parameter V. Also, $E_{b,\text{th2}}^r$ does not fluctuate noticeably over time as it is a function of $-\alpha_r(t)$. The last subplot illustrates the opportunistic behavior of power control strategy. In other words, the proposed algorithms perform based on the channel condition, *i.e.*, the transmission power is higher whenever the channel is stronger.

To study the effect of battery capacity on the performance of the proposed algorithms (Algorithms 3 to 5), we plot the long-term average rate vs. battery capacity in Fig. 3.6. For the proposed algorithms (Algorithms 3 to 5), the long-term average rate significantly

increases under smaller battery capacities. The long-term average rate converges quickly to the maximum value as the battery capacity increases. The converging behavior is due to the influence of the maximum power $P_{\max}$ and charging rate $E_{c,\max}$. It can be seen that the performance of the joint power control policy of the proposed algorithms (Algorithms 3 to 5) are substantially higher than Algorithm 2. Although Algorithm 2 uses the online power control policy for the source and relay individually, performs significantly better than EAWF, power halving and greedy algorithms. Note that EAWF, power halving and greedy algorithms do not depend on the battery size and their performances do not change with the size. As seen in the figure, Algorithm 3 shows a similar performance as that of Algorithm 4 and therefore, only Algorithm 4 and 5 will be presented and discussed in this section.

In Fig. 3.7, we plot the long-term average rate vs. V for $V \in (0, V_{\max}]$. We see the average rate improves as V increases under Algorithm 5 which is consistent with Theorem 3.2 that the gap to the optimal performance decreases as V increases. Also, the average rate of Algorithm 2 increases as V grows, however the increase rate is much lower than Algorithm 5. On the other hand, since EAWF, power halving and greedy algorithms do not change with V, their average rates remain flat.

Finally, we study the long-term average rate under different energy arrival parameters, *i.e.*, arrival rate λ_i and mean arrival amount a_i, in Fig. 3.8. For this plot, we set $a_s = a_r$ and $\lambda_s = \lambda_r$. It can be seen that the average rate is monotonically increasing with both a_i and λ_i. The plot demonstrates clearly that the proposed algorithms outperform significantly over power halving, EAWF and greedy algorithms within a wide range of energy arrival rate λ_i and mean arrival amount a_i. As a_i increases, we see that the improvement of the average rate gradually reduces for all Algorithms 4, 5, EAWF, power halving and greedy algorithms. This is because, as the amount of energy arrival increases, the maximum power $P_{\max}$ and charging rate $E_{c,\max}$ become limiting factors for the performance. As shown in

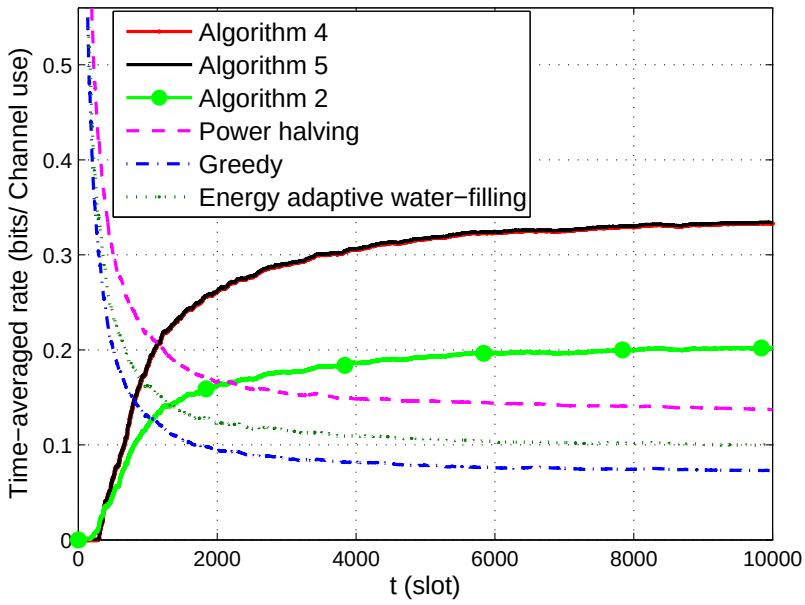

Figure 3.3: Time-averaged expected rate vs. time with initial battery of $\frac{E_{\max}}{2}$

Figs 3.3,3.4, 3.6, 3.7, Algorithm 5 outperforms significantly over Algorithm 2. To avoid confusion in Fig. 3.8, we focus on three other alternative algorithms as benchmarks.

3.7 Summary

In this chapter, we considered an online power control strategy of a two-hop network over wireless fading channels. The transmitter and relay are equipped with energy harvesters and batteries to scavenge the ambient energy. Aiming at maximizing the long-term time-averaged expected rate, we developed an online joint power control algorithm under the battery storage and operation constraints. We derived a combined closed-form and numerical solution for the online power control strategy. The proposed scheme jointly determines the transmission powers for both the transmitter and relay. The method performs based on the energy arrival of both transmitter and rely, battery energy level of both transmitter and relay and also fading condition of both hops. The proposed algorithms do not

require the current information of random events including fading condition and energy arrival. We propose a scheme to tackle the difficulty of unbounded fading channels that cannot be directly handled by Lyapunov technique. We further analytically bounded the performance gap between our proposed algorithm and the optimal solution. The numerical results demonstrate the effectiveness of our proposed online algorithms as compared with three other online approaches.

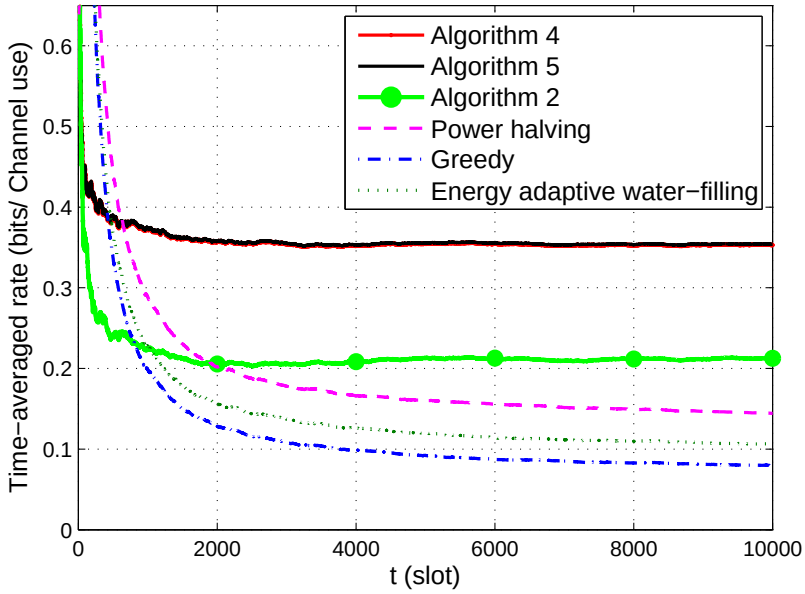

Figure 3.4: Time-averaged expected rate vs. time with battery with full initial value.

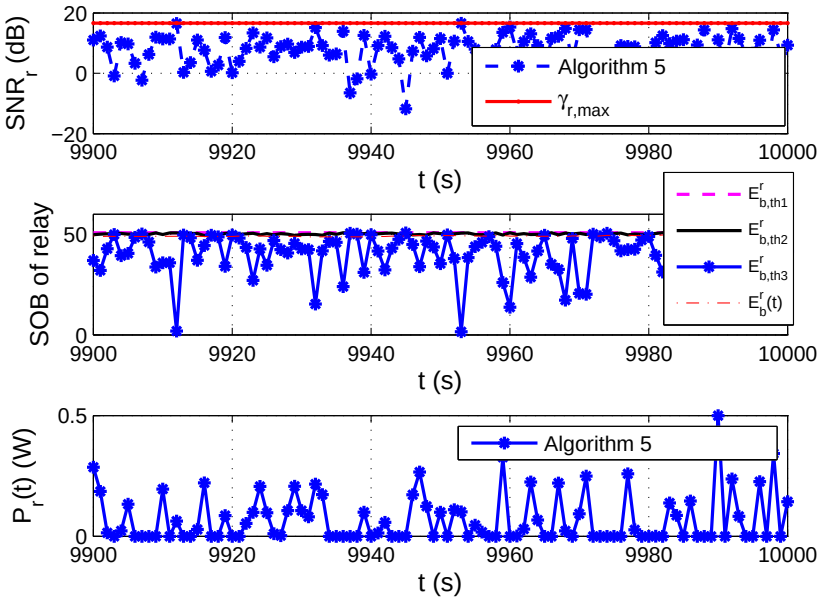

Figure 3.5: Threshold levels of relay battery vs time.

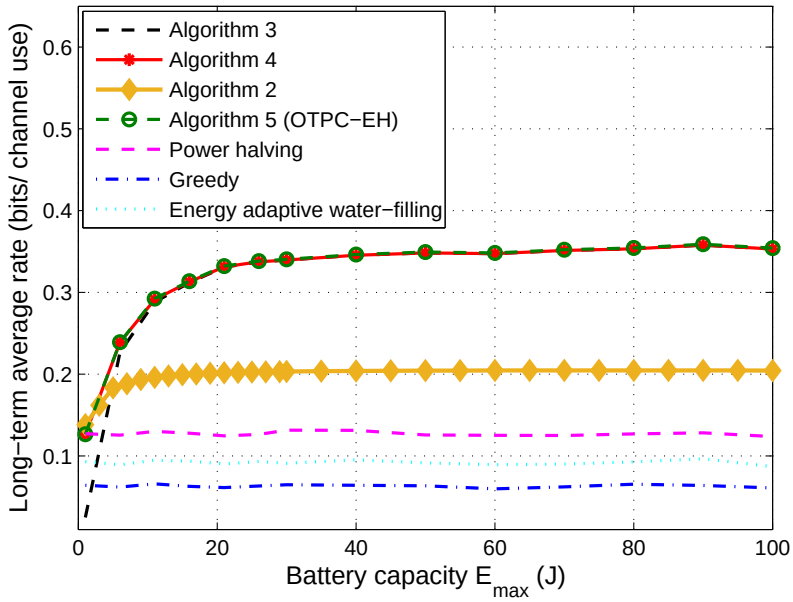

Figure 3.6: Long-term time-averaged expected rate vs. battery size.

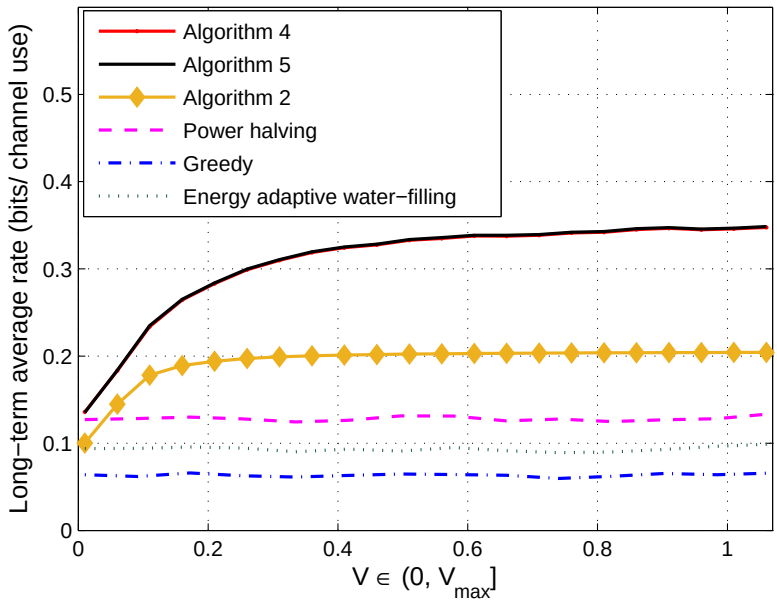

Figure 3.7: Long-term time-averaged expected rate vs. V for $V \in (0, V_{\max}]$.

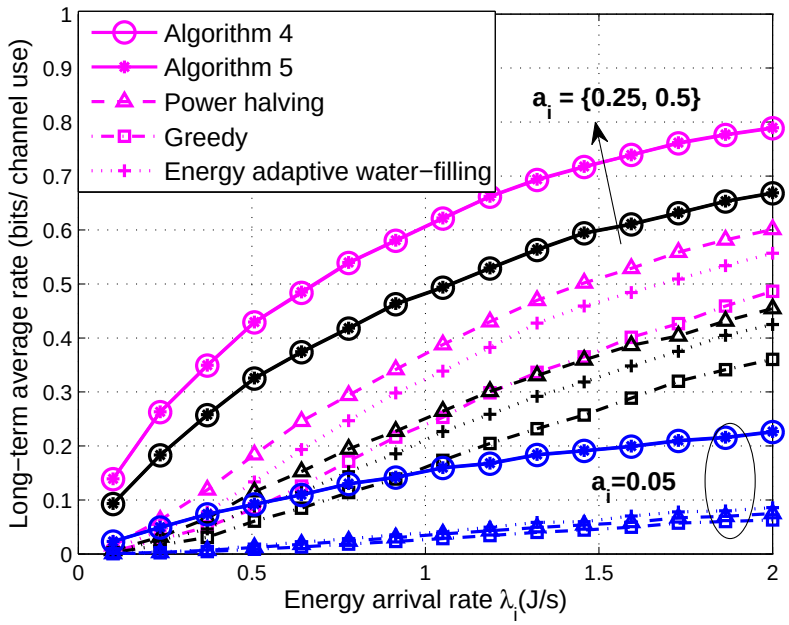

Figure 3.8: Long-term time-averaged expected rate vs. energy arrival rate $\lambda_i(\frac{J}{S})$ for $i = s, r$.

3.8 Appendix

3.8.1 Proof of Lemma 3.1

Proof: From (3.12), the quadratic Lyapunov function for slots t and $t+1$ are as follows

$$L(X_s(t), X_r(t)) = \frac{1}{2}(X_s^2(t) + X_r^2(t)) \tag{3.41}$$

and

$$L(X_s(t+1), X_r(t+1)) = \frac{1}{2}(X_s^2(t+1) + X_r^2(t+1)) \tag{3.42}$$

From the dynamics of $X_i(t)$ in (3.11), we have

$$\begin{aligned} L(X_s(t+1), X_r(t+1)) - L(X_s(t), X_r(t)) &= \frac{X_s^2(t+1) - X_s^2(t)}{2} + \frac{X_r^2(t+1) - X_r^2(t)}{2} \\ = \quad & \frac{(E_h^s(t) - \Delta t P_s(t))^2}{2} + X_s(t)(E_h^s(t) - \Delta t P_s(t)) \\ + & \frac{(E_h^r(t) - \Delta t P_r(t))^2}{2} + X_r(t)(E_h^r(t) - \Delta t P_r(t)). \end{aligned} \tag{3.43}$$

From (3.5), we have $0 \leq E_h^i(t) \leq E_{c,\max}$, for $i = s, r$. Along with constraint (3.2) on $P_i(t)$ for $i = s, r$, we have

$$(E_h^i(t) - \Delta t P_i(t))^2 \leq \max\{E_{c,\max}, \Delta t P_{\max}\}^2. \tag{3.44}$$

Taking expectation at both sides of (3.43) conditioned on $X_s(t)$ and $X_r(t)$ and considering (3.44), we have the per-slot Lyapunov drift being upper bounded by

$$\Delta\left(X_s(t), X_r(t)\right) \leq B + \sum_{i=s,r} X_i(t)\mathbb{E}[E_h^i(t) - \Delta t P_i(t)|X_s(t), X_r(t)] \tag{3.45}$$

where $B \triangleq \max\{E_{c,\max}, \Delta t P_{\max}\}^2/2$. Adding $-V\mathbb{E}\left[R(t)|X_s(t), X_r(t)\right]$ to both sides of (3.45), we have the upper bound on the drift-plus-cost metric as in (3.14). ■

3.8.2 Proof of Lemma 3.2

Proof: Based on the solution of problem **P**3′, all optimal power solutions should satisfy the power constraint (3.2). For part (i), we show in Case 1 in Section 3.4.1.2 that if $X_s(t) \geq 0$ and $X_r(t) \geq 0$, then $P_s^*(t) = P_r^*(t) = P_{\max}$.

For part (ii), considering Case 2 of Section 3.4.1.2, we can show that $X_r(t) \leq -V\zeta_{\max,r}$. Using (3.21) and (3.22), we see that $P_r^*(t) = 0$ if $P_r^o(t) \leq 0$, *i.e.*,

$$\frac{\eta_s(t)P_{\max}}{2(1+\gamma_s(t)P_{\max})}\left(-(2+\gamma_s(t)P_{\max}) + C_r\right) \leq 0. \tag{3.46}$$

Since $\frac{\eta_s(t)P_{\max}}{2(1+\gamma_s(t)P_{\max})}$ is not negative, we conclude that

$$-(2+\gamma_s P_{\max}) + C_r \leq 0. \tag{3.47}$$

Substituting the expression of C_r into (3.47), we have

$$\sqrt{(\gamma_s P_{\max})^2 - 4\frac{\gamma_r V}{\Delta t X_r}(1+\gamma_s P_{\max})} \leq (2+\gamma_s P_{\max}). \tag{3.48}$$

Rearranging equation (3.48), we have $X_r(t) \leq -\frac{V\gamma_r(t)}{\Delta t}$. Therefore, the sufficient condition for $P_r^*(t) = 0$ is $X_r(t) \leq -V\zeta_{\max,r}$. Using the result of Case 3 in Section 3.4.1.2 and

applying the similar approach, we can show part (iii). ■

3.8.3 Proof of Lemma 3.3

Proof: From (3.5), we write the battery evolution of the source as $E_h^s(t) \leq \min\{E_{\max} - E_b^s(t-1) + \Delta t P_s(t-1), E_{c,\max}\}$. Combining this with (3.11), we have

$$X_s(t+1) \leq X_s(t) - \Delta t P_s(t) + \min\{E_{\max} - X_s(t-1) - A_r + \Delta t P_s(t-1), E_{c,\max}\}. \tag{3.49}$$

From the optimal solution of **P3′**, we know that if $X_s(t) > 0$, then $P_s^*(t) = P_{\max}$. Considering this property and maximum possible value of $E_h^s(t)$, the equation (3.49) can be written as $X_s(t+1) \leq X_s(t) - \Delta t P_{\max} + E_{c,\max} \leq X_s(t)$. Thus, $X_s(t+1)$ is decreasing. If $X_s(t) \leq 0$, we have $P_s^*(t) \in [0, P_{\max})$. In this case, the maximum increase from $X_s(t)$ to $X_s(t+1)$ is possible when $P_s^*(t) = 0$ and $E_h^s(t) = E_{c,\max}$. Therefore, we have $X_s(t+1) \leq X_s(t) + E_{c,\max} \leq E_{c,\max}, \forall t$. It follows that $X_s(t)$ is upper bounded as $X_s(t) \leq E_{c,\max} \triangleq X_{\text{up,s}}$. The similar approach is applied for $X_r(t)$.

3.8.4 Proof of Proposition 3.2

Proof: In order for $P_r^*(t)$ to be a feasible solution to **P1**, $E_b^r(t)$ needs to meet the battery capacity constraint (3.1). Using $X_r(t) \geq X_{\text{low,r}}$ and equation (3.10), we have $E_b^r(t) - A_r \geq -V\zeta_{\max,r} - \Delta t P_{\max}$. This means $A_r \leq E_b^r(t) + V\zeta_{\max,r} + \Delta t P_{\max}, \forall t$. It follows that

$$A_r = E_{\min} + V\zeta_{\max,r} + \Delta t P_{\max} \tag{3.50}$$

satisfies the lower bound constraint. Also, in order for $P_r^*(t)$ to be feasible, it requires $X_r(t) = E_b^r(t) - A_r \leq E_{\max} - A_r$. Since $X_r(t) \leq X_{\text{up,r}} = E_{c,\max}$, the feasibility is guaranteed if

$$E_{c,\max} \leq E_{\max} - A_r. \tag{3.51}$$

Using A_r from (3.50) and substituting into (3.51), we have

$$V \leq \frac{E_{\max} - E_{\min} - E_{c,\max} - \Delta t P_{\max}}{\zeta_{\max,r}} \tag{3.52}$$

where the RHS of (3.52) is defined as $V_{\max,r}$. The similar approach is applied for $V_{\max,s}$. Finally, the maximum possible control weight V is derived by choosing $V_{\max}$ as

$$V_{\max} = \min\{V_{\max,s}, V_{\max,r}\}. \tag{3.53}$$

■

3.8.5 Proof of Theorem 3.1

Proof: We adopt a similar approach to Theorem 2.1 to obtain the performance bound. We first consider the stationary randomized power control policy $\{P_s^R(t)\}$ and $\{P_r^R(t)\}$ for **P2**, where $P_i^R(t)$ for $i = s, r$ only depends on the current system state $\mathbf{s}(t)$. Then, we bound the expected values of the cost objective and the constraints for each time slot t. Using these bounds and the upper bound of drift-plus-cost metric in (3.14), we derive the bound in (3.35).

The following results can be obtained straightforwardly from the results in [54] and Lemma 2.5. For the system state $\mathbf{s}(t)$ i.i.d. over time, there exists a stationary randomized

power control solution $P_i^R(t)$ for $i = s, r$ that only depends on the current state $\mathbf{s}(t)$ and guarantees

$$\begin{aligned}\mathbb{E}_{\mathcal{A}}[R^R(t)] &\triangleq \bar{R}^R(\mathcal{A}_s, \mathcal{A}_r) \\ &= \bar{R}^{\text{o}}(\mathcal{A}_s, \mathcal{A}_r), \end{aligned} \tag{3.54}$$

$$\mathbb{E}_{\mathcal{A}}[E_h^{i,R}(t)] = \mathbb{E}_{\mathcal{A}}[\Delta t P_i^R(t)], \quad i = s, r, \tag{3.55}$$

where $P_i^R(t)$, $R^R(t)$ and $E_h^{i,R}(t)$ for $i = s, r$ are the randomized power, instantaneous rate and harvested energy under the stationary randomized solution, and $\mathbb{E}_{\mathcal{A}}[\cdot]$ is taken with respect to the random state $\mathbf{s}(t)$ for the bounded fading, *i.e.*, $\mathbb{E}_{\mathcal{A}}[\cdot] \triangleq E[\cdot|\gamma_i(t) \in \mathcal{A}_i, i = s, r]$. Also, $\bar{R}^R(\mathcal{A}_s, \mathcal{A}_r)$ and $\bar{R}^o(\mathcal{A}_s, \mathcal{A}_r)$ are the objectives of **P2** achieved under stationary randomized policy and the optimal solution, respectively.

Our proposed algorithm is a solution of per slot optimization problem **P3**. The per slot optimization minimizes the upper bound of drift-plus-cost metric in (3.14) over all possible power control solutions, including the optimal stationary randomized solution $P_i^R(t)$ for $i = s, r$.

Plugging $P_i^R(t)$ for $i = s, r$ into the right hand side of (3.14) and using (3.54) and (3.55), we have

$$\begin{aligned}
&\Delta(X_s(t), X_r(t)) - V\mathbb{E}_{\mathcal{A}}[R^s(t)|X_s(t), X_r(t)] \\
&\leq B + X_s(t)\mathbb{E}_{\mathcal{A}}[E_h^{s,R}(t) - \Delta t P_s^R(t)|X_s(t), X_r(t)] \\
&+ X_r(t)\mathbb{E}_{\mathcal{A}}[E_h^{r,R}(t) - \Delta t P_r^R(t)|X_s(t), X_r(t)] - V\mathbb{E}_{\mathcal{A}}[R^R(t)|X_s(t), X_r(t)] \\
&= B + \sum_{i=s,r} X_i(t)\mathbb{E}_{\mathcal{A}}[E_h^{i,R}(t) - \Delta t P_r^{i,R}(t)] - V\mathbb{E}_{\mathcal{A}}[R^R(t)] \\
&= B - V\bar{R}^{\text{o}}(\mathcal{A}_s, \mathcal{A}_r) \\
&\leq B - V\bar{R}^{\text{opt}}(\mathcal{A}_s, \mathcal{A}_r)
\end{aligned} \tag{3.56}$$

where the first equality is due to dependency of $P_i^R(t)$ on $\mathbf{s}(t)$. The second equality is derived by (3.54) and (3.55). The last inequality is since **P2** is a relaxed version of **P1**. Therefore, we have $\bar{R}^{\text{opt}}(\mathcal{A}_s, \mathcal{A}_r) \leq \bar{R}^o(\mathcal{A}_s, \mathcal{A}_r)$.

Replacing $\Delta(X_s(t), X_r(t))$ in (3.13), taking expectations of both sides in (3.56) over $X_i(t)$ for $i = s, r$, and summing over t from 0 to $T-1$, we have

$$\begin{aligned} & V \sum_{t=0}^{T-1} \mathbb{E}_{\mathcal{A}}[R^s(t)] \\ & \geq TV\bar{R}^{\text{opt}}(\mathcal{A}_s, \mathcal{A}_r) - TB + \sum_{i=s,r} \left(\mathbb{E}_{\mathcal{A}}[L(X_i(T))] - \mathbb{E}_{\mathcal{A}}[L(X_i(0))]\right) \\ & \geq TV\bar{R}^{\text{opt}}(\mathcal{A}_s, \mathcal{A}_r) - TB - \sum_{i=s,r} \mathbb{E}_{\mathcal{A}}[L(X_i(0))] \end{aligned} \tag{3.57}$$

where the last inequality is due to $L(X_i(T))$ for $i = s, r$ being non-negative by definition. Dividing both sides by VT and taking limits over T, and noting that $L(X_i(0))$ is bounded, we have

$$\bar{R}^s(V, \mathcal{A}_s, \mathcal{A}_r) \geq \bar{R}^{\text{opt}}(\mathcal{A}_s, \mathcal{A}_r) - \frac{B}{V} \tag{3.58}$$

where $\bar{R}^s(V, \mathcal{A}_s, \mathcal{A}_r) = \lim_{T\to\infty} \frac{1}{T} \sum_{t=0}^{T-1} \mathbb{E}_{\mathcal{A}}[R^s(t)]$. ■

3.8.6 Proof of Lemma 3.4

Proof: To find an upper bound, we know that in each time slot, an optimal rate $R^{\text{opt}}(t)$ is less or equal to the maximum achievable rate which is $R_{\max}(t)$:

$$R^{\text{opt}}(t) \leq \log\left(1 + \text{SNR}_d^{\max}\right) \triangleq R_{\max}(t) \tag{3.59}$$

where $\text{SNR}_d^{\max}$ is obtained by (3.6) using $P_s(t) = P_r(t) = P_{\max}$. Therefore, (3.59) can be written as

$$R^{\text{opt}}(t) - R(t) \leq R_{\max}(t) - R(t) \tag{3.60}$$

where $R(t)$ is the instantaneous rate under random event $\gamma_i(t) \in \mathcal{A}_i^c$, for $i = s, r$. RHS of (3.60) can be written as

$$R_{\max} - R(t) = \log\left(\frac{1 + \text{SNR}_d^{\max}}{1 + \text{SNR}_d^{\delta}(t)}\right) \tag{3.61}$$

where $\text{SNR}_d^{\delta}(t)$ is derived by replacing (3.34) in (3.6). Taking expectation of both sides of (3.60) over $\gamma_i(t)$ and considering (3.61), (3.60) can be written as

$$\mathbb{E}_{\mathcal{A}^c}[R^{\text{opt}}(t)] - \mathbb{E}_{\mathcal{A}^c}[R(t)] \leq \mathbb{E}_{\mathcal{A}^c}\left[\log\left(\frac{1 + \text{SNR}_d^{\max}}{1 + \text{SNR}_d^{\delta}(t)}\right)\right] \tag{3.62}$$

where $\mathbb{E}_{\mathcal{A}^c}$ is taken with respect to the outage event, *i.e.*, $\mathbb{E}_{\mathcal{A}^c}[\cdot] \triangleq E[\cdot|\,(\gamma_s(t) \in \mathcal{A}_s^c) \cup (\gamma_r(t) \in \mathcal{A}_r^c)]$. Summing both sides of (3.62) over T, and let $T \to \infty$, (3.62) is written as follows

$$\lim_{T\to\infty} \frac{1}{T} \sum_{t=0}^{T-1} \mathbb{E}_{\mathcal{A}^c}[R(t)] \geq \bar{R}^{\text{opt}}(\mathcal{A}_s^c, \mathcal{A}_r^c) - G \tag{3.63}$$

where LHS of (3.63) is defined by $\bar{R}^s(\mathcal{A}_s^c, \mathcal{A}_r^c)$ and G is the maximum bound of $g(t)$ as follows

$$g(t) \triangleq \mathbb{E}_{\mathcal{A}^c}\left[\log\left(\frac{1 + \text{SNR}_d^{\max}}{1 + \text{SNR}_d^{\delta}(t)}\right)\right] \leq G \tag{3.64}$$

where $G \triangleq \mathbb{E}_{\mathcal{A}^c}\left[\log\left(1 + \text{SNR}_d^{\max}\right)\right]$. The upper-bound G is finite, *i.e.*, $G < \infty$. ■

3.8.7 Proof of Theorem 3.2

Proof: The achieved long-term time-averaged expected rate under Algorithm 5 can be written as

$$\bar{R}^s(V, p_o) = (1 - p_o)\bar{R}^s(V, \mathcal{A}_s, \mathcal{A}_r) + p_o\bar{R}^s(\mathcal{A}_s^c, \mathcal{A}_r^c) \tag{3.65}$$

where $\bar{R}^s(V, p_o) = \lim_{T\to\infty} \frac{1}{T}\sum_{t=0}^{T-1} \mathbb{E}[R(t)]$. Also, the optimal solution of **P1** can be written as

$$\bar{R}^{\text{opt}} = (1 - p_o)\bar{R}^{\text{opt}}(\mathcal{A}_s, \mathcal{A}_r) + p_o\bar{R}^{\text{opt}}(\mathcal{A}_s^c, \mathcal{A}_r^c). \tag{3.66}$$

By subtracting (3.65) from (3.66), we can write

$$\begin{aligned}\bar{R}^{\text{opt}} - \bar{R}^s(V, p_o) = (1 - p_o)&\left(\bar{R}^{\text{opt}}(\mathcal{A}_s, \mathcal{A}_r) - \bar{R}^s(V, \mathcal{A}_s, \mathcal{A}_r)\right)\\ &+ p_o\left(\bar{R}^{\text{opt}}(\mathcal{A}_s^c, \mathcal{A}_r^c) - \bar{R}^s(\mathcal{A}_s^c, \mathcal{A}_r^c)\right).\end{aligned} \tag{3.67}$$

Combining the results of Theorem 3.1 and Lemma 3.4 , the performance gap of Algorithm 5 to the optimal solution for **P1** in (3.37) can be obtained. ■

Chapter 4

Conclusions and Future Work

4.1 Conclusions

This dissertation focused on designing an online power control policy and storage management using the EH technology in wireless fading networks. A stochastic (time-dependent) optimization was considered to maximize the long-term average rate of a wireless network addressing the stochastic nature of the ambient energy arrival and fading conditions.

In Chapter 2, a point-to-point fading channel was considered in which the transmitter is equipped with the energy harvester and storage device. An online power control algorithm was proposed to maximize the long-term time-averaged rate under the battery operational constraints. A stochastic optimization problem was derived for the power control policy. A technique was proposed to transform the problem into a formulation where the Lyapunov optimization can be applied. However, Lyapunov optimization can not directly be employed for the unbounded channel fading, therefore, an approach was developed that uses the historical average power to tackle this challenge. Unlike most existing online power control algorithms, our proposed algorithm only depends on the current energy arrival and channel fade condition, without requiring their statistical knowledge. The proposed on-

line power control scheme is closed-form and simple to implement. It was shown that our power control solution not only provides energy conservation control of the battery, but also results in an opportunistic transmission style based on fading condition, resembling a ”water-filling” like solution. The proposed algorithm provides a bounded performance gap to the optimal solution. We also presented that our solution is applicable to the general multi-antenna beamforming scenarios. Simulation studies showed that our proposed online power control algorithm significantly outperforms other alternative online algorithms.

In Chapter 3, an amplify-and-forward two-hop relay network was considered where both transmitter and relay are equipped with energy harvesters and batteries. An online joint power control strategy was developed to maximize the long-term time-averaged rate for the two-hop relay network. The proposed scheme jointly determines the transmission power for both the transmitter and relay. A combined closed-form and numerical solution was derived for power control policy based on the energy arrival of both transmitter and rely, battery energy level of both transmitter and relay and also fading condition of both hops. The proposed algorithms do not require the current information of random events including fading condition and energy arrival. We analytically derived the bounded performance gap between our proposed algorithm and the optimal solution. The numerical results showed that our online joint power control algorithms performs significantly better than three online approaches in the literature.

4.2 Future Work

Energy harvesting for the wireless transmission is a promising solution and there are many open problems for leveraging this technology in the wireless network. Some recommendations are provided in the following.

- The proposed methodology developed in this research could be applied to different

wireless networks including broadcast, multiple access, and relay cooperative networks. For instance,

  - The proposed method can be further investigated for the decode and forward (DF) relaying to provide a comprehensive comparison for a relay two-hop model;
  - The relay network can be extended to multi-antenna beamforming scenarios;
  - The proposed methodology for a two-hop network can be extended to consider the direct link between a transmitter and receiver.

- The random packet (data) arrival can be considered along with the energy arrival for EH system. Considering the finite data buffers introduces a new challenge to the existing work. Online scheduling could be considered along with the proposed power control policy for wireless transmission with EH.

- In this thesis, the maximization of the long-term rate (infinite time horizon) of wireless transmission equipped with EH was investigated. The optimization problem can be extended over a finite time period (finite time horizon).

- In this thesis, an ideal charging and discharging for the battery model was considered for simplicity and without loss of generality. However, this methodology could be applied along with leakage parameters of the battery.

References

[1] J. A. Paradiso and T. Starner, “Energy scavenging for mobile and wireless electronics,” *IEEE Pervasive Computing*, vol. 4, no. 1, pp. 18–27, Jan. 2005.

[2] V. Raghunathan, C. Schurgers, S. Park, and M. B. Srivastava, “Energy-aware wireless microsensor networks,” *IEEE Signal Processing Mag.*, vol. 19, no. 2, pp. 40–50, Mar. 2002.

[3] S. Sudevalayam and P. Kulkarni, “Energy harvesting sensor nodes: Survey and implications,” *IEEE Commun. Surveys & Tutorials*, vol. 13, no. 3, pp. 443–461, Third 2011.

[4] K. Joon Kim, F. Cottone, S. Goyal, and J. Punch, “Energy scavenging for energy efficiency in networks and applications,” *Bell Labs Tech. J.*, vol. 15, no. 2, pp. 7–29, Sep. 2010.

[5] I. A. Ieropoulos, J. Greenman, C. Melhuish, and J. Hart, “Comparative study of three types of microbial fuel cell,” *Enzyme and Microbial Technology*, vol. 37, no. 2, pp. 238–245, Jun. 2005.

[6] F. Yildiz, “Potential ambient energy-harvesting sources and techniques,” *J. Technology Studies,*, vol. 35, no. 1, pp. 40–48, Fall 2009.

[7] R. Amirtharajah and A. P. Chandrakasan, "Self-powered signal processing using vibration-based power generation," *IEEE J. of Solid-State Circuits*, vol. 33, no. 5, pp. 687–695, 1998.

[8] D. A. Skoog and D. M. West, *Principles of instrumental analysis*. Saunders College Philadelphia, 1980, vol. 158.

[9] I. Ahmed, M. M. Butt, C. Psomas, A. Mohamed, I. Krikidis, and M. Guizani, "Survey on energy harvesting wireless communications: Challenges and opportunities for radio resource allocation," *Computer Networks*, vol. 88, pp. 234–248, 2015.

[10] H. Venkataraman and G.-M. Muntean, *Green mobile devices and networks: energy optimization and scavenging techniques*. CRC Press, 2012.

[11] C. E. Shannon, "Channels with side information at the transmitter," *IBM J. of Research and Development*, vol. 2, no. 4, pp. 289–293, Oct. 1958.

[12] A. Kansal, J. Hsu, S. Zahedi, and M. B. Srivastava, "Power management in energy harvesting sensor networks," *ACM Trans. Embedded Computing Systems (TECS)*, vol. 6, no. 4, p. 32, 2007.

[13] B. Lo, S. Thiemjarus, A. Panousopoulou, and G. Z. Yang, "Bioinspired design for body sensor networks [life sciences]," *IEEE Signal Processing Mag.*, vol. 30, no. 1, pp. 165–170, Jan. 2013.

[14] M. C. Hamilton, "Recent advances in energy harvesting technology and techniques," in *Proc. of Annual Conf. on IEEE Industrial Electron. Society*, Oct. 2012, pp. 6297–6304.

[15] S. Ulukus, A. Yener, E. Erkip, O. Simeone, M. Zorzi, P. Grover, and K. Huang, "Energy harvesting wireless communications: A review of recent advances," *IEEE J. Select. Areas Commun.*, vol. 33, no. 3, pp. 360–381, Mar. 2015.

[16] A. Goldsmith, *Wireless communications*. Cambridge university press, 2005.

[17] I. Ahmed, A. Ikhlef, D. W. K. Ng, and R. Schober, "Power allocation for an energy harvesting transmitter with hybrid energy sources," *IEEE Trans. Wireless Commun.*, vol. 12, no. 12, pp. 6255–6267, Dec. 2013.

[18] O. Ozel and S. Ulukus, "AWGN channel under time-varying amplitude constraints with causal information at the transmitter," in *Proc. of Asilomar Conf. on Signals, Systems and computers*, Nov. 2011, pp. 373–377.

[19] ——, "On the capacity region of the gaussian MAC with batteryless energy harvesting transmitters," in *Proc. IEEE Global Telecommn. Conf. (GLOBECOM)*, Dec. 2012, pp. 2385–2390.

[20] L. Varshney, "Transporting information and energy simultaneously," in *Proc. IEEE Int. Symposium on Infor. Theory (ISIT)*, Jul. 2008, pp. 1612–1616.

[21] P. Grover and A. Sahai, "Shannon meets tesla: Wireless information and power transfer," in *Proc. IEEE Int. Symposium on Infor. Theory (ISIT)*, Jun. 2010, pp. 2363–2367.

[22] R. Zhang and C. K. Ho, "MIMO broadcasting for simultaneous wireless information and power transfer," *IEEE Trans. Wireless Commun.*, vol. 12, pp. 1989–2001, May 2013.

[23] J. Xu, L. Liu, and R. Zhang, "Multiuser MISO beamforming for simultaneous wireless information and power transfer," *IEEE Trans. Signal Processing*, vol. 62, pp. 4798–4810, Sep. 2014.

[24] Q. Shi, L. Liu, W. Xu, and R. Zhang, "Joint transmit beamforming and receive power splitting for MISO SWIPT systems," *IEEE Trans. Wireless Commun.*, vol. 13, pp. 3269–3280, Jun. 2014.

[25] S. Lee, L. Liu, and R. Zhang, "Collaborative wireless energy and information transfer in interference channel," *IEEE Trans. Wireless Commun.*, vol. 14, pp. 545–557, Jan. 2015.

[26] O. Ozel and S. Ulukus, "Achieving AWGN capacity under stochastic energy harvesting," *IEEE Trans. Inform. Theory*, vol. 58, no. 10, pp. 6471–6483, Oct. 2012.

[27] J. Yang and S. Ulukus, "Optimal packet scheduling in an energy harvesting communication system," *IEEE Trans. Commun.*, vol. 60, pp. 220–230, Jan. 2012.

[28] C. Huang, R. Zhang, and S. Cui, "Throughput maximization for the Gaussian relay channel with energy harvesting constraints," *IEEE J. Select. Areas Commun.*, vol. 31, pp. 1469–1479, Aug. 2013.

[29] K. Tutuncuoglu and A. Yener, "Optimum transmission policies for battery limited energy harvesting nodes," *IEEE Trans. Wireless Commun.*, vol. 11, pp. 4808–4818, Mar. 2012.

[30] ——, "Sum-rate optimal power policies for energy harvesting transmitters in an interference channel," *IEEE J. of Commun and Networks., Special Issue on Energy Harvesting in Wireless Networks*, vol. 29, pp. 151–161, Apr. 2012.

[31] F. Yuan, Q. Zhang, S. Jin, and H. Zhu, "Optimal harvest-use-store strategy for energy harvesting wireless systems," *IEEE Trans. Wireless Commun.*, vol. 14, pp. 698–710, Feb. 2015.

[32] C. K. Ho and R. Zhang, "Optimal energy allocation for wireless communications with energy harvesting constraints," *IEEE Trans. Signal Processing*, vol. 60, pp. 4808–4818, Aug. 2012.

[33] O. Ozel, K. Tutuncuoglu, J. Yang, S. Ulukus, and A. Yener, "Transmission with energy harvesting nodes in fading wireless channels: Optimal policies," *IEEE J. Select. Areas Commun.*, vol. 29, no. 8, pp. 1732–1743, Sep. 2011.

[34] M. A. Antepli, E. Uysal-Biyikoglu, and H. Erkal, "Optimal packet scheduling on an energy harvesting broadcast link," *IEEE J. Select. Areas Commun.*, vol. 29, no. 8, pp. 1721–1731, Sep. 2011.

[35] Z. Wang, V. Aggarwal, and X. Wang, "Iterative dynamic water-filling for fading multiple-access channels with energy harvesting," *IEEE J. Select. Areas Commun.*, vol. 33, no. 3, pp. 382–395, Mar. 2015.

[36] N. Su, O. Kaya, S. Ulukus, and M. Koca, "Cooperative multiple access under energy harvesting constraints," in *Proc. IEEE Global Telecommn. Conf. (GLOBECOM)*, Dec. 2015, pp. 1–6.

[37] P. He, L. Zhao, S. Zhou, and Z. Niu, "Recursive waterfilling for wireless links with energy harvesting transmitters," *IEEE Trans. Veh. Technol.*, vol. 63, no. 3, pp. 1232–1241, 2014.

[38] P. He and L. Zhao, "Noncommutative composite water-filling for energy harvesting and smart power grid hybrid system with peak power constraints," *IEEE Trans. Vehicular Technology*, vol. 65, no. 4, pp. 2026–2037, Apr. 2016.

[39] Z. Wang, A. Tajer, and X. Wang, "Communication of energy harvesting tags," *IEEE Trans. Commun.*, vol. 60, pp. 1159–1166, Apr. 2012.

[40] V. Sharma, U. Mukherji, and V. J. S. Gupta, "Optimal energy management policies for energy harvesting sensor nodes," *IEEE Trans. Wireless Commun.*, vol. 9, pp. 1326–1336, Apr. 2010.

[41] J. Lei, R. Yates, and L. Greenstein, "A generic model for optimizing single-hop transmission policy of replenishable sensors," *IEEE Trans. Wireless Commun.*, vol. 8, pp. 547–551, Feb. 2009.

[42] P. Blasco, D. Gunduz, and M. Dohler, "A learning theoretic approach to energy harvesting communication system optimization," *IEEE Trans. Wireless Commun.*, vol. 12, no. 4, pp. 1872–1882, Apr. 2013.

[43] M. B. Khuzani, H. E. Saffar, E. H. M. Alian, and P. Mitran, "On optimal online power policies for energy harvesting with finite-state markov channels," in *Proc. IEEE Int. Symposium on Infor. Theory (ISIT)*, Jul. 2013, pp. 1586–1590.

[44] Q. Wang and M. Liu, "When simplicity meets optimality: Efficient transmission power control with stochastic energy harvesting," in *Proc. IEEE Conf. on Computer Commun. (INFOCOM)*, Apr. 2013, pp. 580–584.

[45] K. Tutuncuoglu and A. Yener, "Optimal power policy for energy harvesting transmitters with inefficient energy storage," in *Proc. of Annual Conf. on Information Sciences and Systems (CISS)*, Mar. 2012, pp. 1–6.

[46] J. Xu and R. Zhang, "Throughput optimal policies for energy harvesting wireless transmitters with non-ideal circuit power," *IEEE J. Select. Areas Commun.*, vol. 32, pp. 322–332, Feb. 2014.

[47] O. Orhan, D. Gunduz, and E. Erkip, "Optimal packet scheduling for an energy harvesting transmitter with processing cost," in *Proc. IEEE Int. Conf. Commun. (ICC)*, Jun. 2013, pp. 3110–3114.

[48] R. Nagda, S. Satpathi, and R. Vaze, "Optimal offline and competitive online strategies for transmitter-receiver energy harvesting," in *Proc. IEEE Int. Conf. Commun. (ICC)*, Jun. 2015, pp. 74–79.

[49] N. Michelusi and M. Zorzi, "Optimal adaptive random multi-access in energy harvesting wireless sensor networks," *IEEE Trans. Commun.*, vol. 63, no. 4, pp. 1355–1372, Apr. 2015.

[50] D. Zhao, C. Huang, Y. Chen, F. Alsaadi, and S. Cui, "Resource allocation for multiple access channel with conferencing links and shared renewable energy sources," *IEEE J. Select. Areas Commun.*, vol. 33, no. 3, pp. 423–437, Mar. 2015.

[51] M. B. Khuzani and P. Mitran, "On online energy harvesting in multiple access communication systems," *IEEE Trans. Inform. Theory*, vol. 60, no. 3, pp. 1883–1898, Mar. 2014.

[52] Z. Mao, C. Koksal, and N. Shroff, "Near optimal power and rate control of multi-hop sensor networks with energy replenishment:basic limitations with finite energy and data storage," *IEEE Trans. Autom. Control*, vol. 57, pp. 815–829, Apr. 2012.

[53] L. Huang and M. Neely, "Utility optimal scheduling in energy-harvesting networks," *IEEE/ACM Trans. Networking*, vol. 21, no. 4, pp. 1117–1130, Aug. 2013.

[54] M. J. Neely, *Stochastic Network Optimization with Application to Communication and Queueing Systems*. Morgan & Claypool, 2010.

[55] B. Varan and A. Yener, "Two-hop networks with energy harvesting: The (non-)impact of buffer size," in *Proc. IEEE Global Conf. on Signal and Information Processing (GlobalSIP)*, Dec. 2013, pp. 399–402.

[56] Y. Luo, J. Zhang, and K. Letaief, "Optimal scheduling and power allocation for two-hop energy harvesting communication systems," *IEEE Trans. Wireless Commun.*, vol. 12, no. 9, pp. 4729–4741, Sep. 2013.

[57] O. Orhan and E. Erkip, "Energy harvesting two-hop networks: Optimal policies for the multi-energy arrival case," in *IEEE Sarnoff Symposium*, May 2012, pp. 1–6.

[58] I. Ahmed, A. Ikhlef, R. Schober, and R. Mallik, "Joint power allocation and relay selection in energy harvesting AF relay systems," *IEEE Wireless Commun. Letter.*, vol. 2, no. 2, pp. 239–242, Apr. 2013.

[59] Y. Mao, J. Zhang, S. Song, and K. Letaief, "Joint link selection and relay power allocation for energy harvesting relaying systems," in *Proc. IEEE Global Telecommn. Conf. (GLOBECOM)*, Dec. 2014, pp. 2568–2573.

[60] O. Orhan and E. Erkip, "Energy harvesting two-hop communication networks," *IEEE J. Select. Areas Commun.*, vol. 33, no. 12, pp. 2658–2670, Dec. 2015.

[61] A. Minasian, S. ShahbazPanahi, and R. S. Adve, "Energy harvesting cooperative communication systems," *IEEE Trans. Wireless Commun.*, vol. 13, no. 11, pp. 6118–6131, Nov. 2014.

[62] Z. Ding and H. V. Poor, "Cooperative energy harvesting networks with spatially random users," *IEEE Signal Processing Lett.*, vol. 20, no. 12, pp. 1211–1214, Dec. 2013.

[63] K. Tutuncuoglu and A. Yener, "Energy harvesting networks with energy cooperation: Procrastinating policies," *IEEE Trans. Commun.*, vol. 63, no. 11, pp. 4525–4538, Nov. 2015.

[64] S. Bi, C. K. Ho, and R. Zhang, "Wireless powered communication: opportunities and challenges," *IEEE Commun. Mag.*, vol. 53, no. 4, pp. 117–125, Apr. 2015.

[65] X. Lu, P. Wang, D. Niyato, D. I. Kim, and Z. Han, "Wireless networks with RF energy harvesting: A contemporary survey," *IEEE Commun. Surveys Tutorials*, vol. 17, no. 2, pp. 757–789, Second 2015.

[66] L. Liu, R. Zhang, and K. C. Chua, "Wireless information transfer with opportunistic energy harvesting," *IEEE Trans. Wireless Commun.*, vol. 12, no. 1, pp. 288–300, Jan. 2013.

[67] Y. Zeng and R. Zhang, "Optimized training design for wireless energy transfer," *IEEE Trans. Commun.*, vol. 63, no. 2, pp. 536–550, Feb. 2015.

[68] H. J. Visser and R. J. M. Vullers, "RF energy harvesting and transport for wireless sensor network applications: Principles and requirements," *Proc. of the IEEE*, vol. 101, no. 6, pp. 1410–1423, Jun. 2013.

[69] K. M. Farinholt, G. Park, and C. R. Farrar, "RF energy transmission for a low-power wireless impedance sensor node," *IEEE Sensor J.*, vol. 9, no. 7, pp. 793–800, Jul. 2009.

[70] A. Al-Khayari, H. Al-Khayari, S. Al-Nabhani, M. M. Bait-Suwailam, and Z. Nadir, "Design of an enhanced RF energy harvesting system for wireless sensors," in *Proc. of IEEE GCC Conf. and Exh. (GCC)*, Nov. 2013, pp. 479–482.

[71] M. Al-Lawati, M. Al-Busaidi, and Z. Nadir, "RF energy harvesting system design for wireless sensors," in *Proc. of Int. Multi-Conf. on Systems, Signals Devices*, Mar. 2012, pp. 1–4.

[72] N. Barroca, H. M. Saraiva, P. T. Gouveia, J. Tavares, L. M. Borges, F. J. Velez, C. Loss, R. Salvado, P. Pinho, R. Gonçalves, N. BorgesCarvalho, R. Chavéz-Santiago, and I. Balasingham, "Antennas and circuits for ambient RF energy harvesting in wireless body area networks," in *Proc. of IEEE Annual Int. Symposium on Personal, Indoor, and Mobile Radio Commun. (PIMRC)*, Sep. 2013, pp. 532–537.

[73] L. Xia, J. Cheng, N. E. Glover, and P. Chiang, "0.56 V, 20 dBm RF-powered, multi-node wireless body area network System-on-a-Chip with harvesting-efficiency tracking loop," *IEEE J. of Solid-State Circuits*, vol. 49, no. 6, pp. 1345–1355, Jun. 2014.

[74] Y. Zuo, "Survivable RFID systems: Issues, challenges, and techniques," *IEEE Trans. on Sys., Man, and Cybernetics, Part C (Applications and Reviews)*, vol. 40, no. 4, pp. 406–418, Jul. 2010.

[75] U. Olgun, C. C. Chen, and J. L. Volakis, "Wireless power harvesting with planar rectennas for 2.45 GHz RFIDs," in *Proc. of URSI Int. Symposium on Electromagnetic Theory*, Aug. 2010, pp. 329–331.

[76] V. Kuhn, F. Seguin, C. Lahuec, and C. Person, "A multi-tone RF energy harvester in body sensor area network context," in *Proc. of Loughborough Antennas Propag. Conf. (LAPC)*, Nov. 2013, pp. 238–241.

[77] S. Mandal, L. Turicchia, and R. Sarpeshkar, "A battery-free tag for wireless monitoring of heart sounds," in *Proc. of Int. Workshop on Wearable and Implantable Body Senor Networks*, Jun. 2009, pp. 201–206.

[78] K. Huang and V. K. N. Lau, "Enabling wireless power transfer in cellular networks: Architecture, modeling and deployment," *IEEE Trans. Wireless Commun.*, vol. 13, no. 2, pp. 902–912, Feb. 2014.

[79] H. Lee, K. J. Lee, H. Kim, B. Clerckx, and I. Lee, "Resource allocation techniques for wireless powered communication networks with energy storage constraint," *IEEE Trans. Wireless Commun.*, vol. 15, no. 4, pp. 2619–2628, Apr. 2016.

[80] J. O. McSpadden and J. C. Mankins, "Space solar power programs and microwave wireless power transmission technology," *IEEE Microwave Mag.*, vol. 3, no. 4, pp. 46–57, Dec. 2002.

[81] K. Huang and E. Larsson, "Simultaneous information and power transfer for broadband wireless systems," *IEEE Trans. Signal Processing*, vol. 61, no. 23, pp. 5972–5986, Dec. 2013.

[82] L. Liu and R. Zhang, "Wireless information and power transfer: A dynamic power splitting approach," *IEEE Trans. Commun.*, vol. 61, no. 8, pp. 4754–4767, Sept. 2013.

[83] Z. Zong, H. Feng, F. R. Yu, N. Zhao, T. Yang, and B. Hu, "Optimal transceiver design for SWIPT in K-user MIMO interference channels," *IEEE Trans. Wireless Commun.*, vol. 15, no. 1, pp. 430–445, Jan. 2016.

[84] Q. Shi, W. Xu, T. H. Chang, Y. Wang, and E. Song, "Joint beamforming and power splitting for miso interference channel with swipt: An socp relaxation and decen-

tralized algorithm," *IEEE Trans. Signal Processing*, vol. 62, no. 23, pp. 6194–6208, Dec. 2014.

[85] Z. Zong, H. Feng, F. R. Yu, N. Zhao, T. Yang, and B. Hu, "Optimal transceiver design for swipt in k -user mimo interference channels," *IEEE Trans. Wireless Commun.*, vol. 15, no. 1, pp. 430–445, Jan. 2016.

[86] X. Zhou, R. Zhang, and C. K. Ho, "Wireless information and power transfer: Architecture design and rate-energy tradeoff," *IEEE Trans. Commun.*, vol. 61, no. 11, pp. 4754–4767, Jan. 2013.

[87] T. A. Zewde and M. C. Gursoy, "Energy-efficient resource allocation for SWIPT in multiple access channels," in *Proc. of Annual Conf. on Information Sciences and Systems (CISS)*, Mar. 2016, pp. 246–251.

[88] H. Ju and R. Zhang, "A novel mode switching scheme utilizing random beamforming for opportunistic energy harvesting," *IEEE Trans. Wireless Commun.*, vol. 13, no. 4, pp. 2150–2162, Apr. 2014.

[89] X. Zhou, R. Zhang, and C. K. Ho, "Wireless information and power transfer in multiuser OFDM systems," *IEEE Trans. Wireless Commun.*, vol. 13, no. 4, pp. 2282–2294, Apr. 2014.

[90] S. Park, S. Lee, B. Kim, D. Hong, and J. Lee, "Energy-efficient opportunistic spectrum access in cognitive radio networks with energy harvesting," in *Proc. of the 4th int. conf. on cognitive radio and advanced spectrum management*. ACM, 2011, p. 62.

[91] S. Park, H. Kim, and D. Hong, "Cognitive radio networks with energy harvesting," *IEEE Trans. Wireless Commun.*, vol. 12, no. 3, pp. 1386–1397, 2013.

[92] S. Park, J. Heo, B. Kim, W. Chung, H. Wang, and D. Hong, "Optimal mode selection for cognitive radio sensor networks with RF energy harvesting," in *2012 IEEE 23rd Int. Sym. on Personal, Indoor and Mobile Radio Commun. - (PIMRC)*, Sept. 2012, pp. 2155–2159.

[93] A. Sultan, "Sensing and transmit energy optimization for an energy harvesting cognitive radio," *IEEE Wireless Communications Letters*, vol. 1, no. 5, pp. 500–503, Oct. 2012.

[94] N. Pappas, J. Jeon, A. Ephremides, and A. Traganitis, "Optimal utilization of a cognitive shared channel with a rechargeable primary source node," *Journal of Commun. and Networks*, vol. 14, no. 2, pp. 162–168, Apr. 2012.

[95] S. Lee, R. Zhang, and K. Huang, "Opportunistic wireless energy harvesting in cognitive radio networks," *IEEE Trans. Wireless Commun.*, vol. 12, no. 9, pp. 4788–4799, Sep. 2013.

[96] A. E. Shafie and A. Sultan, "Optimal random access and random spectrum sensing for an energy harvesting cognitive radio," in *Proc. of IEEE 8th International Conf. on Wireless and Mobile Computing, Networking and Commun. (WiMob)*, Oct. 2012, pp. 403–410.

[97] ——, "Optimal random access for a cognitive radio terminal with energy harvesting capability," *IEEE Commun. Letter.*, vol. 17, no. 6, pp. 1128–1131, Jun. 2013.

[98] X. Gao, W. Xu, S. Li, and J. Lin, "An online energy allocation strategy for energy harvesting cognitive radio systems," in *Proc. of Int. Conf. on Wireless Commun. and Signal Processing (WCSP)*, Oct. 2013, pp. 1–5.

[99] S. Park and D. Hong, "Achievable throughput of energy harvesting cognitive radio networks," *IEEE Trans. Wireless Commun.*, vol. 13, no. 2, pp. 1010–1022, Feb. 2014.

[100] W. Chung, S. Park, S. Lim, and D. Hong, "Spectrum sensing optimization for energy-harvesting cognitive radio systems," *IEEE Trans. Wireless Commun.*, vol. 13, no. 5, pp. 2601–2613, May 2014.

[101] S. Lee, K. Huang, and R. Zhang, "Cognitive energy harvesting and transmission from a network perspective," in *2012 IEEE Int.l Conf. on Commun. Systems (ICCS)*, Nov. 2012, pp. 225–229.

[102] G. Zheng, Z. Ho, E. A. Jorswieck, and B. Ottersten, "Information and energy cooperation in cognitive radio networks," *IEEE Trans. Signal Processing*, vol. 62, no. 9, pp. 2290–2303, May 2014.

[103] K. Huang and V. K. N. Lau, "Enabling wireless power transfer in cellular networks: Architecture, modeling and deployment," *IEEE Trans. Wireless Commun.*, vol. 13, no. 2, pp. 902–912, Feb. 2014.

[104] I. Ahmed, A. Ikhlef, D. W. K. Ng, and R. Schober, "Power allocation for an energy harvesting transmitter with hybrid energy sources," *IEEE Trans. Wireless Commun.*, vol. 12, no. 12, pp. 6255–6267, Dec. 2013.

[105] O. Ozel, K. Shahzad, and S. Ulukus, "Optimal energy allocation for energy harvesting transmitters with hybrid energy storage and processing cost," *IEEE Trans. Signal Processing*, vol. 62, no. 12, pp. 3232–3245, Jun. 2014.

[106] J. Gong, S. Zhou, Z. Niu, and J. S. Thompson, "Energy-aware resource allocation for energy harvesting wireless communication systems," in *Proc. of IEEE 77th Vehicular Technology Conf. (VTC Spring)*, Jun. 2013, pp. 1–5.

[107] P. Viswanath, D. N. C. Tse, and R. Laroia, "Opportunistic beamforming using dumb antennas," in *Proc. IEEE Int. Symposium on Infor. Theory (ISIT)*, 2002, pp. 449–.

[108] N. Tekbiyik, T. Girici, E. Uysal-Biyikoglu, and K. Leblebicioglu, "Proportional fair resource allocation on an energy harvesting downlink," *IEEE Trans. Wireless Commun.*, vol. 12, no. 4, pp. 1699–1711, April 2013.

[109] H. Erkal, F. M. Ozcelik, and E. Uysal-Biyikoglu, "Optimal offline broadcast scheduling with an energy harvesting transmitter," *EURASIP Journal on Wireless Commun. and Networking*, vol. 2013, no. 1, p. 197, 2013.

[110] J. Yang and S. Ulukus, "Optimal packet scheduling in a multiple access channel with energy harvesting transmitters," *IEEE Journal of Commun. and Networks*, vol. 14, no. 2, pp. 140–150, Apr. 2012.

[111] M. J. Neely, "Super-fast delay tradeoffs for utility optimal fair scheduling in wireless networks," *IEEE J. Select. Areas Commun.*, vol. 24, no. 8, pp. 1489–1501, Aug. 2006.

[112] ——, "Optimal energy and delay tradeoffs for multiuser wireless downlinks," *IEEE Trans. Inform. Theory*, vol. 53, no. 9, pp. 3095–3113, Sep. 2007.

[113] L. Georgiadis, M. J. Neely, and L. Tassiulas, *Resource allocation and cross-layer control in wireless networks*. Now Publishers Inc, 2006.

[114] A. Eryilmaz and R. Srikant, "Joint congestion control, routing, and mac for stability and fairness in wireless networks," *IEEE J. Select. Areas Commun.*, vol. 24, no. 8, pp. 1514–1524, Aug. 2006.

[115] A. L. Stolyar, "Maximizing queueing network utility subject to stability: Greedy primal-dual algorithm," *Queueing Systems*, vol. 50, no. 4, pp. 401–457, 2005.

[116] L. Tassiulas and A. Ephremides, "Stability properties of constrained queueing systems and scheduling policies for maximum throughput in multi-hop radio networks," *IEEE Trans. Autom. Control*, vol. 37, no. 12, pp. 1936–1948, Dec. 1992.

[117] L. Huang and M. J. Neely, "Delay reduction via lagrange multipliers in stochastic network optimization," *IEEE Trans. Autom. Control*, vol. 56, no. 4, pp. 842–857, Apr. 2011.

[118] "Sony fortelion," SONY, 2011. [Online]. Available: http://www.solarshop-europe.net/product_info.php?products_id=2562

[119] "Lg resu 5.0," LG Chem., 2013. [Online]. Available: http://de.krannichsolar.com/en/products/storage-solutions/lg-chem.html

[120] D. P. Bertsekas, *Dynamic programming and optimal control*. Athena Scientific, 2007.

[121] A. Sinha and P. Chaporkar, "Optimal power allocation for a renewable energy source," in *National Conf. on Commuincations Proceedings*, Kharagpur, Feb. 2012, pp. 1–5.

[122] G. Strang, *Introduction to Linear Algebra*. Wellesley-Cambridge Press, 2003. [Online]. Available: https://books.google.ca/books?id=Gv4pCVyoUVYC

[123] S. Boyd and L. Vandenberghe, *Convex Optimization*. New York: Cambridge University Press, 2004.